AD-A077 651 OHIO STATE UNIV COLUMBUS ELECTROSCIENCE LAB F/G 9/1
ASYMPTOTIC HIGH FREQUENCY TECHNIQUES FOR UHF AND ABOVE ANTENNAS--ETC(U)
SEP 79 R C RUDDUCK, R J MARHEFKA N00123-76-C-1371
UNCLASSIFIED ESL-784508-20 NL

1 OF 1
ADA 077651

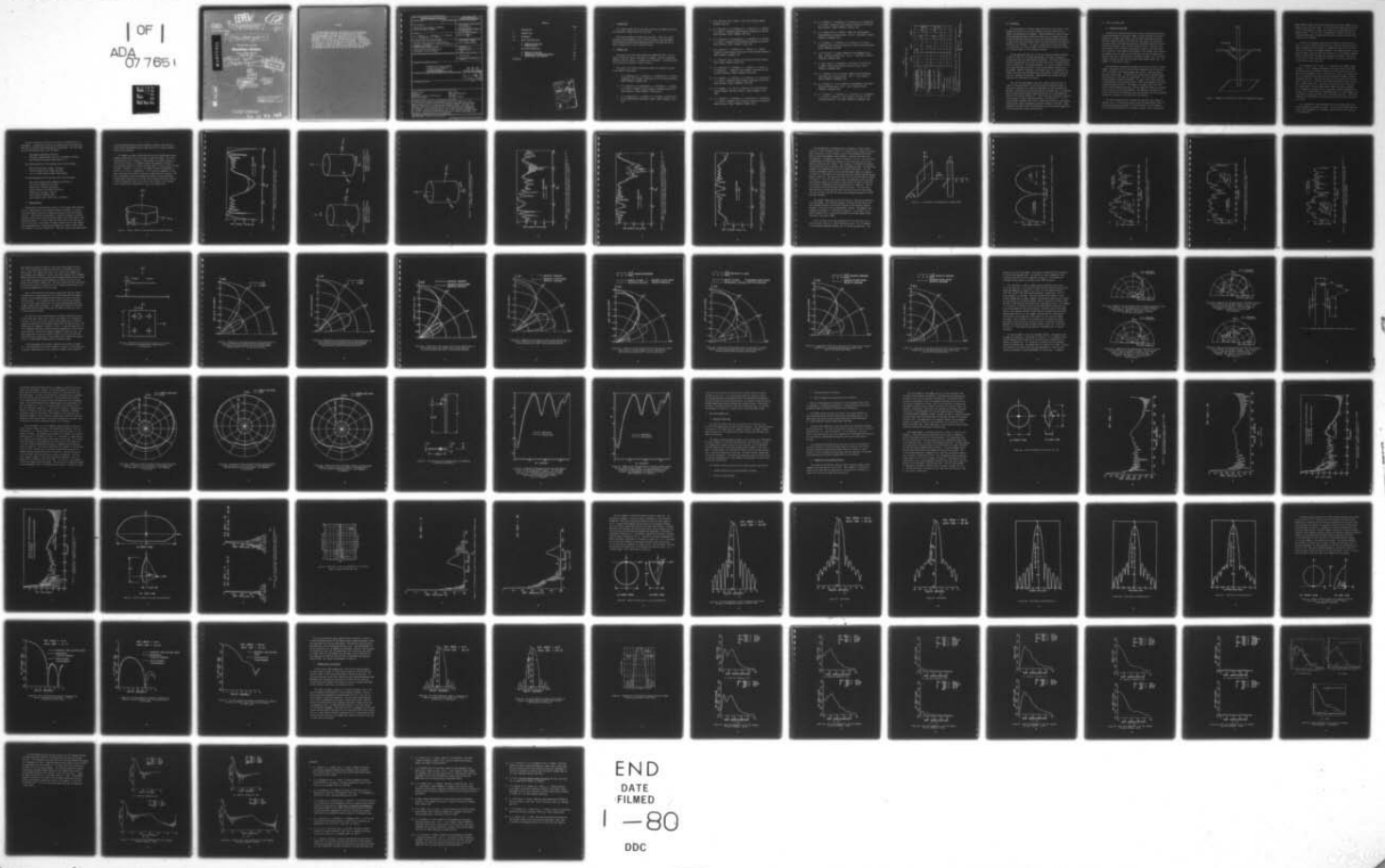

END
DATE FILMED
1 -80
DDC

LEVEL II

12

OSU

The Ohio State University

ASYMPTOTIC HIGH FREQUENCY TECHNIQUES FOR UHF AND ABOVE ANTENNAS

NOSC Con 4204

R. C. Rudduck, R. J. Marhefka, W. D. Burnside, R. G. Kouyoumjian, C. H. Walter

The Ohio State University

ElectroScience Laboratory

Department of Electrical Engineering
Columbus, Ohio 43212

Final rept. 1 Aug 76 - 31 Jul 79

ESL-

Final Report 784508-20

Sept 1979

Contract N00123-76-C-1371

88

Naval Regional Procurement Office
Long Beach, California 90822

NOTICES

When Government drawings, specifications, or other data are used for any purpose other than in connection with a definitely related Government procurement operation, the United States Government thereby incurs no responsibility nor any obligation whatsoever, and the fact that the Government may have formulated, furnished, or in any way supplied the said drawings, specifications, or other data, is not to be regarded by implication or otherwise as in any manner licensing the holder or any other person or corporation, or conveying any rights or permission to manufacture, use, or sell any patented invention that may in any way be related thereto.

SECURITY CLASSIFICATION OF THIS PAGE *(When Data Entered)*

REPORT DOCUMENTATION PAGE

READ INSTRUCTIONS BEFORE COMPLETING FORM

1. REPORT NUMBER	2. GOVT ACCESSION NO. / 3. RECIPIENT'S CATALOG NUMBER
4. TITLE *(and Subtitle)* ASYMPTOTIC HIGH FREQUENCY TECHNIQUES FOR UHF AND ABOVE ANTENNAS	5. TYPE OF REPORT & PERIOD COVERED Final Report 8/1/76-7/31/79
	6. PERFORMING ORG. REPORT NUMBER ESL 784508-20
7. AUTHOR(s) R. C. Rudduck, R. J. Marhefka, W. D. Burnside, R. G. Kouyoumjian, C. H. Walter	8. CONTRACT OR GRANT NUMBER(s) N00123-76-C-1371
9. PERFORMING ORGANIZATION NAME AND ADDRESS The Ohio State University ElectroScience Laboratory, Department of Electrical Engineering Columbus, Ohio 43212	10. PROGRAM ELEMENT, PROJECT, TASK AREA & WORK UNIT NUMBERS Project N00953/6/009121
11. CONTROLLING OFFICE NAME AND ADDRESS Naval Regional Procurement Office Long Beach, California 90822	12. REPORT DATE September 1979 13. NUMBER OF PAGES 84
14. MONITORING AGENCY NAME & ADDRESS *(if different from Controlling Office)*	15. SECURITY CLASS. *(of this report)* Unclassified 15a. DECLASSIFICATION/DOWNGRADING SCHEDULE

16. DISTRIBUTION STATEMENT *(of this Report)*

This document has been approved for public release and sale; its distribution is unlimited.

17. DISTRIBUTION STATEMENT *(of the abstract entered in Block 20, if different from Report)*

18. SUPPLEMENTARY NOTES

19. KEY WORDS *(Continue on reverse side if necessary and identify by block number)*

Computer code
Algorithm
Geometrical Theory of Diffraction
Far Field Pattern
Near field
Aperture integration
Cylinders
Reflector antenna

20. ABSTRACT *(Continue on reverse side if necessary and identify by block number)*

The overall scope of the program on Contract No. N00123-76-C-1371 between The Ohio State University ElectroScience Laboratory and the Naval Ocean Systems Center is to develop the necessary theory, algorithms and computer codes for simulating antennas at UHF and above in a complex ship environment. The work consists of a) basic scattering code development, b) reflector antenna code development and c) basic studies to support items a) and b). This report describes the progress in each of these areas for the period 1 August 1976 to 31 July 1979.

DD FORM 1 JAN 73 1473 EDITION OF 1 NOV 65 IS OBSOLETE

SECURITY CLASSIFICATION OF THIS PAGE *(When Data Entered)*

CONTENTS

I. INTRODUCTION

This report summarizes the work done on Contract No. N00123-76-C-1371 for the period 1 August 1976 to 31 July 1979.

The overall program is divided into two areas. These are 1) basic scattering code development, and 2) reflector antenna code development. The following sections present background material and describe the research accomplished in each of these two areas.

II. PROGRAM SCOPE

The scope of the work under Contract No. N00123-76-C-1371 is to develop the necessary theory, algorithms and computer codes for simulating antennas at UHF and above in a complex ship environment. A milestone chart for the three year program is shown in Table 1.

More details on the work accomplished under this contract are given in the reports listed below:

1. R. G. Kouyoumjian, R. C. Rudduck, R. J. Marhefka and C. H. Walter, "Asymptotic High Frequency Techniques for UHF and Above Antennas," Report 784508-1, November 1976.

2. W. D. Burnside, R. G. Kouyoumjian, R. J. Marhefka, R. C. Rudduck, C. H. Walter, "Asymptotic High Frequency Techniques for UHF and Above Antennas," Report 784508-2, February 1977.

3. R. G. Kouyoumjian, R. J. Luebbers, R. C. Rudduck, "A GTD Analysis of the LAMPS Antennas Blocked by a Mast," Report 784508-3, June 1977.

4. W. D. Burnside, "User's Manual - Flat Plate Program," Report 784508-4, May 1977.

5. W. D. Burnside, R. G. Kouyoumjian, R. J. Marhefka, R. C. Rudduck, C. H. Walter, "Asymptotic High Frequency Techniques for UHF and Above Antennas," Report 784508-5, May 1977.

6. W. D. Burnside, R. G. Kouyoumjian, R. J. Marhefka, R. C. Rudduck, C. H. Walter, "Asymptotic High Frequency Techniques for UHF and Above Antennas," Report 784508-6, August 1977.

7. W. D. Burnside, R. J. Marhefka, R. C. Rudduck, C. H. Walter, "Asymptotic High Frequency Techniques for UHF and Above Antennas," Report 784508-7, November 1977.

8. R. J. Marhefka, "User's Manual for Plates and Cylinder Computer Code," Report 784508-8, March 1978.

9. W. D. Burnside, R. J. Marhefka, R. C. Rudduck, C. H. Walter, R. G. Kouyoumjian, "Asymptotic High Frequency Techniques for UHF and Above Antennas," Report 784508-9, March 1978.

10. R. C. Rudduck, R. J. Marhefka, W. D. Burnside, R. G. Kouyoumjian, C. H. Walter, "Asymptotic High Frequency Techniques for UHF and Above Antennas," Report 784508-10, June 1978.

11. R. C. Rudduck, S. H. Lee, W. D. Burnside, "Far Field Reflector Antenna Computer Code User's Manual," Report 784508-11, July 1978.

12. R. C. Rudduck, R. J. Marhefka, W. D. Burnside, R. G. Kouyoumjian, C. H. Walter, "Asymptotic High Frequency Techniques for UHF and Above Antennas," Report 784508-12, October 1978.

13. R. C. Rudduck, R. J. Marhefka, W. D. Burnside, R. G. Kouyoumjian, C. H. Walter, "Asymptotic High Frequency Techniques for UHF and Above Antennas," Report 784508-13, January 1979.

14. F. W. Schmidt and R. J. Marhefka, "Numerical Electromagnetic Code (NEC)-Basic Scattering Code. Part II: Code Manual," Report 784508-14, September 1979.

15. R. C. Rudduck, R. J. Marhefka, W. D. Burnside, C. H. Walter, "Asymptotic High Frequency Techniques for UHF and Above Antennas," Report 784508-15, May 1979.

16. S. H. Lee and R. C. Rudduck, "Numerical Electromagnetic Code (NEC) - Reflector Antenna Code. Part II: Code Manual," Report 784508-16, September 1979.

17. R. Tiberio and R. G. Kouyoumjian, "An Analysis of Diffraction at Edges Illuminated by Transition Region Fields," Report 784508-17, September 1979.

18. R. J. Marhefka and W. D. Burnside, "Numerical Electromagnetic Code (NEC)-Basic Scattering Code. Part I: User's Manual," Report 784508-18, September 1979.

19. R. C. Rudduck, S. H. Lee, "Numerical Electromagnetic Code (NEC)-Reflector Antenna Code. Part I: User's Manual," Report 784508-19, September 1979.

20. R. C. Rudduck, R. J. Marhefka, W. D. Burnside, R. G. Kouyoumjian, C. H. Walter, "Asymptotic High Frequency Techniques for UHF and Above Antennas," Final Report 784508-20, September 1979.

TABLE I

REVISED MILESTONE CHART (04/12/78)

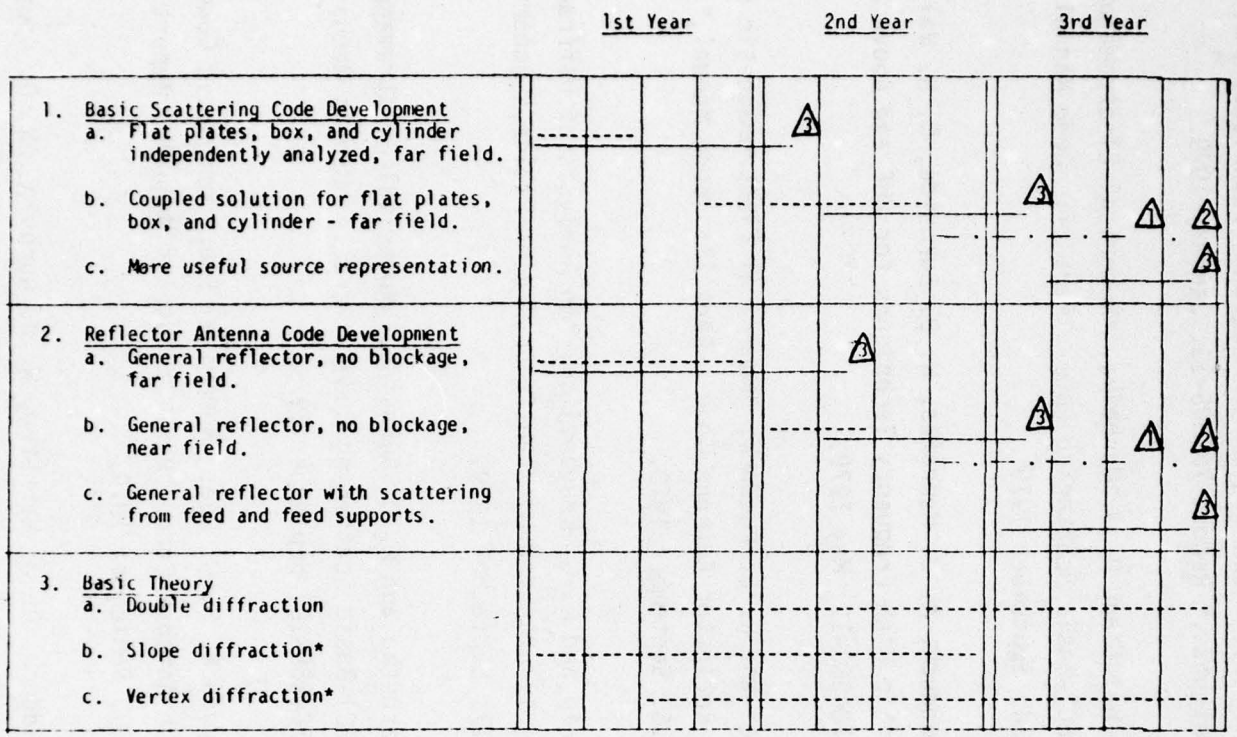

----- Theoretical development

——— Formulate algorithms and write and implement codes (including integration with NEC and User's Manual)

—·— Write Code Manual

*To be jointly supported by ONR Block Funding (Associate JSEP)

1 Rough Draft

2 Final Version

3 Computer Code Delivered to NOSC

III. BACKGROUND

The performance of shipboard communications and radar systems is dependent on the abilities of their antennas to operate effectively in a complex electromagnetic environment. System performance at UHF and above can be degraded by pattern distortion effects due to blockage and scattering by shipboard structures or by strong coupling between antennas[1]. In many cases, these detrimental effects can be minimized by the judicious location of the antennas. This task is complicated by the large number of systems that are used on a modern ship where many systems must compete for a limited number of prime antenna locations.

The two approaches that can be used for modeling shipboard antennas at UHF and above are scale model measurements and numerical modeling. In many ways these are complimentary techniques. Scale model measurements have the disadvantage of the cost and time required for a thorough design that will address all anticipated problems. It is very desirable to foresee as many problems as possible so that costly remedial solutions can be avoided. Numerical modeling, on the other hand, is a relatively cost effective and fast way of modeling the many possible situations that can arise in a shipboard environment. Measurements need be made only when necessary for confirmation of results.

Two user oriented computer codes have recently been developed in order to allow the analysis of far field pattern distortion effects of the ship's structure on an antenna's performance at UHF and above: the NEC Basic Scattering Code and the NEC Reflector Antenna Code. The development of these codes has been accomplished by the use of the Geometrical Theory of Diffraction (GTD)[2,3,4]. The GTD has been successfully applied to many types of complex modeling problems in the past[5,6,7]. It is a high frequency technique that allows a complicated structure to be approximated by basic shapes representing canonical problems in the GTD. These canonical solutions include the diffraction at flat and curved wedges and the scattering from convex curved surfaces.

IV. BASIC SCATTERING CODE

A. Features of the Code

The NEC Basic Scattering Code can be used to simulate many practical scattering problems by using basic shapes to model the major scattering features of a complex environment, such as those encountered on a ship. The basic shapes included in the code allow the analysis of scattering structures that can be modeled by perfectly conducting convex and concave flat plate structures, and a finite elliptic cylinder. The basic scattering shapes can be arbitrarily positioned in space to form the various ship structures in the immediate environment of the antenna under analysis. For example, the flat plates can be fashioned into box-like shapes that represent the ship's superstructure, platforms, yardarms, etc. The finite elliptic cylinder can be used to represent smoke stacks, masts, etc. An example is illustrated in Figure 1.

The scattering structures are assumed to be large in terms of a wavelength. The general rule is that the lower frequency limit of this solution is dictated by the spacing between the various scattering centers and their overall size. In practice, this means that the smallest dimensions should be on the order of a wavelength. This can often be relaxed to approximately a quarter-wavelength. The upper limit on the frequency is dictated by the fine structural details that can be modeled by the basic scattering shapes available. The antenna is assumed to be in the near field of the scattering structures, but the scattering centers are assumed to be in the far field of the antennas. The observer is assumed to be in the far field of the structures, thus the scattered rays are all parallel leaving the structure in the direction of the observer.

The basic scattering code is capable of analyzing a wide range of antennas since it is basically a Green's function type solution, that is, the solution has been developed for infinitely small current elements. If the current distribution of an antenna is known, such as from the NEC

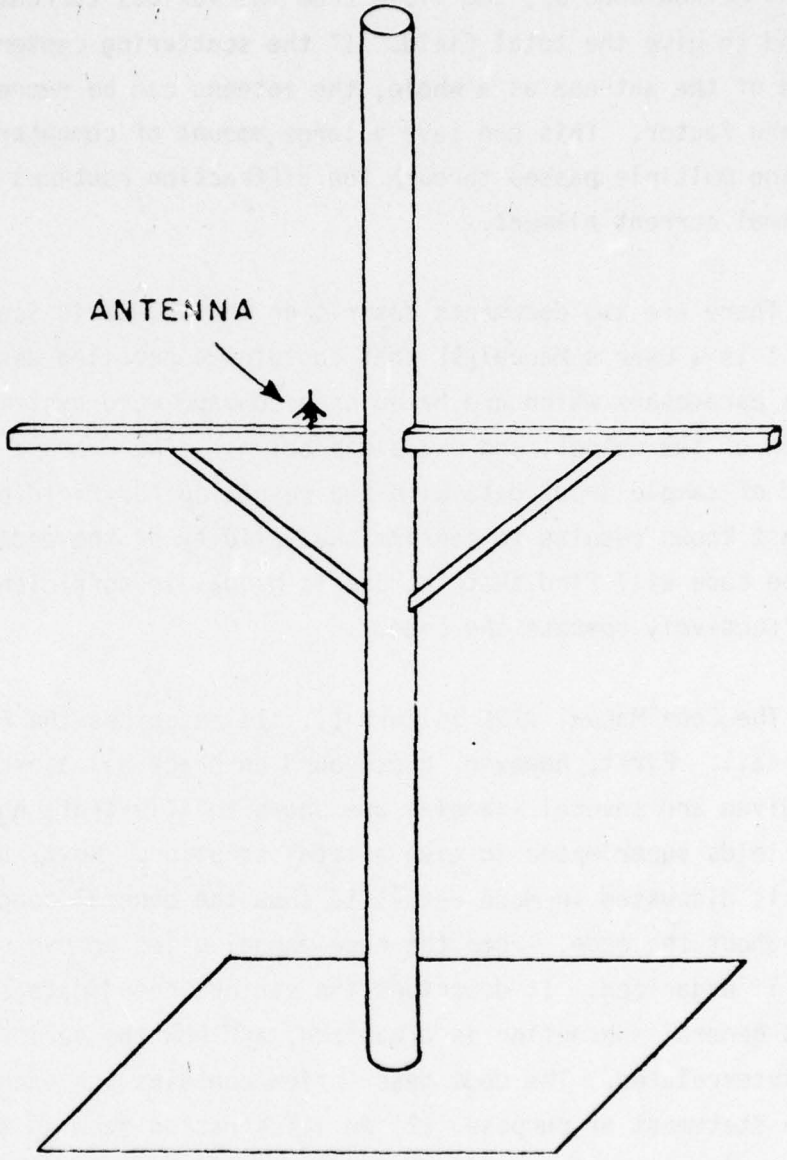

Figure 1. Example of an antenna in a typical shipboard environment.

Moment Method Code[8], the field from the various current segments can be summed to give the total field. If the scattering centers are in the far field of the antenna as a whole, the antenna can be represented by its pattern factor. This can save a large amount of computer time by eliminating multiple passes through the diffraction routines for each infinitesimal current element.

There are two documents describing the NEC-Basic Scattering Code. Part I is a User's Manual[9] that contains a detailed description of the input parameters which are based on a command word system, an interpretation of the output, and example problems. The example problems are composed of sample input data with the resulting far field patterns compared against known results to confirm the validity of the code. Most users of the code will find that the User's Manual is sufficient to learn how to effectively operate the code.

The Code Manual [10] is Part II. It describes the FORTRAN coding in detail. First, however, background on practical aspects of the GTD are given and several examples are shown to illustrate how the various GTD fields superimpose to give a total solution. Next, a particular GTD term is discussed in more detail to show the general concepts involved throughout the code. Then the code manual gives an overview on how the code is organized. It describes the various coordinate systems involved, how a general subroutine is organized, and how the various subroutines are interrelated. The code description contains for each subroutine: (1) a statement of purpose, (2) an illustration showing the geometry involved, (3) a brief narrative on the method used, (4) a flow diagram, (5) a dictionary of major variables, (6) a listing of the code. Finally the common blocks are defined and system library functions used by the code are listed.

The information in the Code Manual will be of primary interest to someone attempting to modify the code. It will also be helpful when the code is being implemented on a computer system on which the coding may not be compatible.

The basic scattering code has been very much in demand during its development. The agencies to which various generations of the code have been sent by The Ohio State University are listed below. The first generation of the code was sent to the following:

- Westinghouse (Baltimore, Maryland)
- Electronic Communications, Inc. (St. Petersburg, Florida)
- Naval Research Laboratory (Washington, D.C.).

The second generation of the code was sent to the following:

- Martin Marietta Corp. (Denver, Colorado)
- Atlantic Research Corp. (Rome, New York)
- H. R. B. Singer (State College, Pennsylvania)

The third generation of the code was sent to the following:

- Naval Post Graduate School (Monterey, California)
- Harris Corp. (Melbourne, Florida)
- Boeing Corp. (Seattle, Washington)
- General Dynamics (San Diego, California)
- Andrew Corp. (Chicago, Illinois)
- Ohio University (Athens, Ohio)
- Naval Weapons Center (China Lake, California).

B. Example Results

The NEC Basic Scattering Code, with all of the capabilities mentioned above, is applicable to a wide range of practical problems. Of course, with such a general code not all possible situations can be anticipated a priori. Every effort has been made to include the dominant scattering mechanisms that could be cost-effectively added to the code to give a good engineering answer. In order to show the versatility of the code and to test its accuracy a large number of example problems were run and compared with measurements over a wide range of geometries. Many of these results are included in the User's Manuals [9]. The code's results have been tested

against measurements made at OSU and whenever possible, they have been tested against measurements made at other facilities or against results found in the literature.

For example, the basic scattering code has been checked against measurements made by Bach [11] on a variety of satellite shapes. The code's calculated results for a dipole in the presence of an eight sided box as illustrated in Figure 2, is compared against measurements in Figure 3. The calculated results for various locations about a finite circular cylinder as shown in Figures 4 a, b, and c, are compared against measurements in Figures 5 a, b, and c, respectively. In all cases the agreement is very good, confirming the validity of the basic scattering code's results. The small discrepencies that exist between the patterns can be contributed to measurement inaccuracies and to the lack of double diffraction effects in both the geometries and, in the case of the cylinder, to the pseudo caustic caused by the coalescence of rays on the endcap rims.

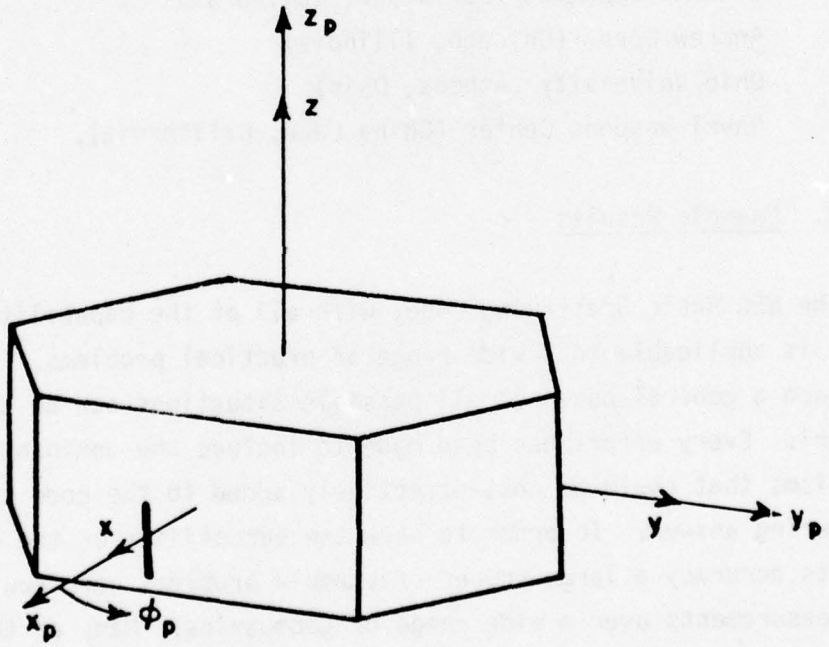

Figure 2. Electric dipole in the presence of an eight sided box.

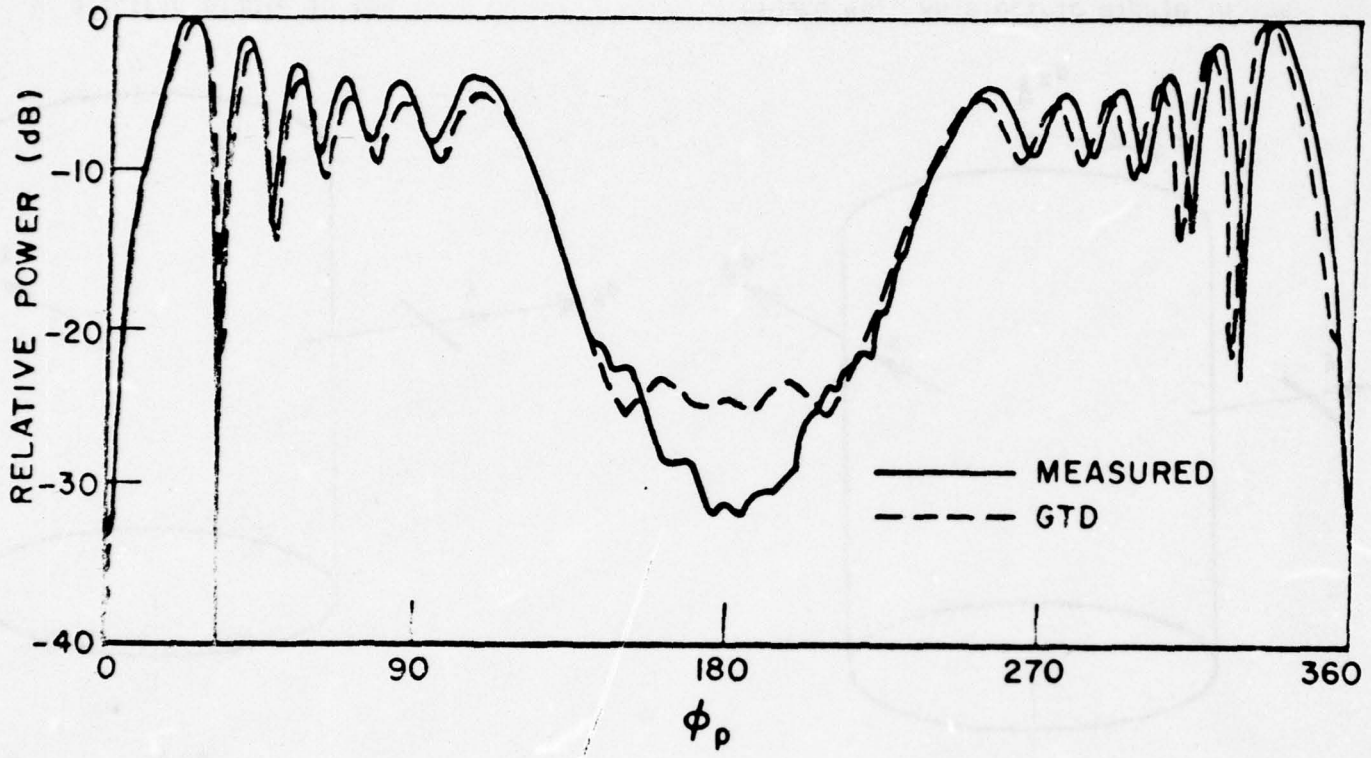

Figure 3. Comparison of measured (Bach) and calculated radiation pattern for $E_{\theta p}$ for an electric dipole in the presence of an eight sided box.

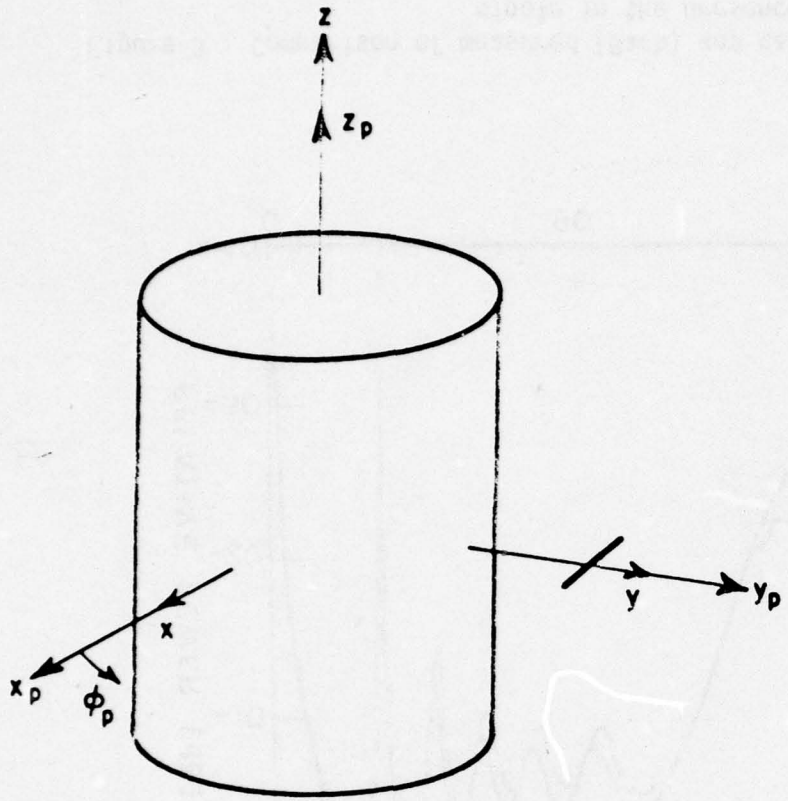

Figure 4a. An electric dipole in the presence of a finite circular cylinder (pattern taken in x-y plane).

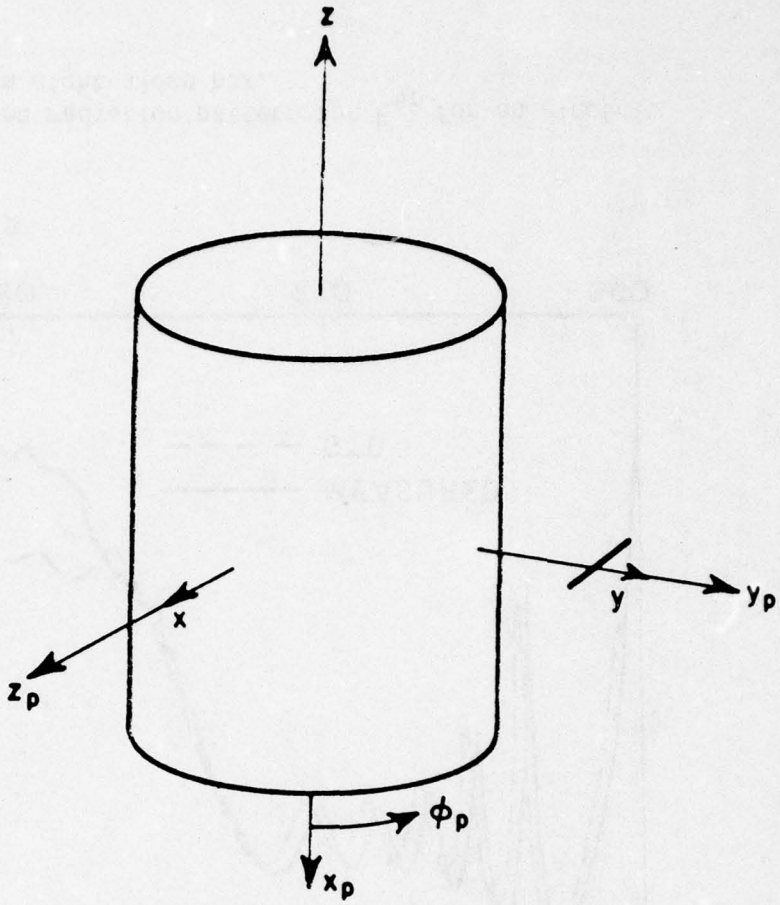

Figure 4b. An electric dipole in the presence of a finite circular cylinder (pattern taken in y-z plane).

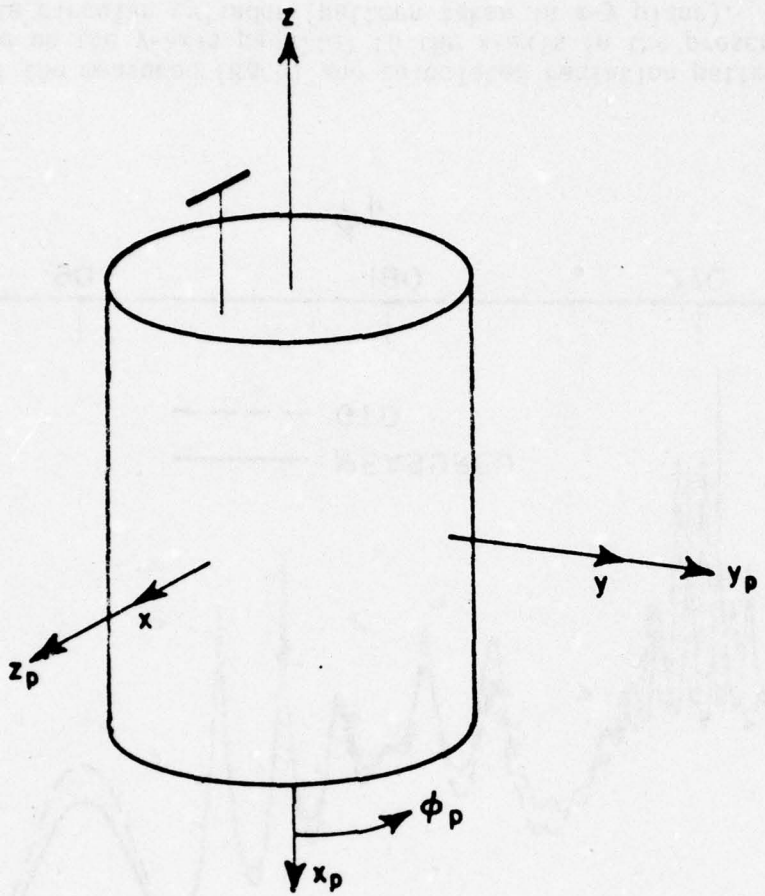

Figure 4c. An electric dipole in the presence of a finite circular cylinder (pattern in the y-z plane).

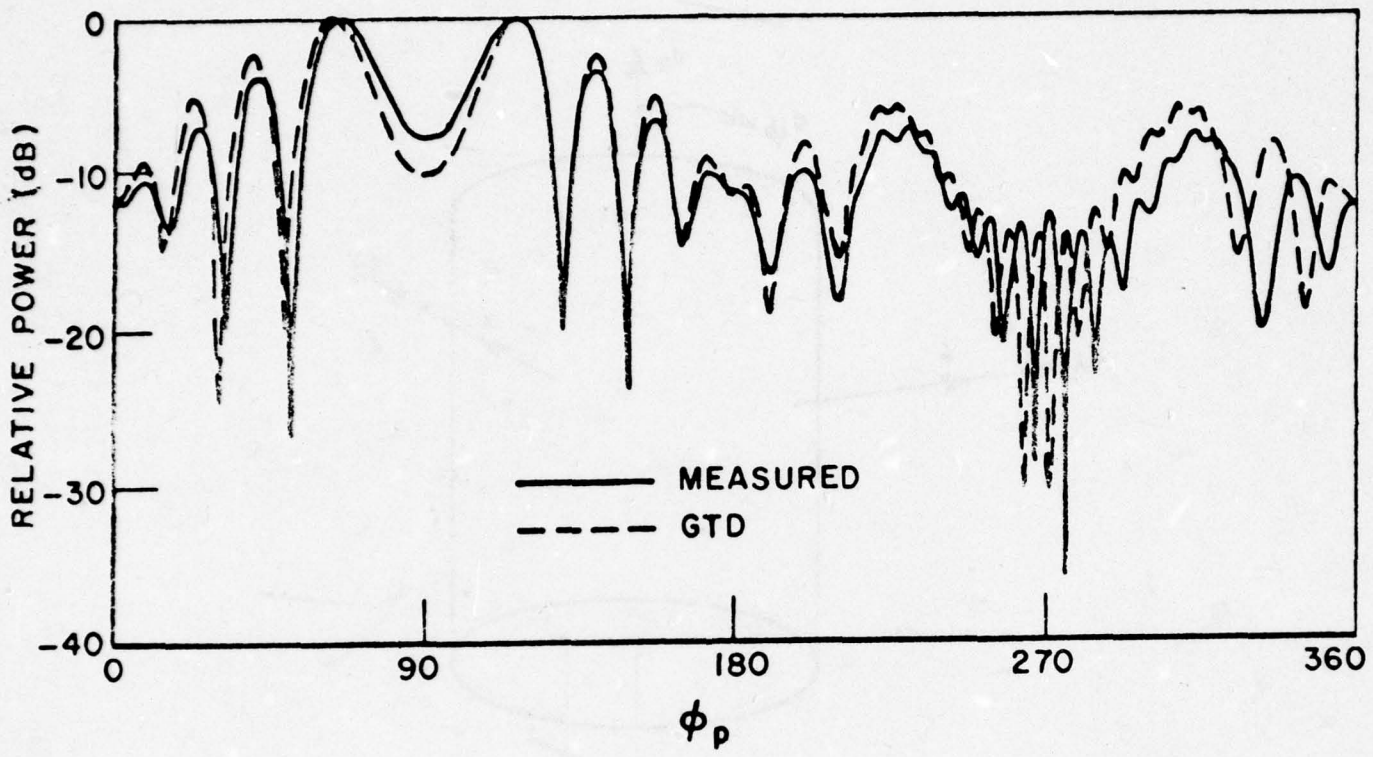

Figure 5a. Comparison of the measured (Bach) and calculated radiation pattern for $E_{\phi p}$ of an electric dipole on the y-axis parallel to the x-axis in the presence of a finite circular cylinder (pattern taken in x-y plane).

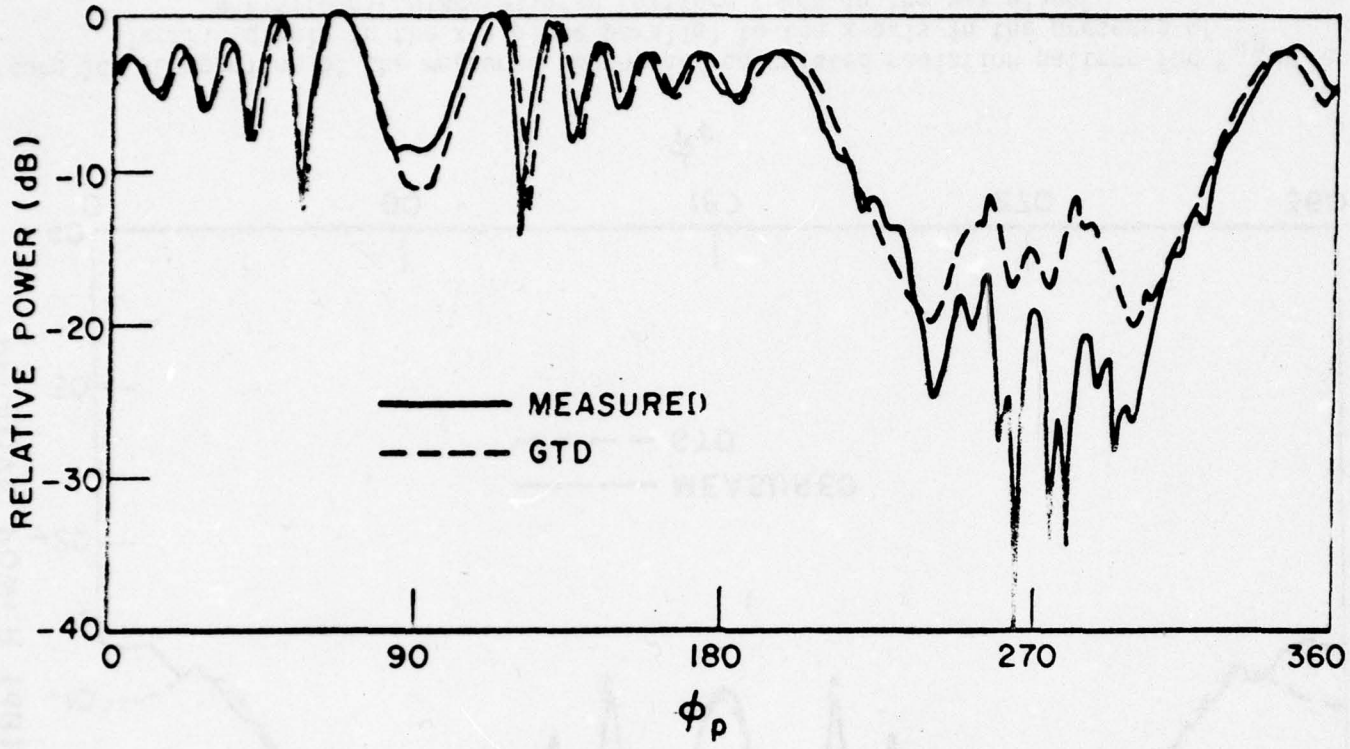

Figure 5b. Comparison of the measured (Bach) and calculated radiation pattern for $E_{\theta p}$ of an electric dipole on the y-axis parallel to the x-axis in the presence of a finite circular cylinder (pattern taken in y-z plane).

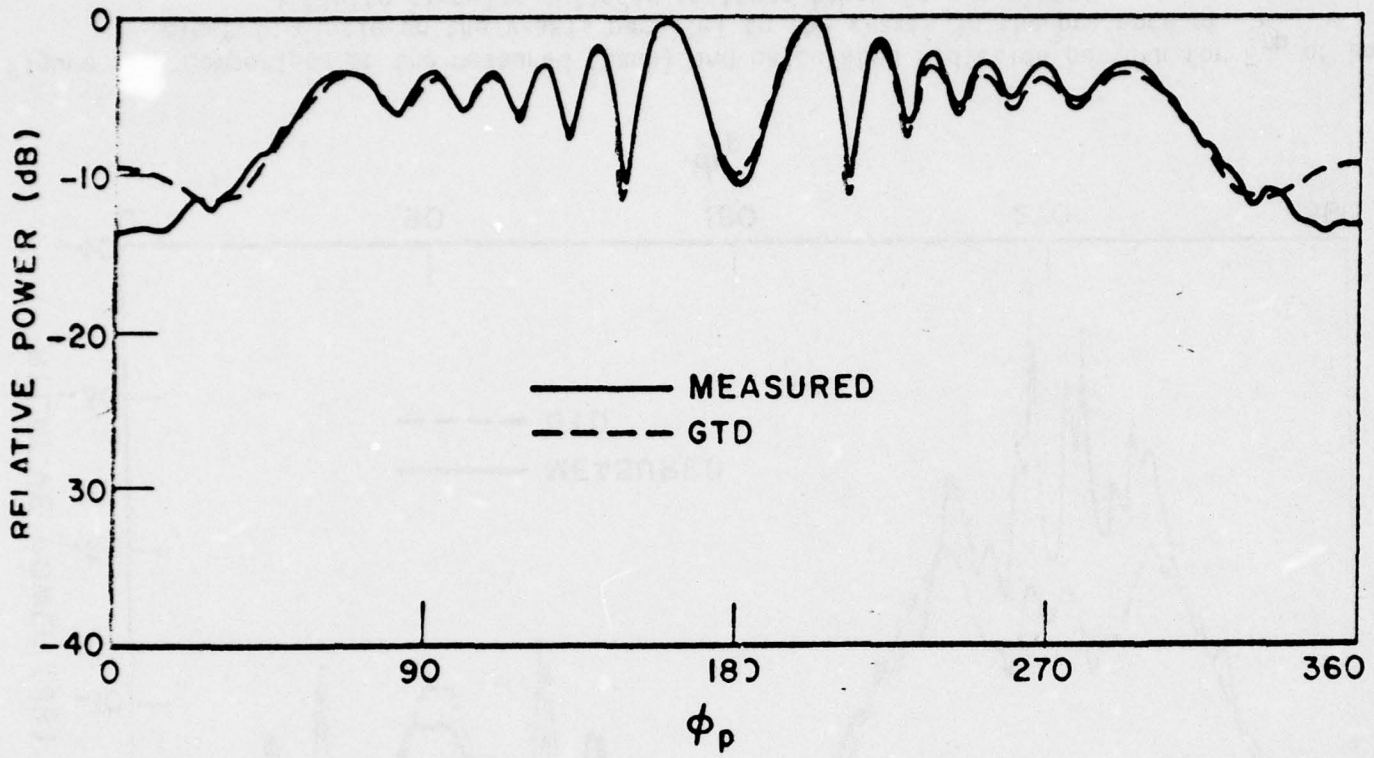

Figure 5c. Comparison of the measured (Bach) and calculated radiation pattern for $E_{\theta p}$ of an electric dipole in the x-z plane parallel to the x-axis in the presence of a finite circular cylinder (pattern taken in the y-z plane).

The two geometries considered above are composed of either plates alone or a finite cylinder by itself. In order to test a problem containing both a plate and a finite cylinder a series of measurements were made at OSU on a simplified geometry that resembles a situation that may arise on shipboard. The geometry is shown in Figure 6. This is a very difficult problem because of the multiple bounces of the fields that can occur between the plate and the cylinder. This, however, illustrates the engineering solution that can be obtained using the scattering code. For comparison purposes, the separate pieces are first studied individually. The calculated and measured patterns of the half-wavelength dipole are compared in Figure 7a. The results for the square plate are compared against measurements in Figure 7b. The results for the finite circular cylinder are shown in Figure 7c. In all of these three cases the comparisons are quite good. The radiation pattern of the dipole in the presence of both the plate and the cylinder is compared to the calculated result in Figure 7d. This result contains five plate-cylinder interaction fields. It can be noted that the levels are good and that the fine details have the right trends. This verifies that the code can provide good engineering answers to rather difficult problems.

The examples shown above verify the ability of the code to model general type shapes. The following examples illustrate how the code can be used to model antennas of particular interest to the shipboard antenna designer. The first is for an AS-2410/WSC-1 antenna. The geometry used to model this antenna is illustrated in Figure 8. The currents on the dipole elements of the antenna were obtained from the NEC moment method code by Mr. Jim Logan of NOSC.

First, in order to test the compatibility of the two codes for exactly the same situation, a simpler problem was used. This is composed of four quarter wavelength dipoles over an infinite ground plane. The

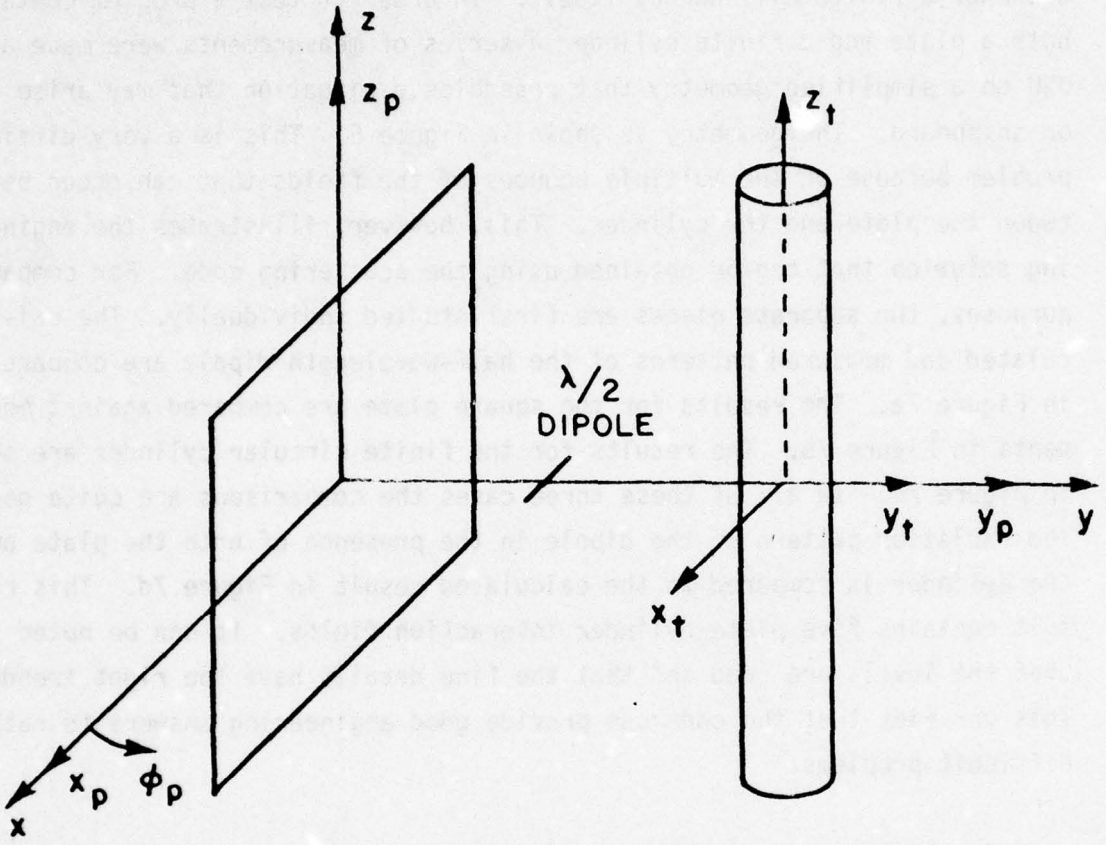

Figure 6. A λ/2 dipole in the presence of a square plate.

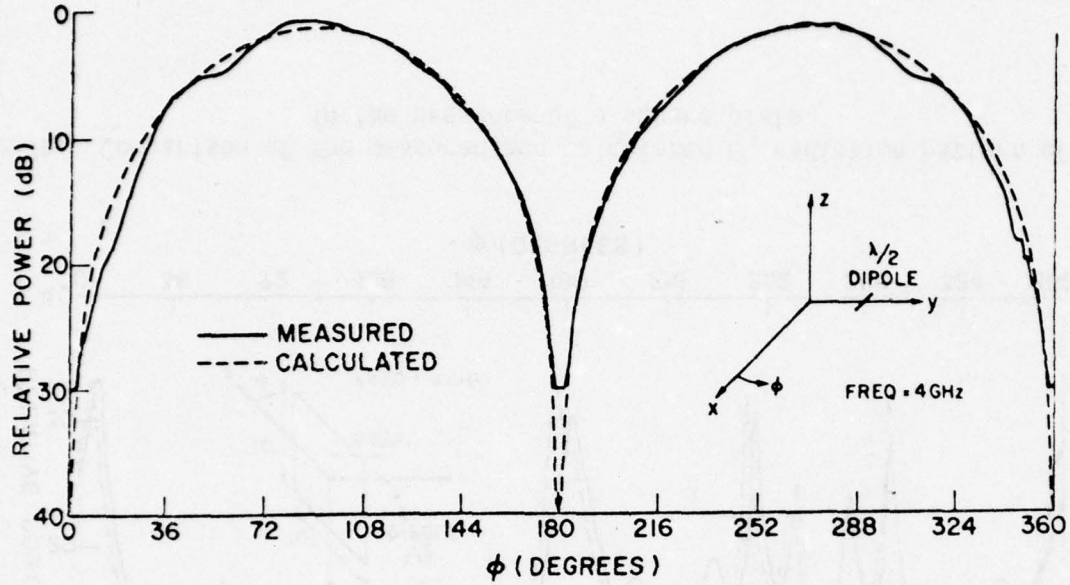

Figure 7a. Comparison of the measured and calculated E_ϕ radiation pattern of a $\lambda/2$ dipole.

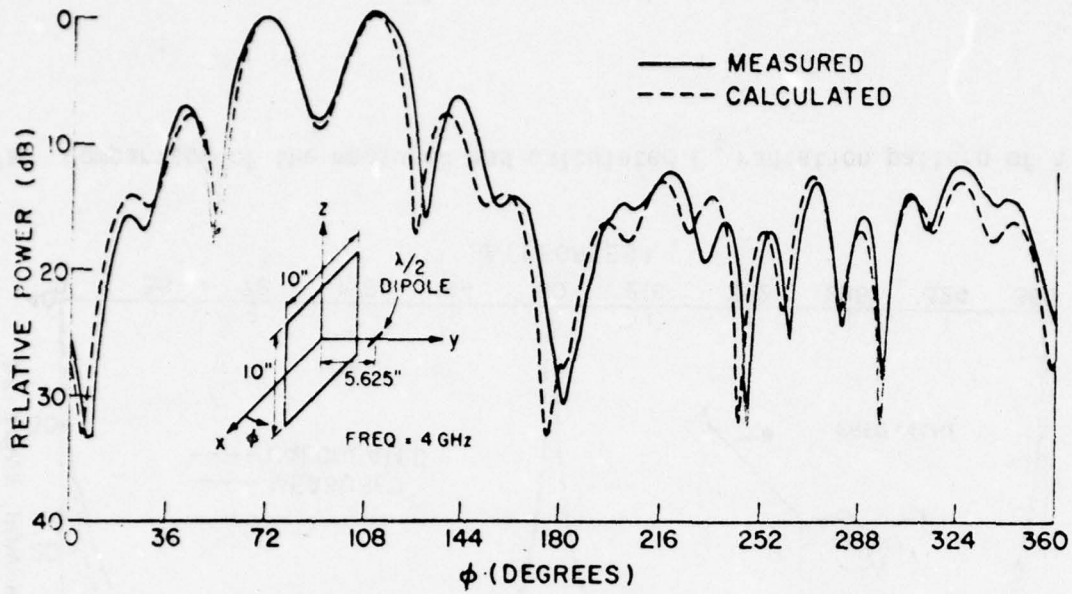

Figure 7b. Comparison of the measured and calculated E_ϕ radiation pattern of a dipole in the presence of a square plate.

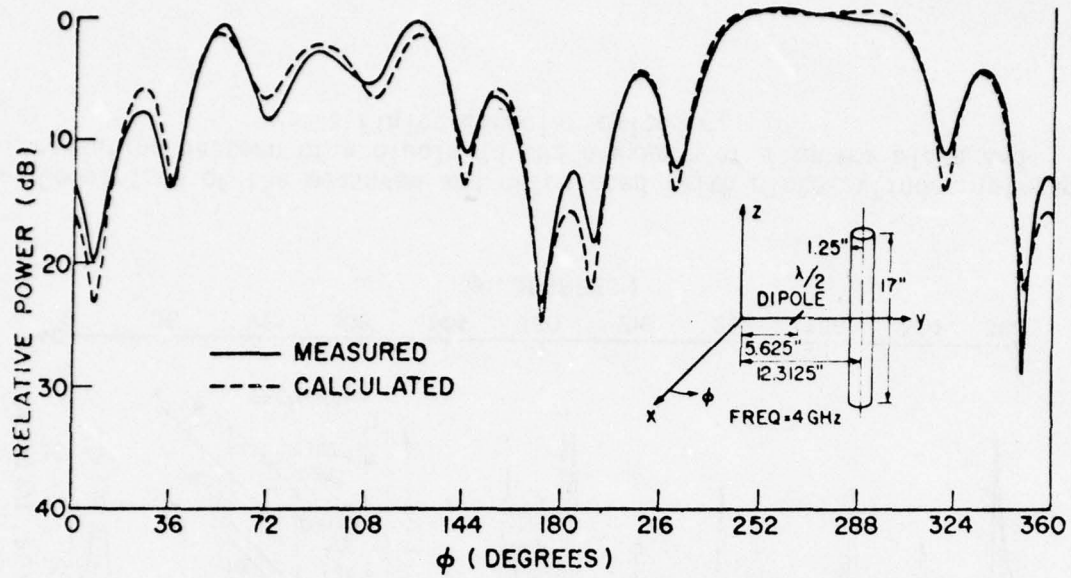

Figure 7c. Comparison of the measured and calculated E_ϕ radiation pattern of a dipole in the presence of a finite circular cylinder.

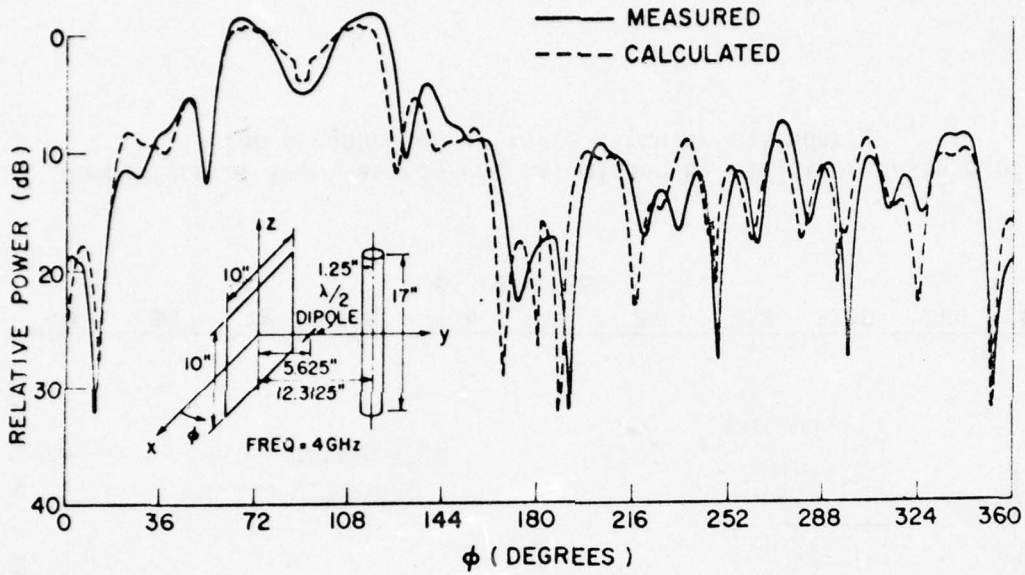

Figure 7d. Comparison of the measured and calculated (with plate-cylinder interactions) E_ϕ radiation pattern of a dipole in the presence of a square plate and a finite circular cylinder.

four dipoles are shown in Figure 8 as the solid lines parallel to the x-axis. The infinite ground plane for this case is coincident with the square plate. The dipoles were broken into a total of 20 segments and the frequency was 0.2998 GHz. The far zone fields obtained from the moment method code and the fields obtained using the moment method current weights in the basic scattering code are compared in Figures 9 a and b for the planes $\phi=0^{o}$ and $\phi=90^{o}$, respectively. The basic scattering code calculations for the directive gain is within 0.2 dB of the moment method results confirming the compatibility of the two codes.

Next, to show how the directive gain changes when the four dipoles are placed over a square plate over an infinite ground plane as shown in Figure 8, the same moment method current weights are used in the basic scattering code. It is assumed that the current distribution obtained for the infinite ground plane case will not be perturbed appreciably by slightly changing the environment. The comparisons between the infinite ground plane and the square plate cases are shown in Figures 10 a and b for the two pattern planes.

For the case of the crossed dipoles of the WSC-1 antenna of Figure 8, the dipoles were broken into a total of 48 segments at a frequency of 0.25 GHz. The far zone fields for the crossed dipoles over an infinite ground plane obtained from the moment method (AMP) code and the basic scattering code are compared in Figures 11 a and b. Figure 11a shows the vertical component and Figure 11b the horizontal component of the circularly polarized field. Again the two results compared to within 0.2 dB. The square plate results are also shown in Figures 12 a and b for the $\phi=0^{o}$ and $\phi=45^{o}$ planes, respectively. Again these results confirm the compatibility of the NEC moment method and basic scattering codes.

A few measurements for the WSC-1 antennas are available from NOSC [1]. The simple model of the WSC-1 antenna in Figure 8 is used along with an analytic representation of the 8 dipoles to compare with a measured

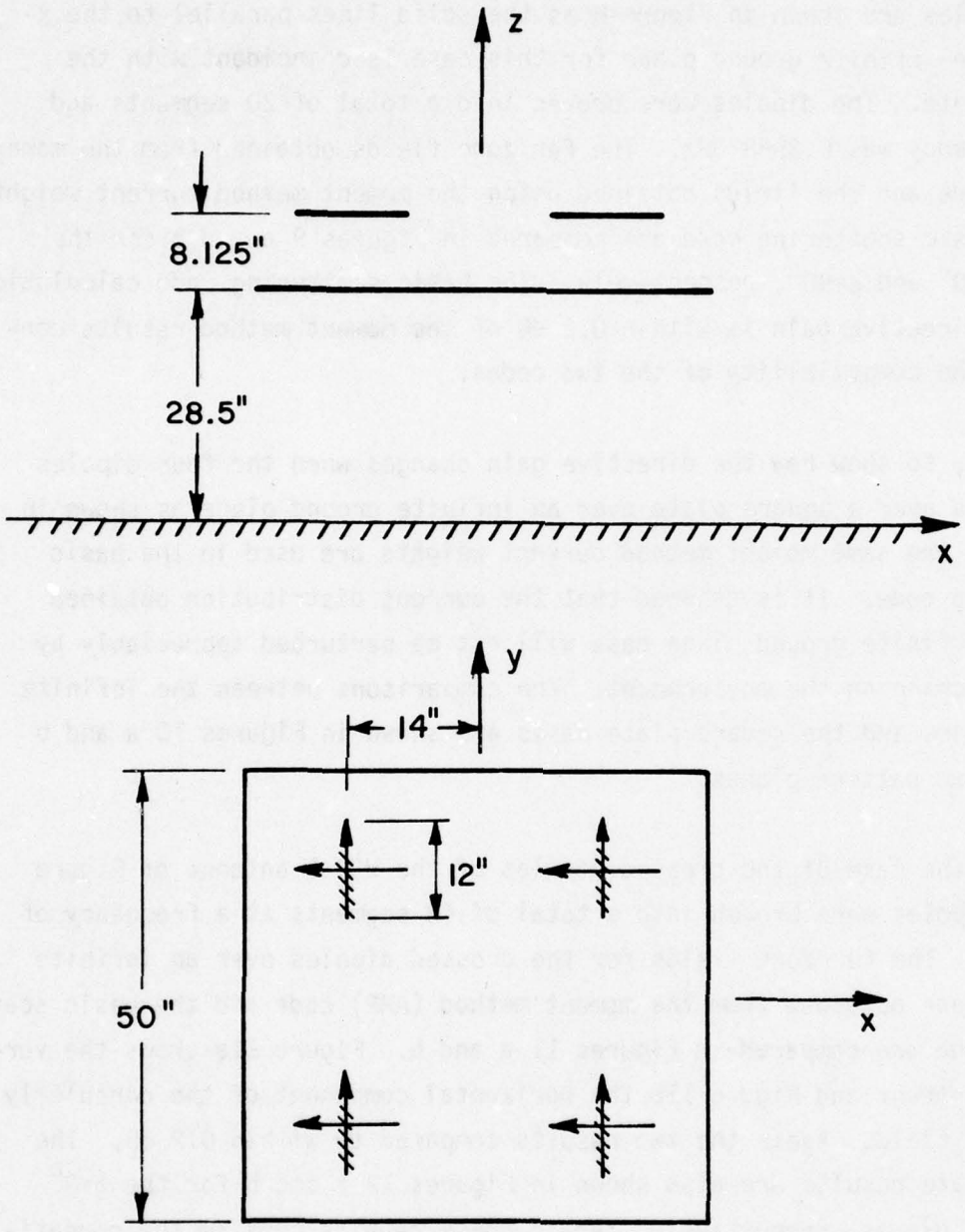

Figure 8. Geometry for the problems of dipoles over a square plate and infinite ground plane showing the side and top views.

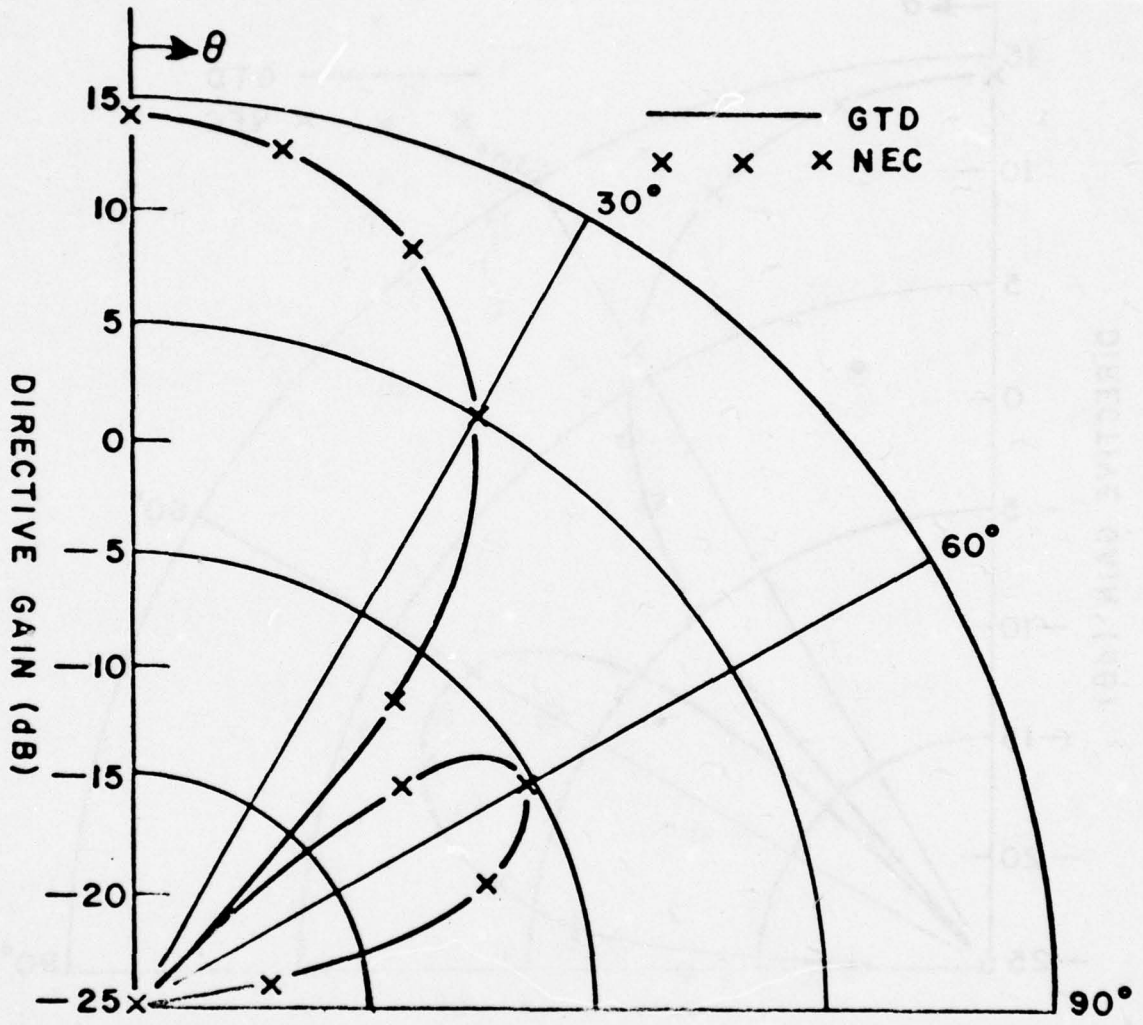

Figure 9a. Comparison of the directive gain of four dipoles over an infinite ground plane obtained from the NEC moment method code and from the basic scattering code using the moment method currents ($\phi=0^0$ vertical polarization).

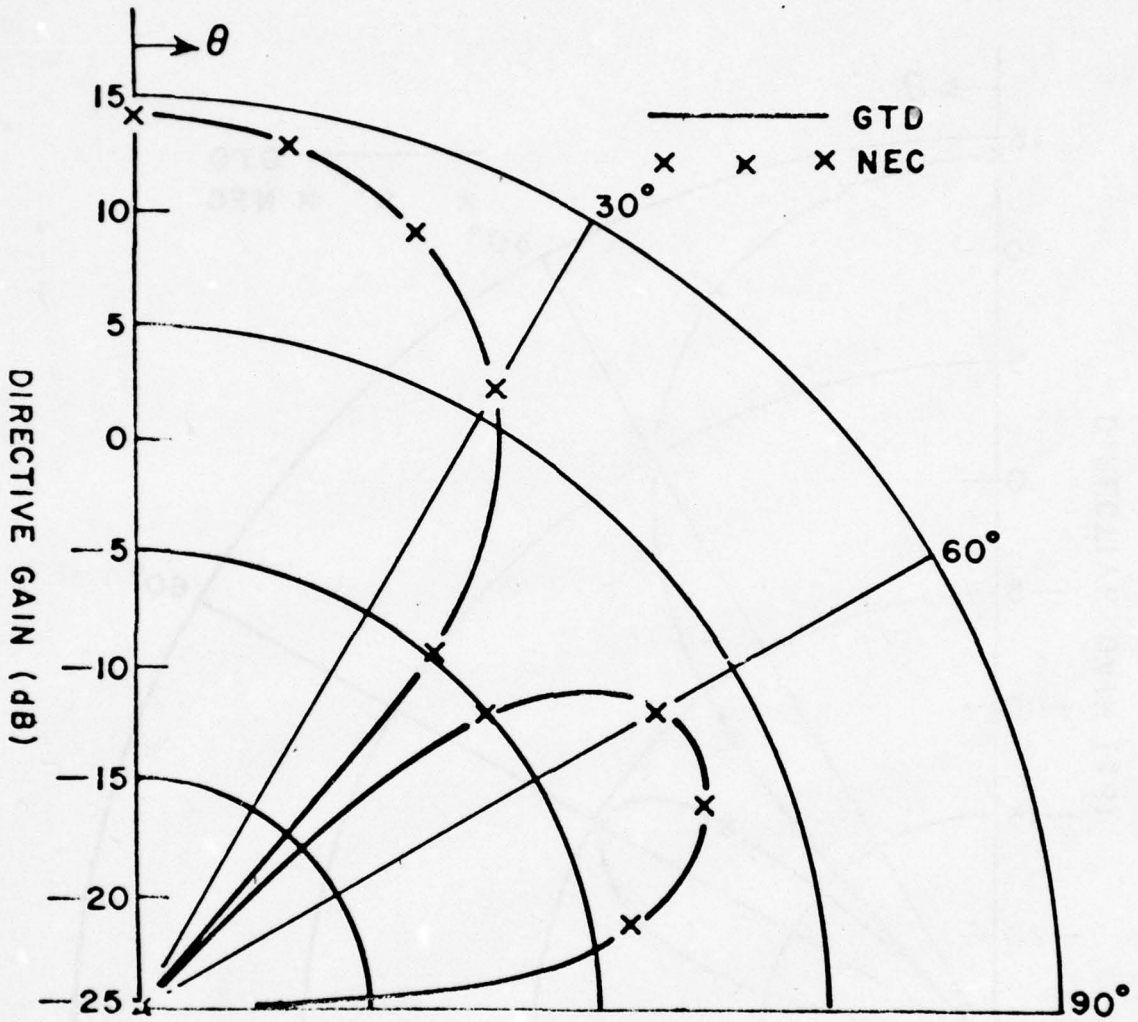

Figure 9b. Comparison of the directive gain of four dipoles over an infinite ground plane obtained from the NEC moment method code and from the basic scattering code using the moment method currents (ϕ=90^0 horizontal polarization).

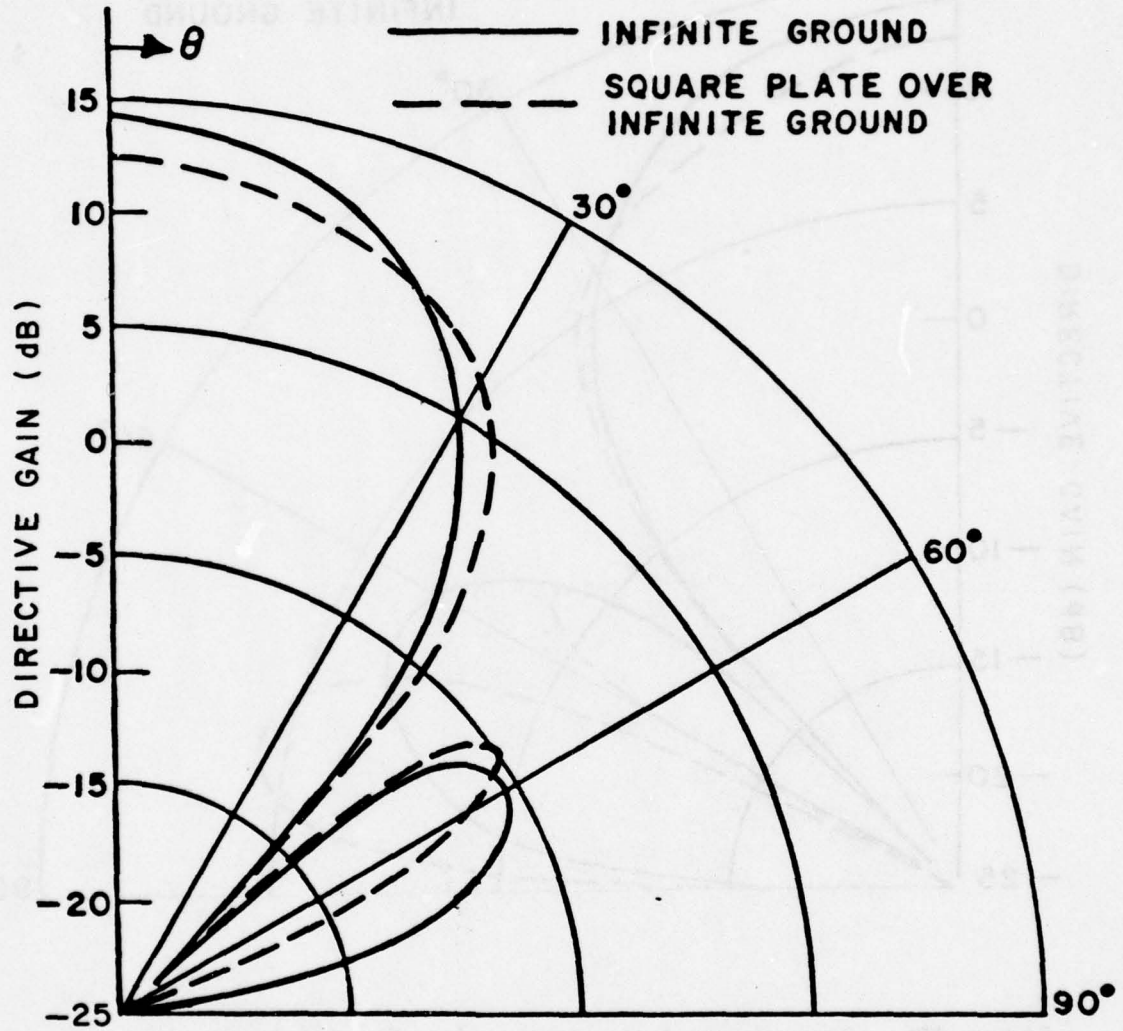

Figure 10a. Comparison of the directive gain of four dipoles over an infinite ground with four dipoles over a square plate over an infinite ground plane ($\phi=0^{o}$, vertical polarization).

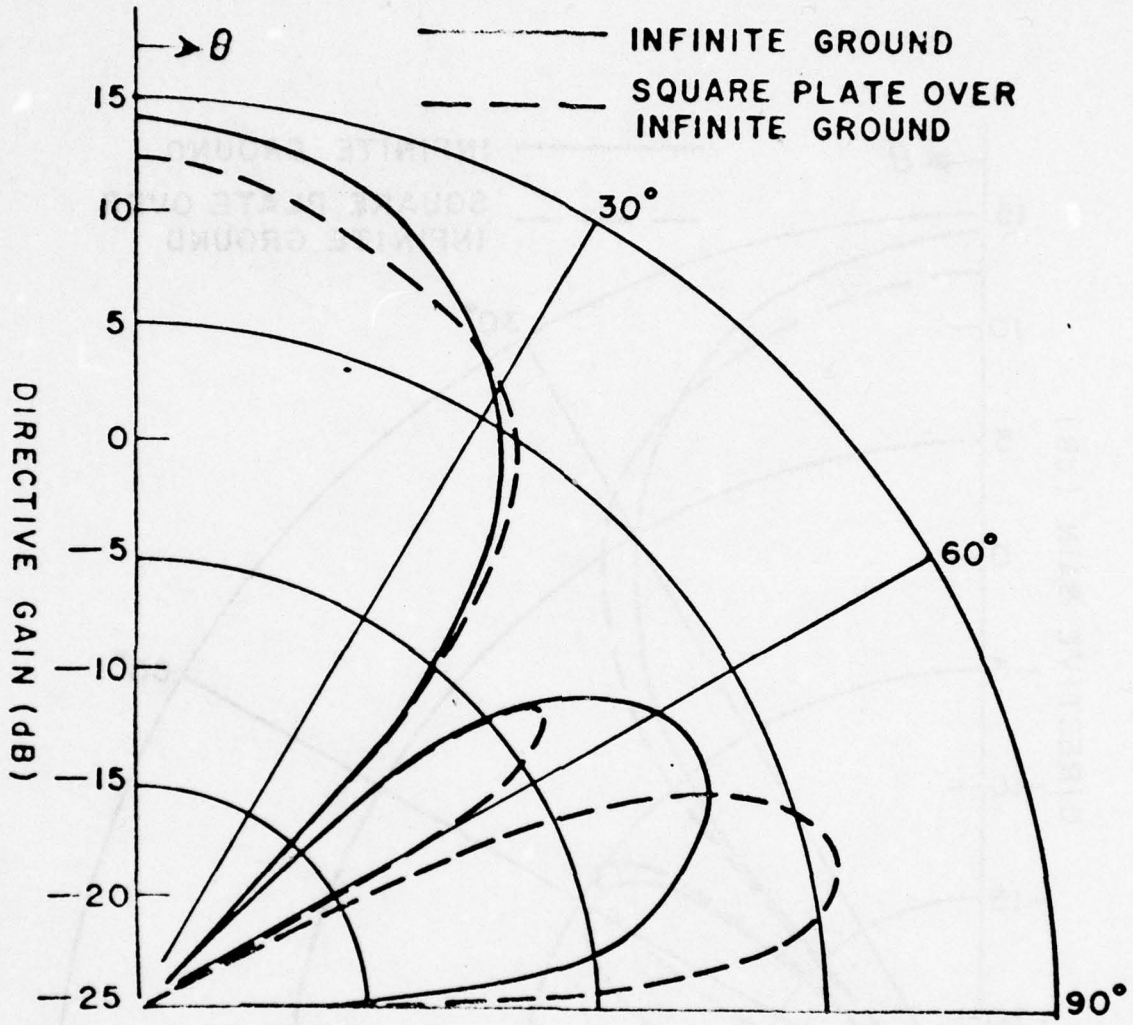

Figure 10b. Comparison of the directive gain of four dipoles over an infinite ground with four dipoles over a square plate over an infinite ground plane (ϕ=90^{0}, horizontal polarization).

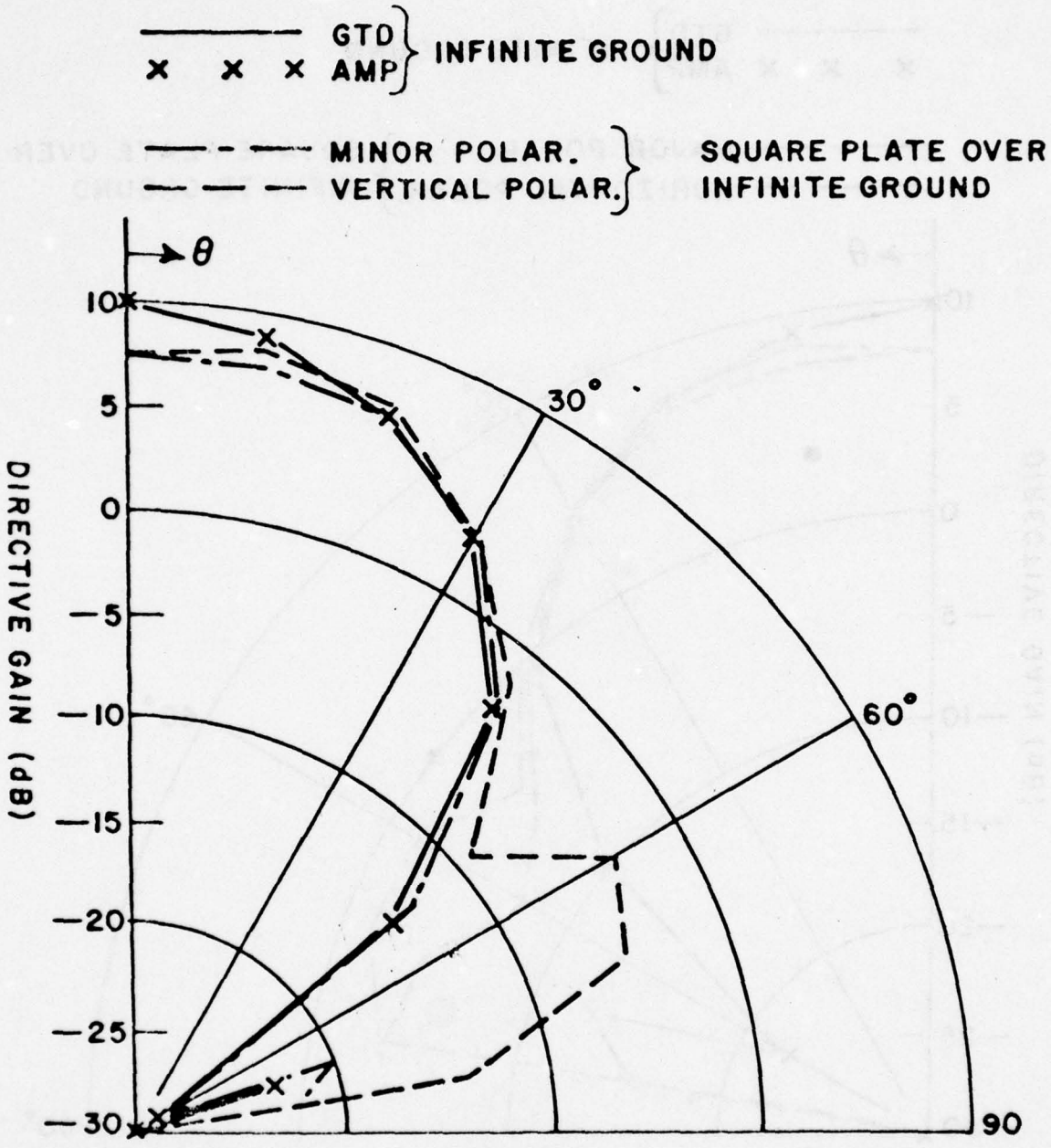

Figure 11a. Comparison of the directive gain of four sets of crossed dipoles over an infinite ground and over a square plate over an infinite ground ($\phi=0^{o}$, vertical polarization).

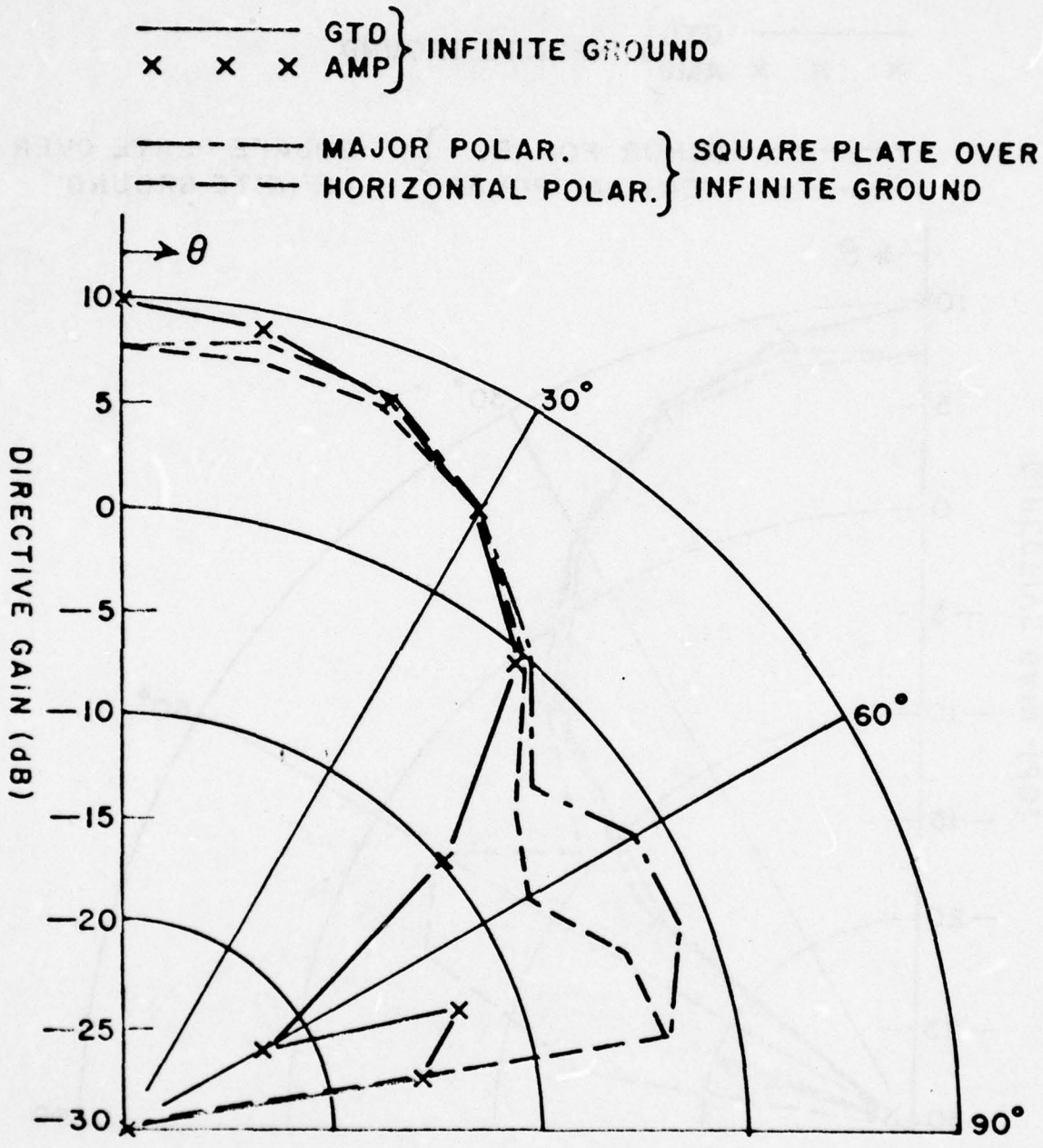

Figure 11b. Comparison of the directive gain of four sets of crossed dipoles over an infinite ground and over a square plate over an infinite ground ($\phi=0^{o}$, horizontal polarization).

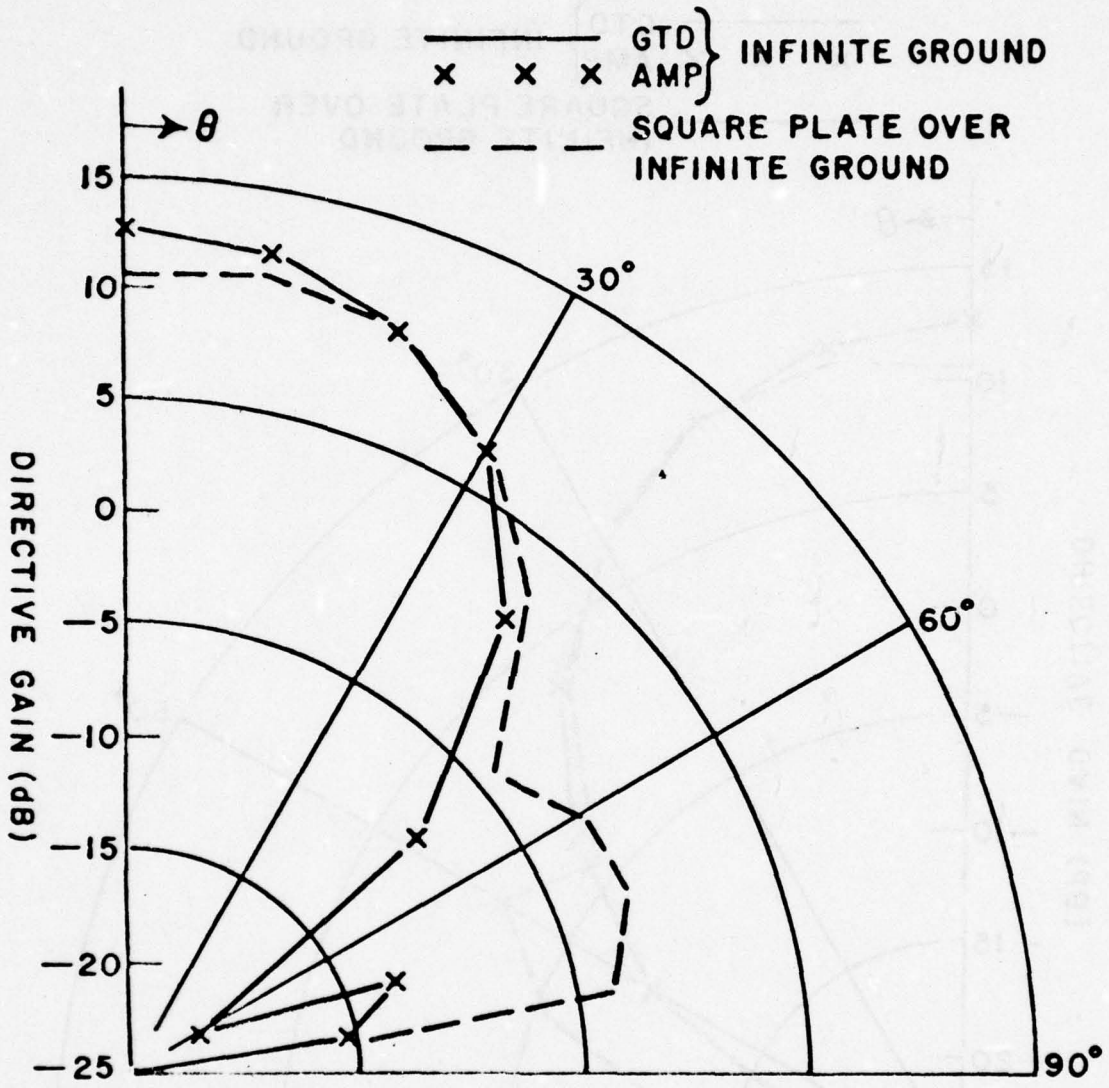

Figure 12a. Comparison of the total directive gain of four sets of crossed dipoles over an infinite ground and over a square plate over an infinite ground ($\phi=0^{o}$).

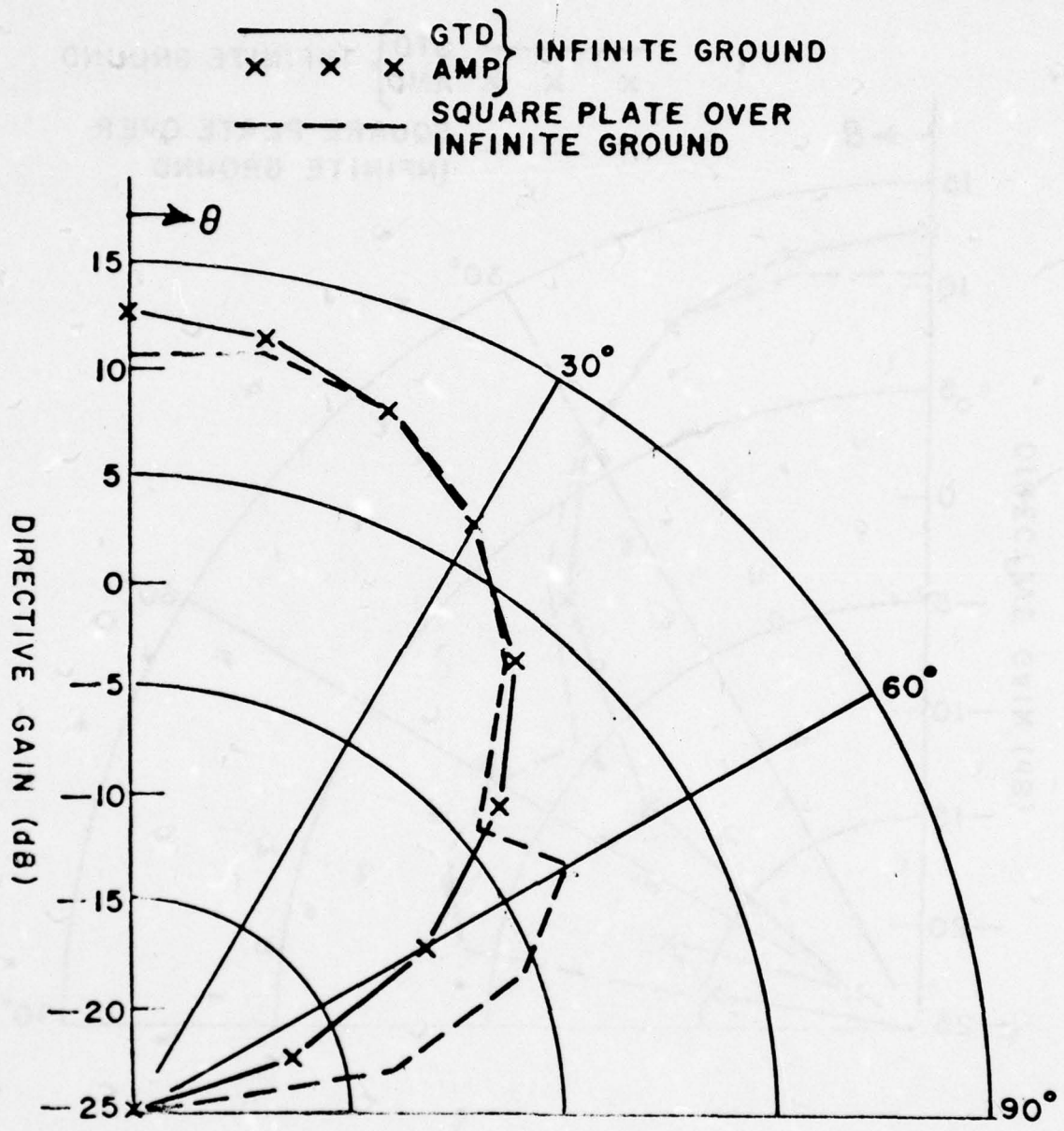

Figure 12b. Comparison of the total directive gain of four sets of crossed dipoles over an infinite ground and over a square plate over an infinite ground ($\phi=45^{o}$).

pattern from a full scale model. The analytic representation of the dipole is used to save computer time. The results for the E_θ component of the circularly polarized field are compared in Figure 13. The frequency is 0.250 GHz and the antenna is pointed at $\theta=0^o$ (90^o elevation).

This same model is used to compare against measured results from a 1/10 scale model [1]. The results for the circularly polarized field (total field) and compared in Figures 14 a, b and c for the antenna pointed at $\theta=0^o$, 30^o, and 60^o (90^o, 60^o and 30^o elevation), respectively. The full scale frequency is 0.320 GHz. The basic feature of the patterns in all of these comparisons are good. However, the secondary lobes are off slightly. This may be due to the simplified model used to calculate the results using the basic scattering code along with normal experimental errors. For example, it is difficult to simulate circularly polarized antennas because the low level fields depend on the precise phasing. The model used for the computations can be greatly improved if more details are known about the experimental models and set up. For example, the polarization of the pattern could be more closely matched if more details of the receiving antenna are known. Also, the model of the antenna could be improved by adding more detail, such as using a circular cylinder to represent the antenna pedestal and using more plates to model the back plate, etc. These capabilities are in the code but the necessary information was not readily available.

The second example is for an AS-1735/SRC antenna. The geometry used to model this antenna is illustrated in Figure 15. It is composed of four dipoles mounted around a mast and is used to provide an omnidirectional pattern in azimuth [12]. This antenna is to operate over the frequency range of 0.225-0.46 GHz. This means that for a mast of 5.5 inches in radius, the electrical size varies from 0.10-0.19 wavelengths in radius and the dipoles are mounted 0.17-0.29 wavelengths off the surface. In general,

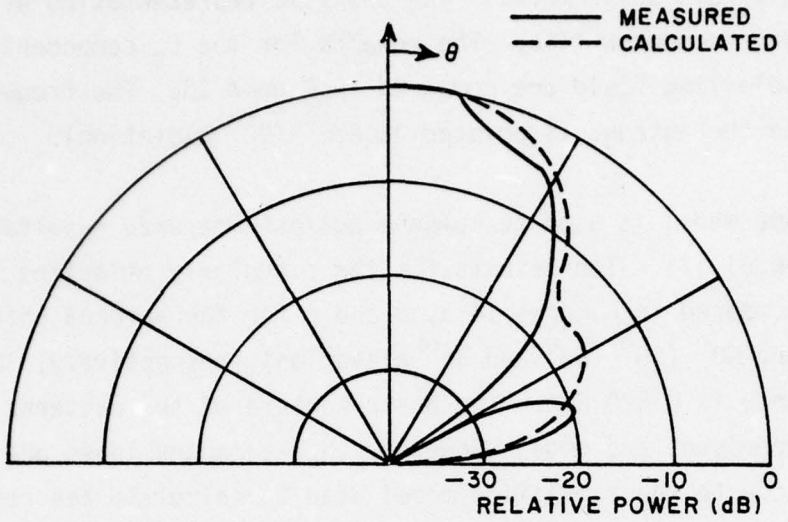

Figure 13. Comparison of the measured and calculated E_θ patterns for the WSC-1 antenna. The calculated result is from the NEC-Basic Scattering Code. The measurements were made on a full scale model at NOSC[1]. The antenna is pointed at $\theta=0^o$ (90^o elevation).

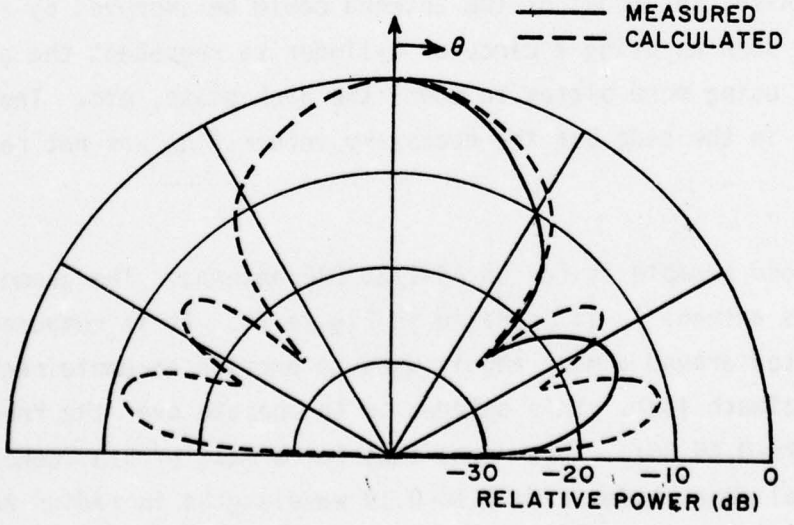

Figure 14a. Comparison of the measured and calculated circularly polarized pattern for the WSC-1 antenna. The calculated result is from the NEC-Basic Scattering Code. The measurements were made on a 1/10 scale model at NOSC[1]. The antenna is pointed at $\theta=0^o$ (90^o elevation).

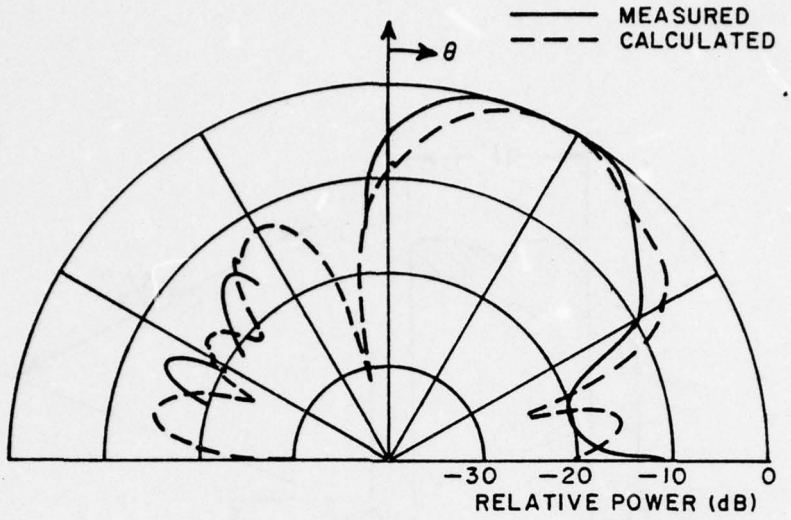

Figure 14b. Comparison of the measured and calculated circularly polarized pattern for the WSC-1 antenna. The calculated result is from the NEC-Basic Scattering Code. The measurements were made on a 1/10 scale model at NOSC[1]. The antenna pointed at $\theta=30^{0}$ (60^{0} elevation).

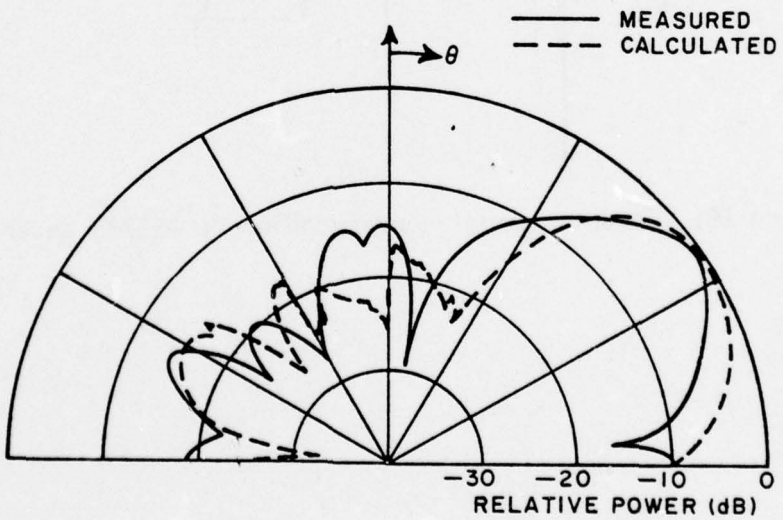

Figure 14c. Comparison of the measured and calculated circularly polarized pattern for the WSC-1 antenna. The calculated result is from the NEC-Basic Scattering Code. The measurements were made on a 1/10 scale model at NOSC [1]. The antenna is pointed at $\theta=60^{0}$ (30^{0} elevation).

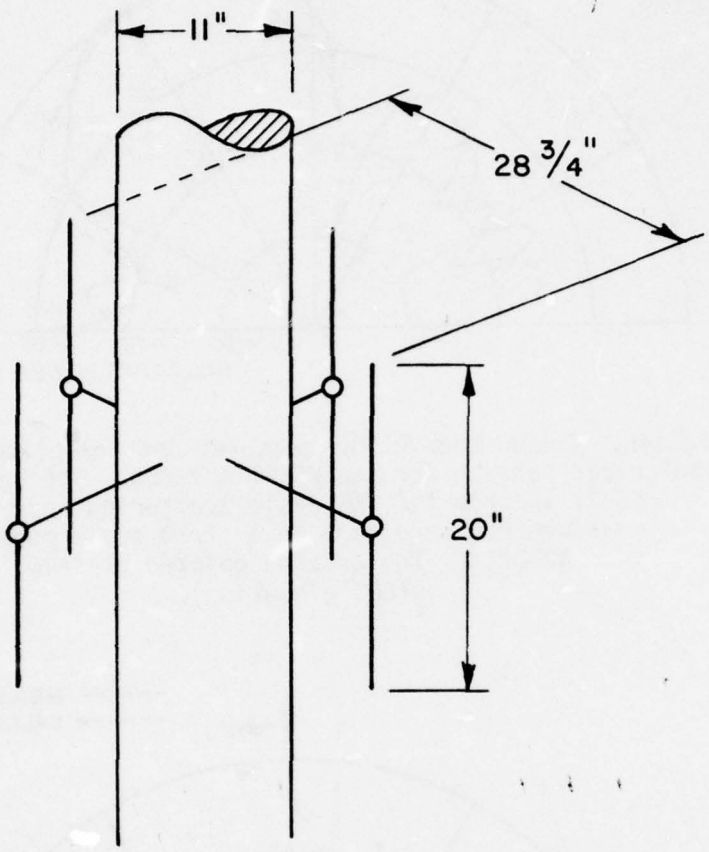

Figure 15. Computer model corresponding to AS1735 antenna example.

the smallest applicable dimensions for an asymptotic solution are on the order of one wavelength. However, the uniform asymptotic solutions are often used for sizes on the order of a quarter of a wavelength for engineering purposes. In order to test the basic scattering code's usefulness for this problem, the far zone field of a single dipole was calculated in the azimuth plane at the lower, middle and upper ends of the frequency range. The resulting patterns are compared against the exact modal solution in Figures 16a, b, and c for the frequencies of 0.225 GHz, 0.3125 GHz, and 0.400 GHz, respectively. These results produce an omnidirectional pattern in azimuth for the four dipole case as is expected. Therefore, the patterns have not been shown. The agreement is very good and even though the asymptotic results should be viewed with caution for such small dimensions, these results seem to verify the usefulness of the basic scattering code in giving an engineering answer to this problem.

The third example is for an AS-390/SRC antenna mounted on the yard arm of a mast as shown in Figure 1. Measurements were made for this configuration by L. S. Hansen of NOSC [1] using a 1/10 scale model at a frequency of 4.0 GHz. The geometry used to model this structure for the basic scattering code is illustrated in Figure 17. The AS-390 is simply modeled as a dipole of scale model length 1.925 inches for the code. The far zone field calculated in the azimuth plane for the antenna in the presence of a circular cylinder representing the mast is compared with the measured result in Figure 18. The results calculated for an antenna in the presence of the circular cylinder and a flat plate representing the yard arm is compared against the measured result in Figure 19. Note that the result for the cylinder alone gives the basic shape to the pattern. The flat plate, however, appears to give the result better agreement in the null depths and in the shape of the lobe at 180^{o}. The lack of a small feature at about 160 degrees needs more study. This may be due to something present in the measurements that is not modeled by the code or it could be a higher

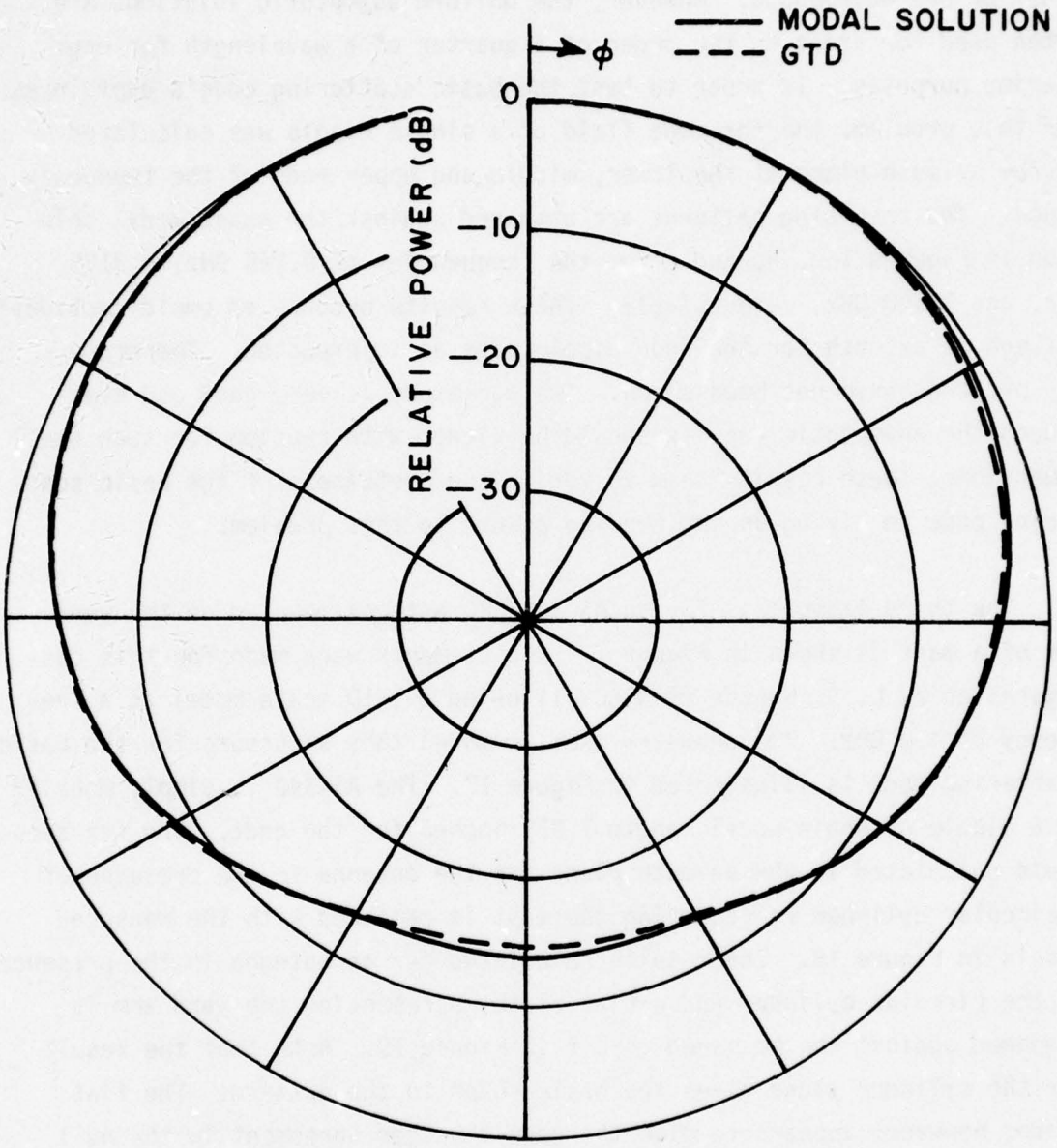

Figure 16a. Comparison of the exact modal solution and the uniform asymptotic solution of the E_θ pattern in the azimuth plane for one dipole of an AS-1735 antenna. The frequency is 0.225 GHz.

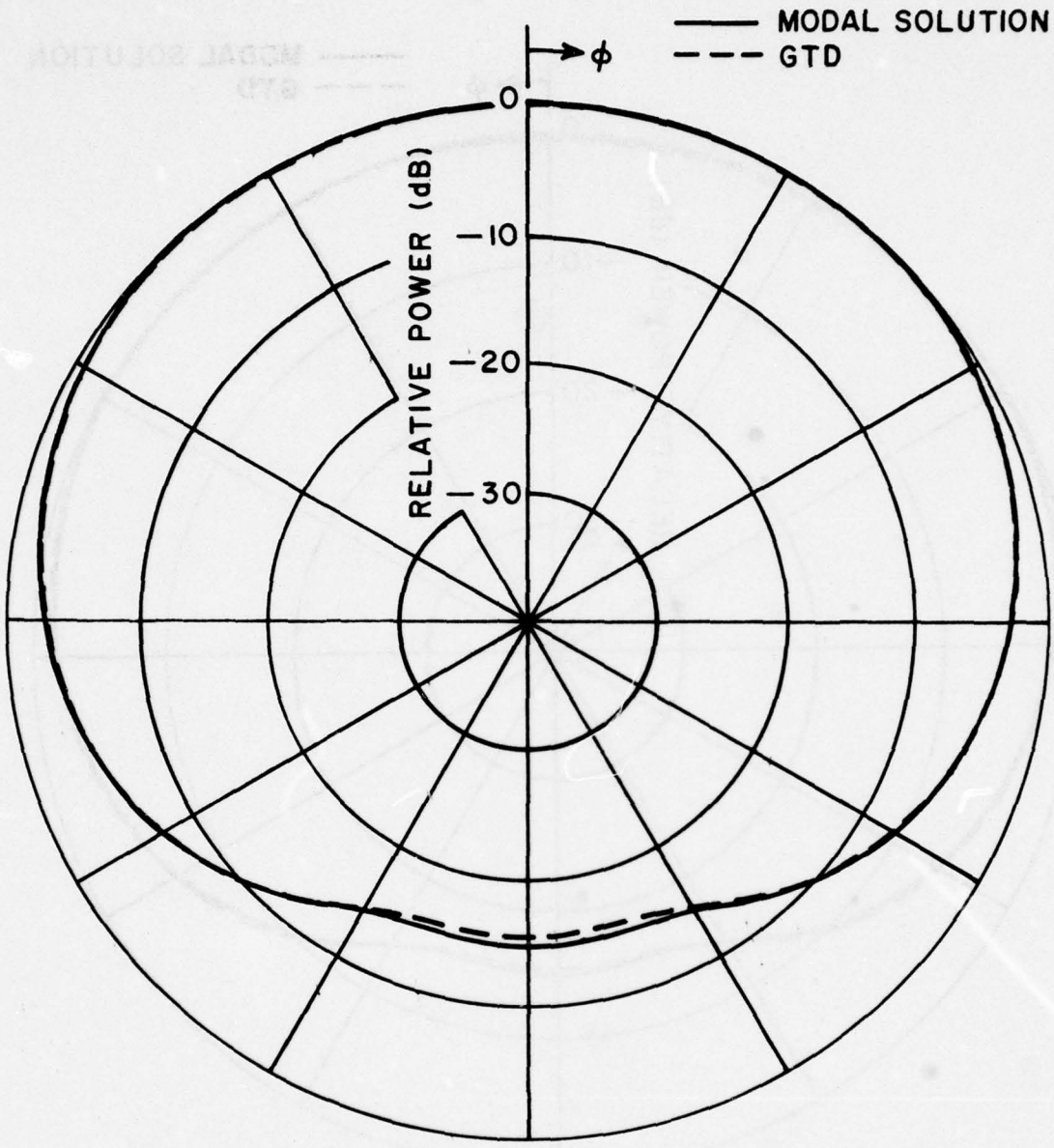

Figure 16b. Comparison of the exact modal solution and the uniform asymptotic solution of the E_θ pattern in the azimuth plane for one dipole of an AS-1735 antenna. The frequency is 0.3125 GHz.

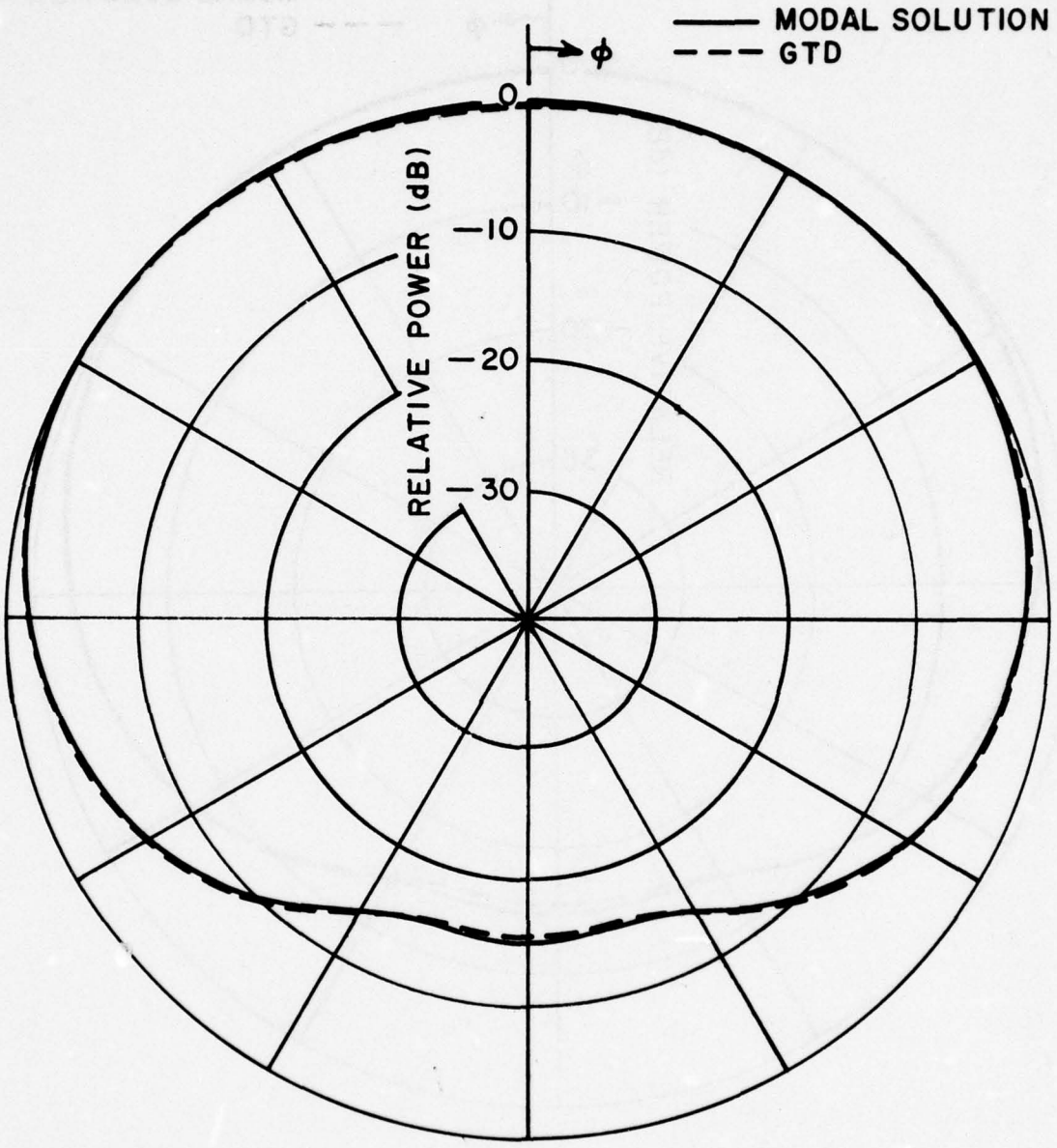

Figure 16c. Comparison of the exact modal solution and the uniform asymptotic solution of the E_θ pattern in the azimuth plane for one dipole of an AS-1735 antenna. The frequency is 0.400 GHz.

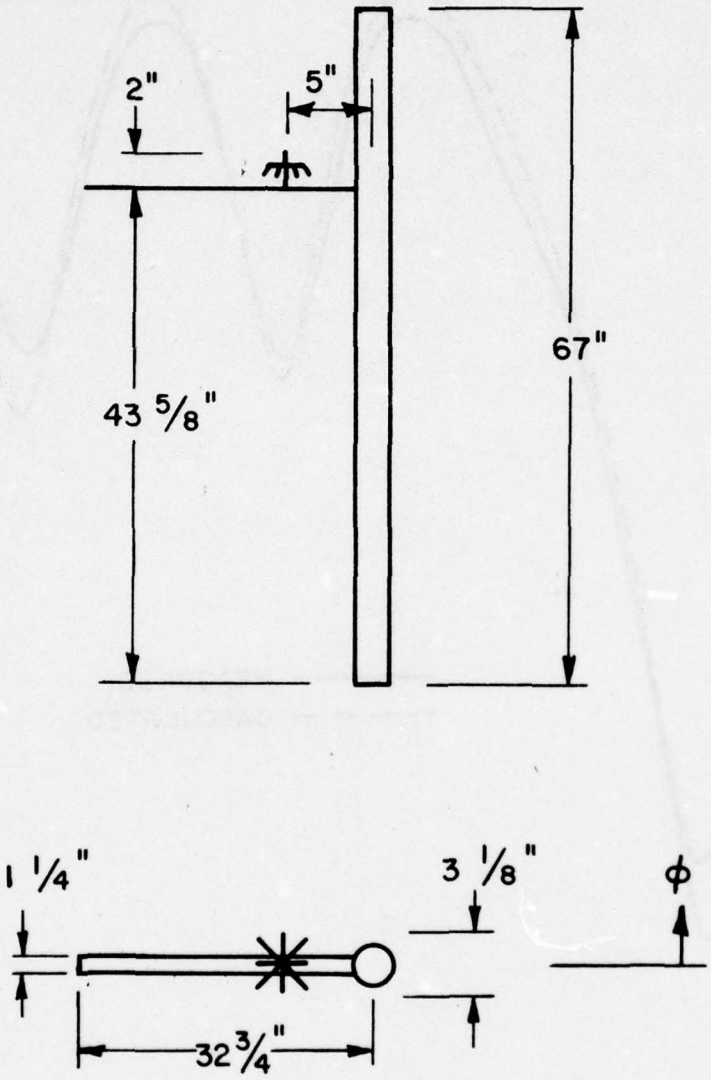

Figure 17. Top and side view of computer model corresponding to AS-390 antenna example.

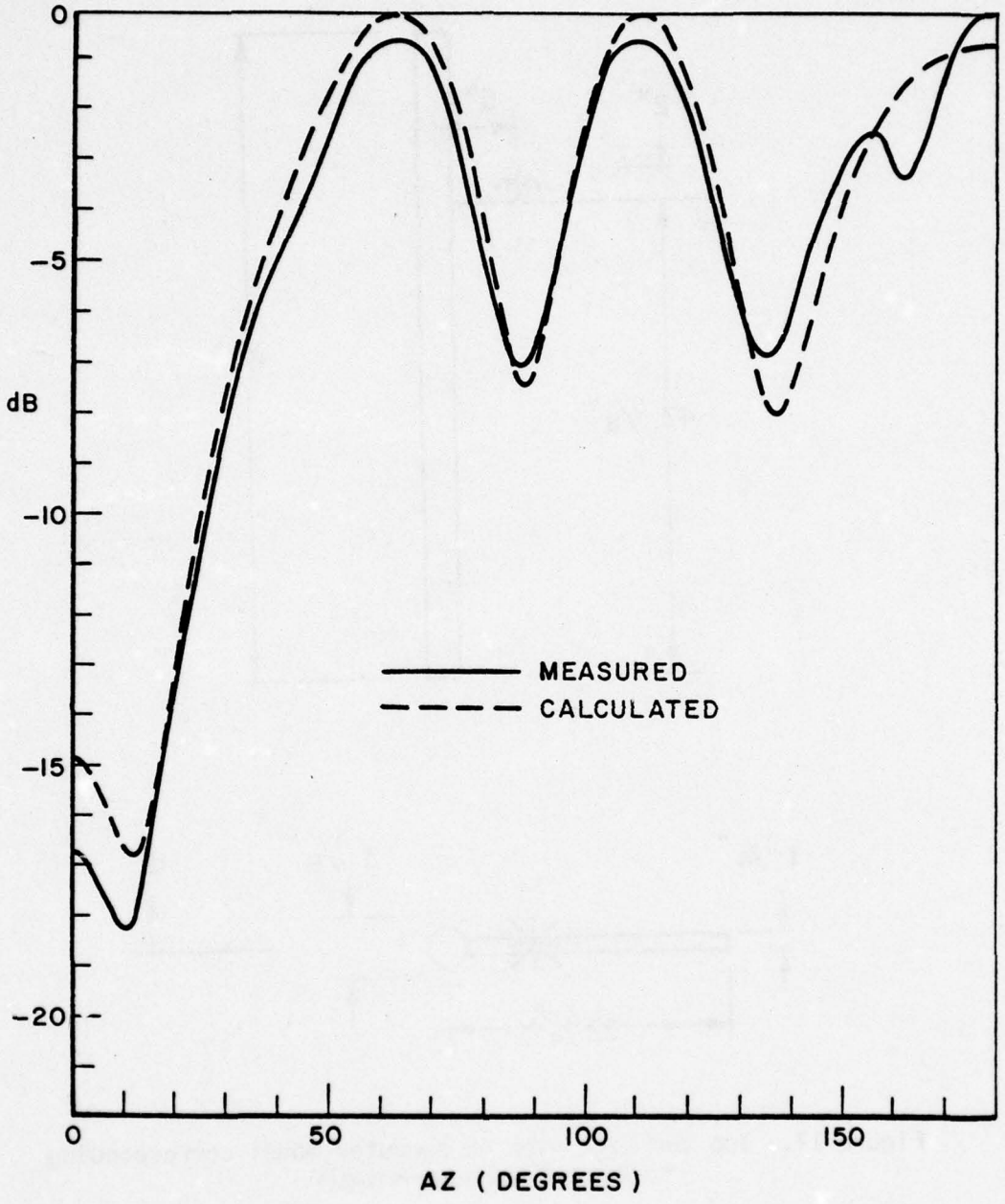

Figure 18. Comparison of the measured and calculated azimuth pattern for the AS-390 antenna example. The calculated result is from the NEC-Basic Scattering Code including the mast only. The measurements were made on a 1/10 scale model including yardarms at NOSC by L. S. Hansen[1].

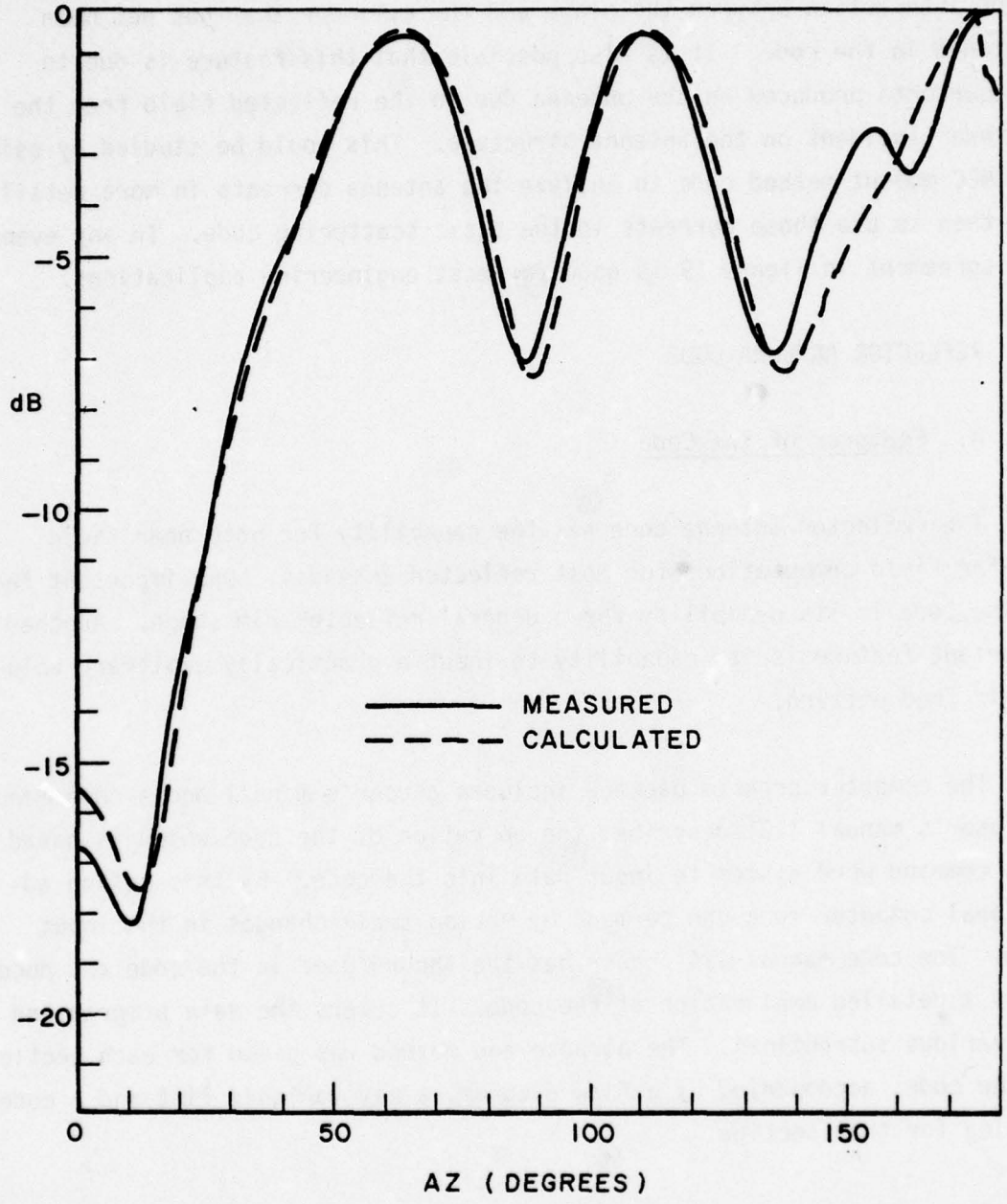

Figure 19. Comparison of the measured and calculated azimuth pattern for the AS-390 antenna example. The calculated result is from the NEC-Basic Scattering Code including the mast and the yardarm. The measurements were made on a 1/10 scale model at NOSC by L. S. Hansen[1].

order interaction between the plate and the cylinder that has not been included in the code. It is also possible that this feature is due to the currents produced on the antenna due to the reflected field from the cylinder incident on the antenna structure. This could be studied by using the NEC moment method code to analyze the antenna currents in more detail and then to use those currents in the basic scattering code. In any event the agreement in Figure 19 is good for most engineering applications.

V. REFLECTOR ANTENNA CODE

A. Features of the Code

The reflector antenna code has the capability for both near field and far field computations for most reflector antennas. One important feature of the code is its capability for a general reflector rim shape. Another important feature is its capability to input a practically arbitrary volumetric feed pattern.

The computer program package includes a user's manual and a code manual. The user's manual [13] describes the operation of the code which is based on a command word system to input data into the code. By this method additional computer runs can be made by making small changes in the input data. The code manual [14] describes the theory used in the code and documents a detailed explanation of the code. It covers the main program and its various subroutines. The purpose and method was given for each section of the code, accompanied by a flow diagram, a key variable list and a code listing for that section.

The reflector code can be used for the following basic applications:

1. Pattern prediction of existing reflector antennas.

2. Reflector antenna design.

3. Radiation hazard calculations.

4. EMC or coupling calculations with small antennas.

The far field capability of the code is used for applications 1 and 2 listed above. For pattern prediction it is necessary to have sufficient information about the reflector dimensions and feed pattern.

For antenna design the code can be used in an iterative manner to seek a practical design having a given pattern performance goal or, the code can be used to give a more accurate prediction of the performance of a design obtained from more approximate techniques.

The near field capability of the code can be used to EMC and radiation hazard applications. The code can accurately calculate the field at virtually any point that is at least one diameter from the reflector. Since the code is efficient even for near field computations it eliminates the necessity to rely entirely on approximate techniques as has usually been done in the past.

For radiation hazard applications the code is used to calculate the level of the electric field or the power density at the near field point. For EMC or coupling calculations the power density incident on a small antenna is first calculated using the code; then the coupling is calculated by multiplying by the effective aperture of the small antenna.

B. Computed Far Field Pattern Results

The results of the general reflector code for several example antenna geometries are presented in this section. These examples illustrate the versatility of the code for computing far field patterns of reflector antennas with various rim shapes and feed patterns.

The first example is the common case of a circular reflector with an on-axis feed as shown in Figure 20. A GTD analysis was previously developed for this case as reported in Reference 15. Calculated results are given in Reference 15 for a 24" diameter reflector with an F/D ratio of 1/3 and a frequency of 11 GHz. The far field patterns as computed by the general reflector code are shown in Figures 21 a and b for the H- and E-planes, respectively. The results from the general reflector code were found to be in good agreement with the calculated results of Reference 15 without aperture blockage as shown in Figures 22 and 23. Aperture blockage and feed strut scattering effects have not yet been included in the general reflector code. The comparison of the computed results with the measured patterns in Figures 22 and 23 is one indication of the validity of the general reflector code. Other comparisons are given below to further demonstrate the accuracy of the general reflector code.

The second example is an offset reflector as shown in Figure 24. Fortunately, sufficient data were published by Silver [16] to completely specify the antenna and most of its feed pattern. The feed pattern data for this reflector had to be extracted from the published dB contours [16] of the aperture field. The feed is horizontally polarized. The feed patterns were specified by using the option for an offset feed tilt angle (PSIT=20^{o}) and the feed pattern symmetry option (ISYM=3). This feed symmetry option specifies the feed pattern to be symmetrical about the y-z plane. The E- and H-plane patterns as computed for 9.2 GHz from the general reflector code are shown in Figures 25 a and b. The corresponding measured patterns as published in Silver [16] are shown in Figure 26. The measured and computed patterns are in good agreement considering that feed strut scattering effects are not included in the reflector code. The full 180^{o} patterns as computed by the general reflector code are shown in Figures 27 a and b. The feed spillover is evident from the lobes near 90^{o} and 110^{o} in the E- and H-plane, respectively.

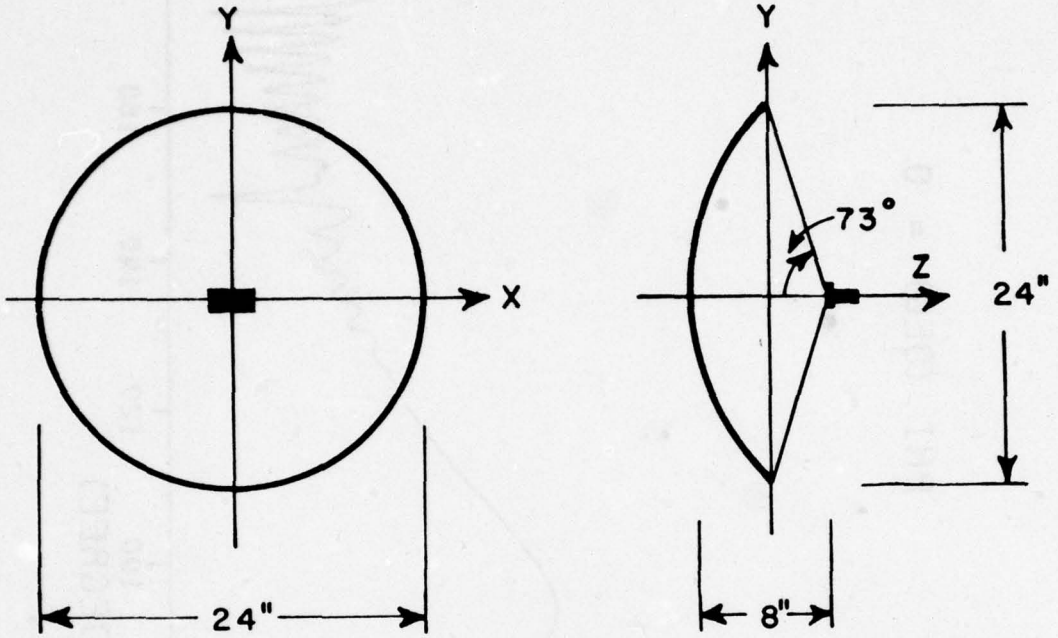

(a) FRONT VIEW

(b) SIDE VIEW

Figure 20. Circular reflector antenna with F/D = $\frac{1}{3}$.

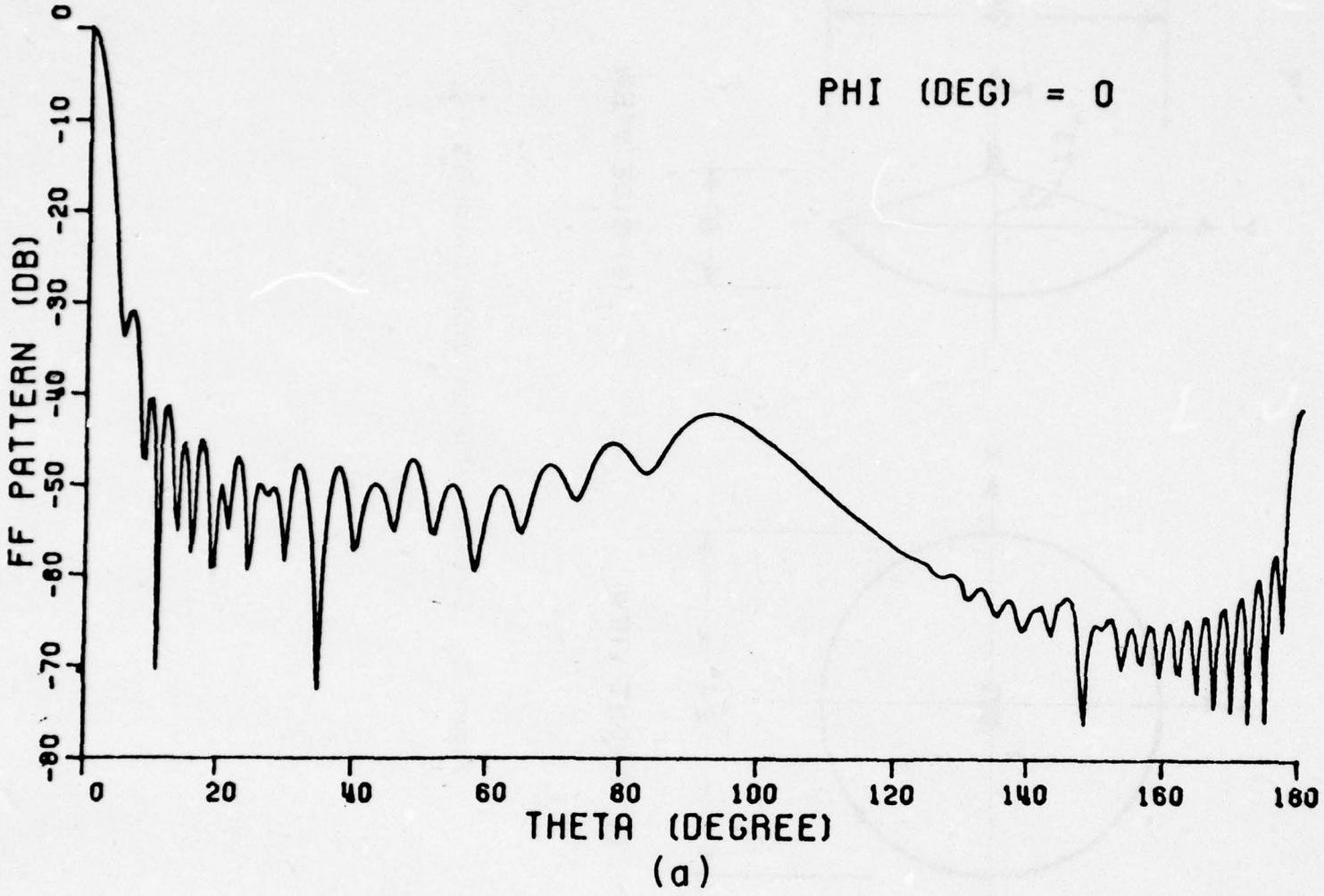

Figure 21. Far field patterns of circular reflector example computed by general reflector code.

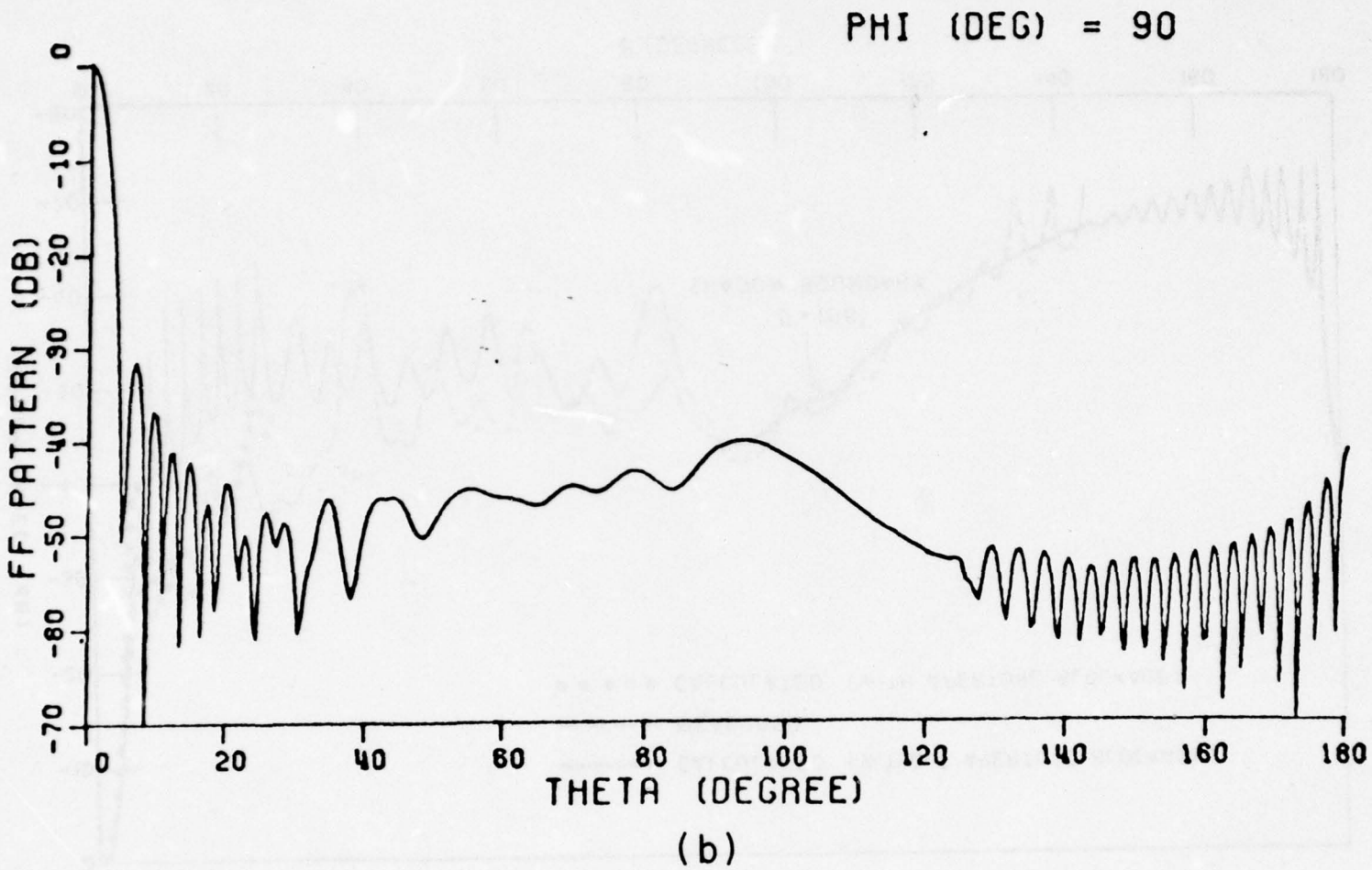

(b)

Figure 21. (Continued)

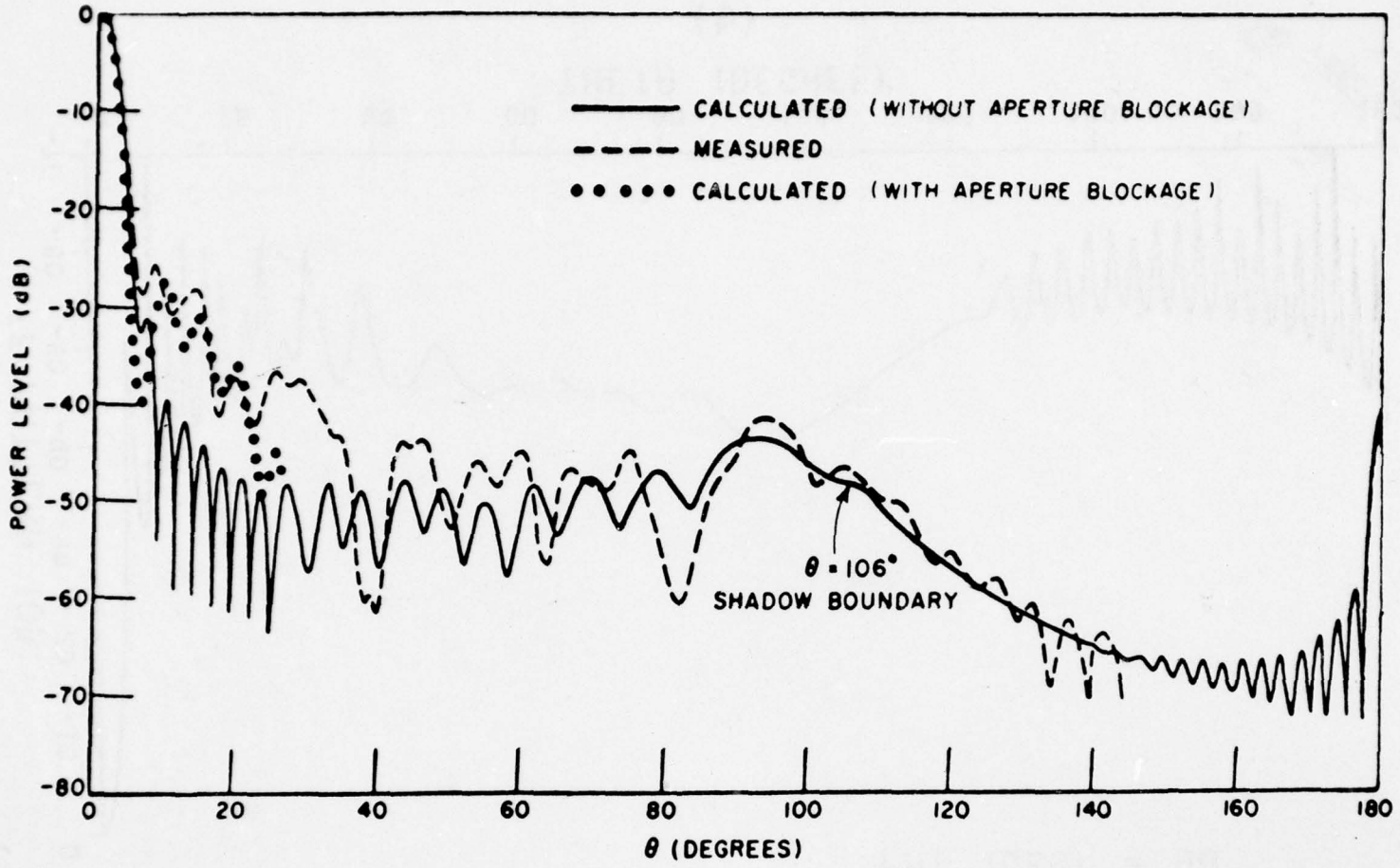

Figure 22. H-plane pattern of a parabolic reflector with a flanged waveguide feed. Computed in Reference 15.

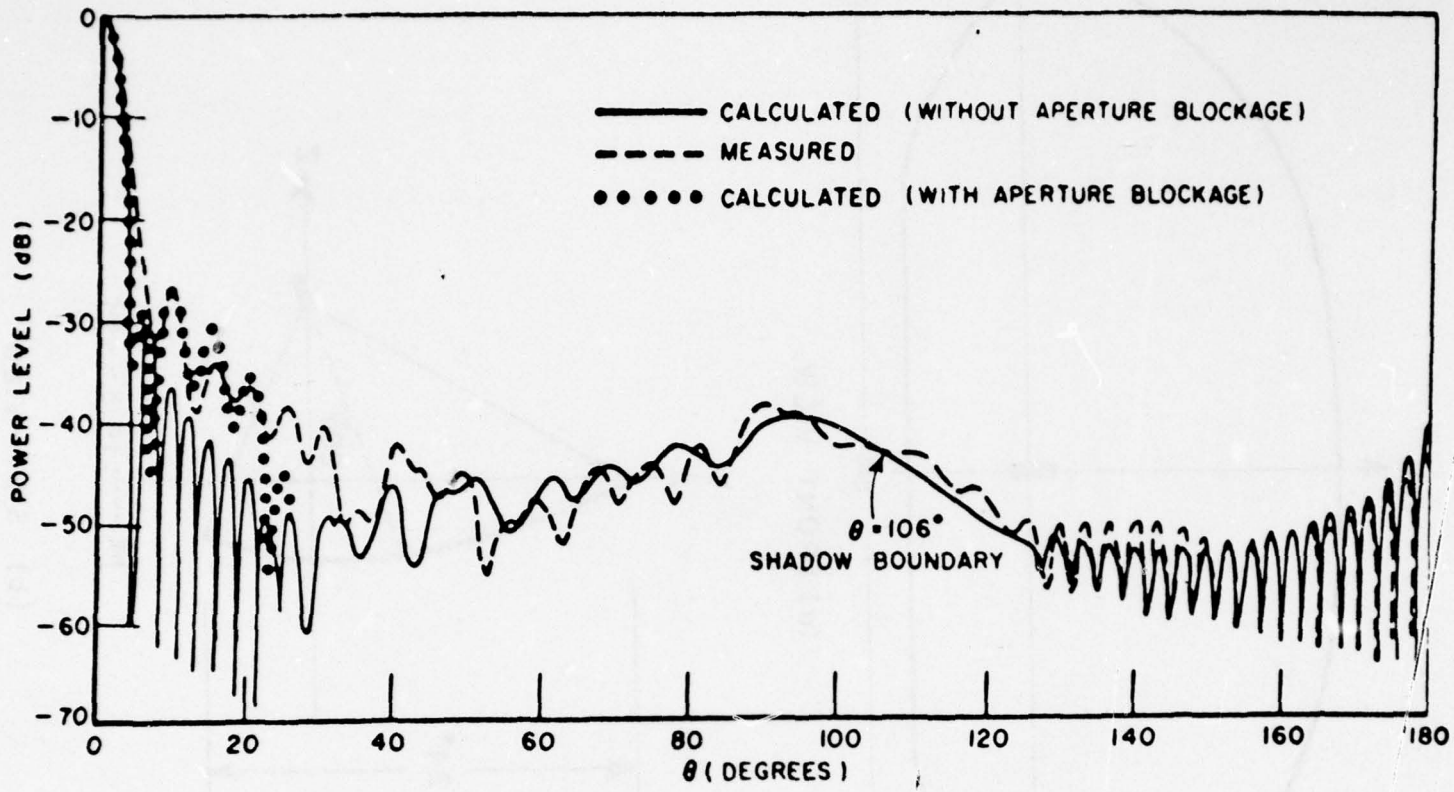

Figure 23. E-plane pattern of a parabolic reflector with a flanged waveguide feed. Computed in Reference 15.

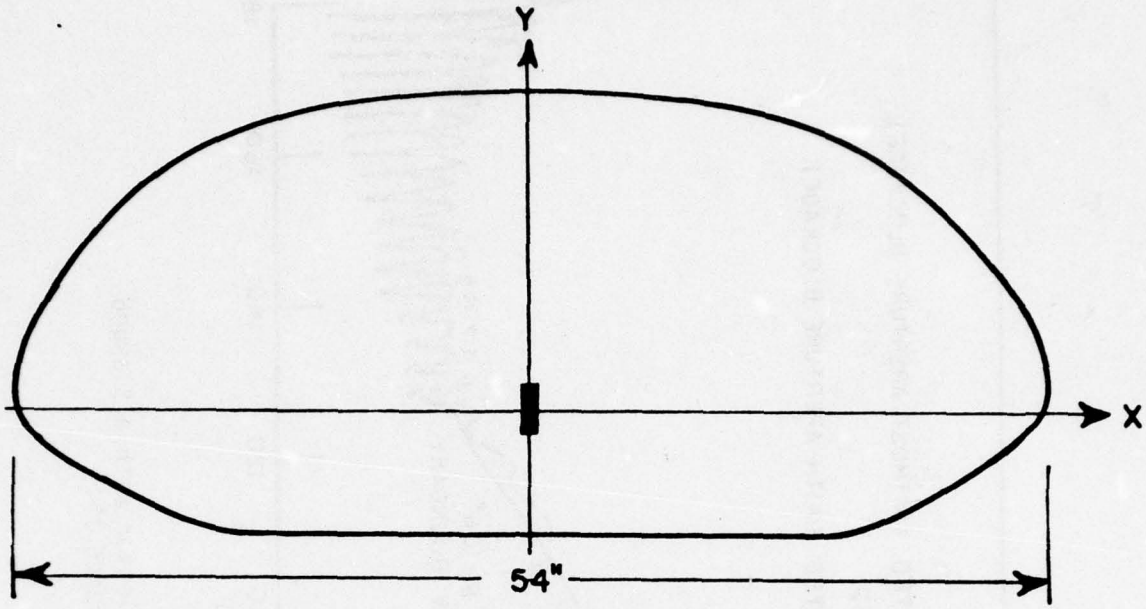

(a) FRONT VIEW

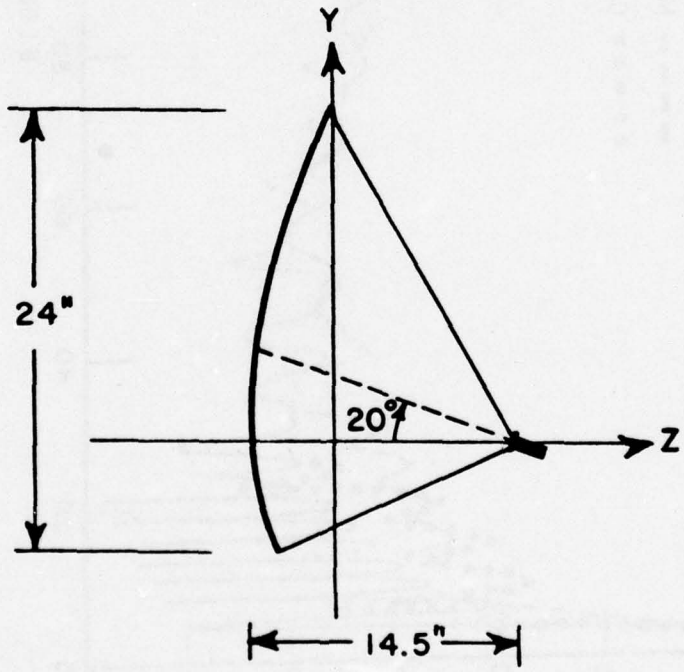

(b) SIDE VIEW

Figure 24. Offset reflector rim shape and crosssection.

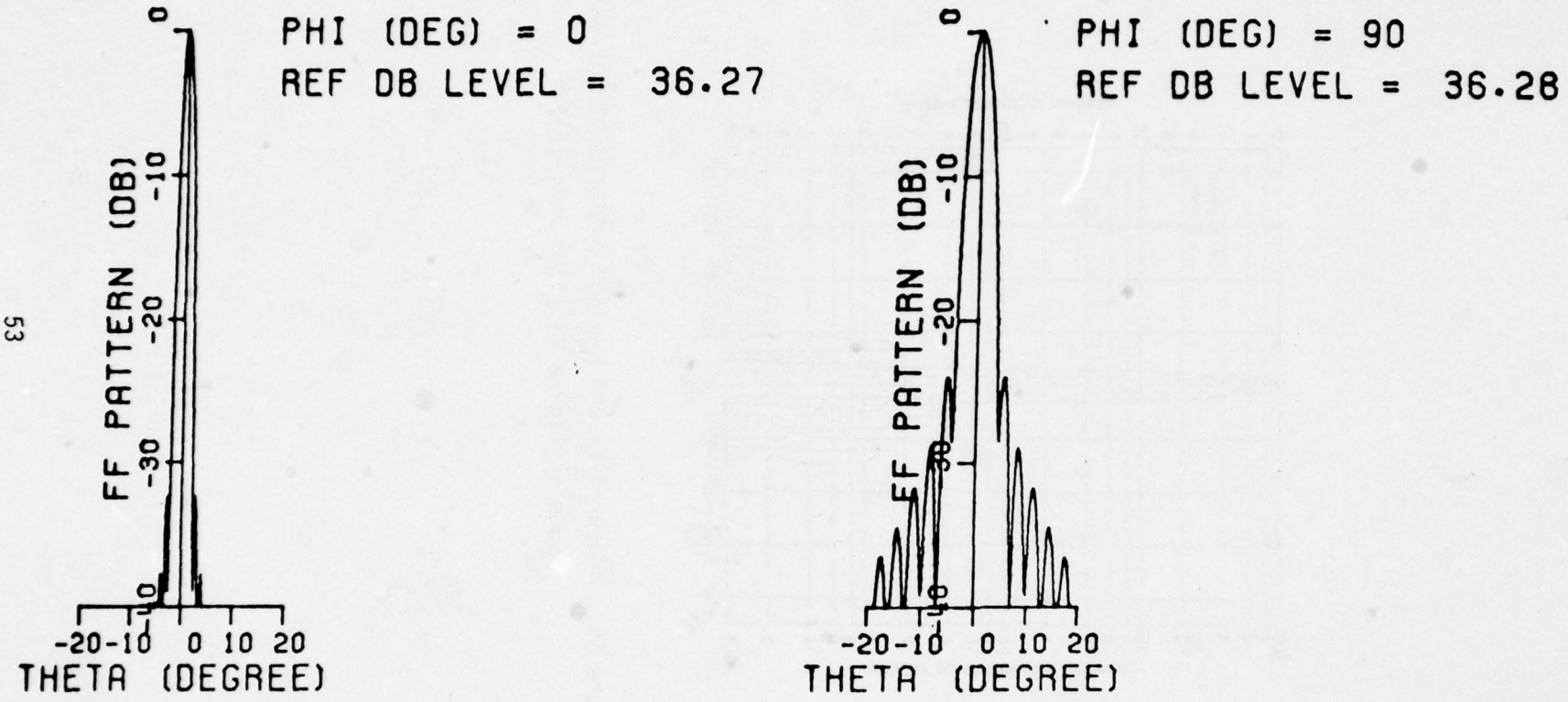

Figure 25. Far field patterns of offset reflector example computed by general reflector code. Main beam and near sidelobes.

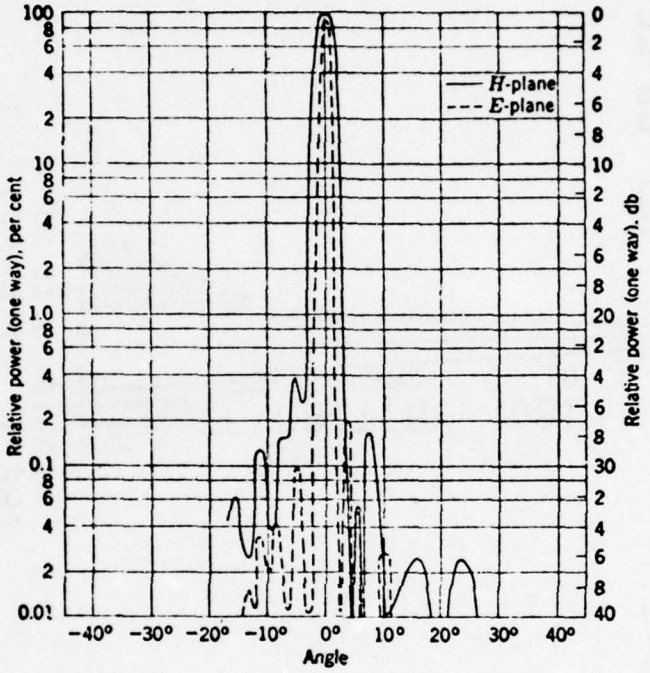

Figure 26. Measured E- and H-plane patterns of the antenna shown in Figure 24 (from Ref. 16).

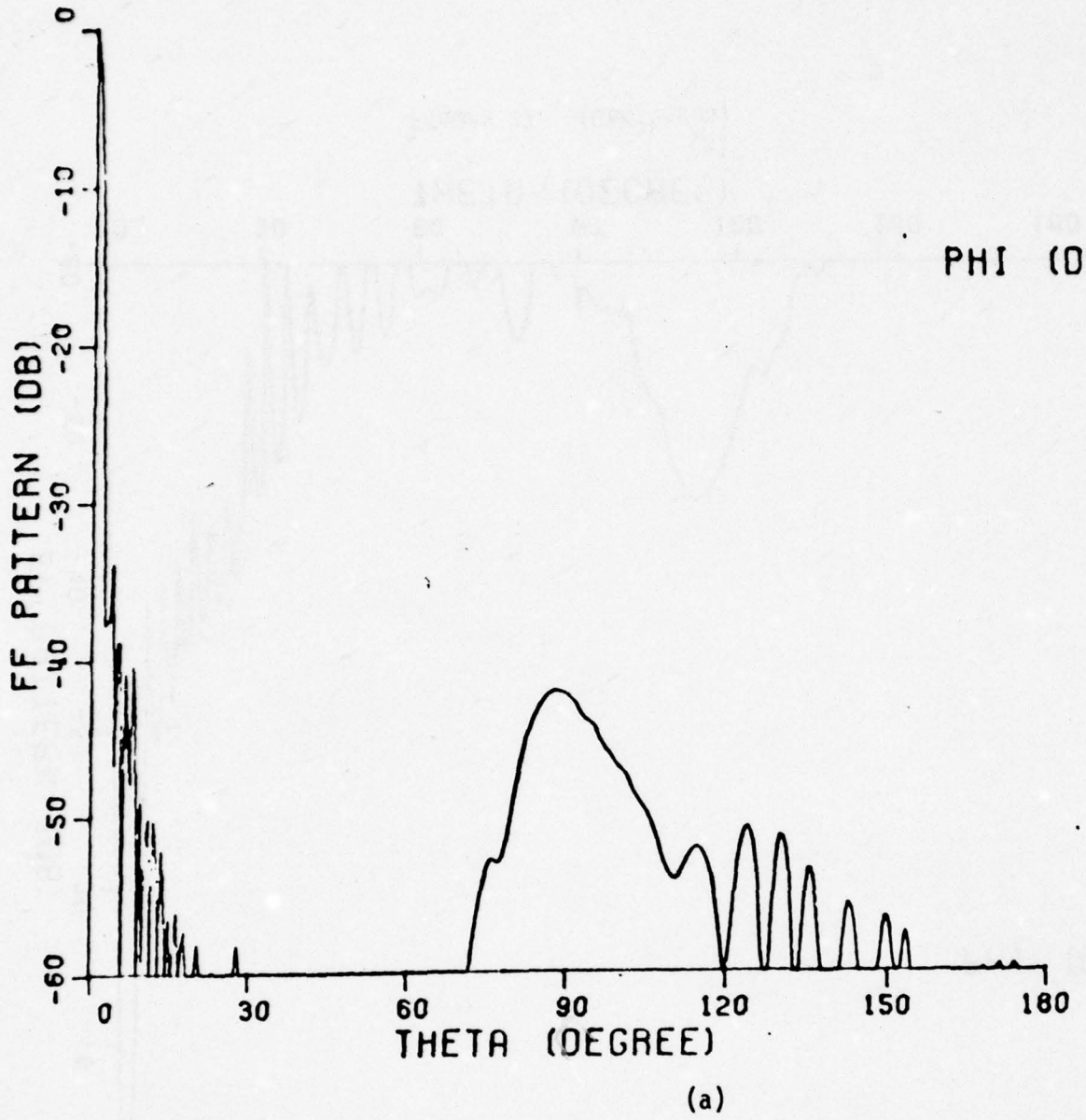

(a)

Figure 27. Far field patterns of offset reflector example computed by general reflector code.

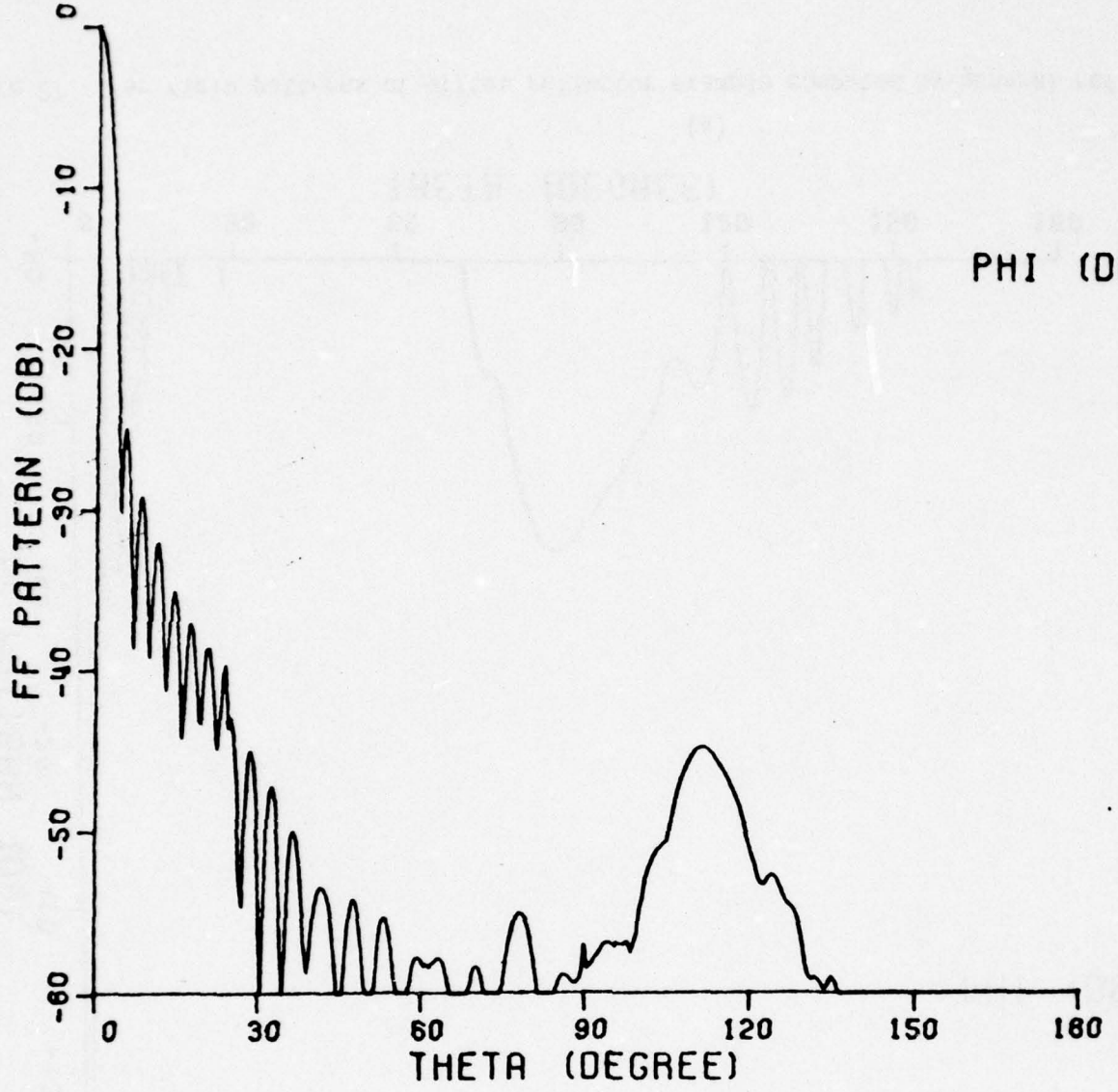

(b)

Figure 27. (Continued)

The next example is the offset reflector shown in Figure 28. The projected rim shape is circular as shown, although the rim is actually elliptical. The feed is horizontally polarized with an offset angle of 51.5^{o}. A specialized computer code was previously developed by Mentzer et al [17] which is applicable only for this particular antenna. Although the mid-C band frequency was not precisely known, several frequencies were tried until one was obtained which matched the beamwidths of the patterns calculated in Reference 17. The patterns computed by the general reflector code are shown in Figures 29 a to c. They are in excellent agreement with those calculated in Reference 17 and shown in Figures 30 a to c. An antenna gain of 65 dB was computed by the general reflector code; and the gain of the feed horn was computed to be about 37 dB. Thus the general reflector code predicts the antenna gain as 26 dB above the feed horn gain. This is within about 1 dB of that shown in Figure 30.

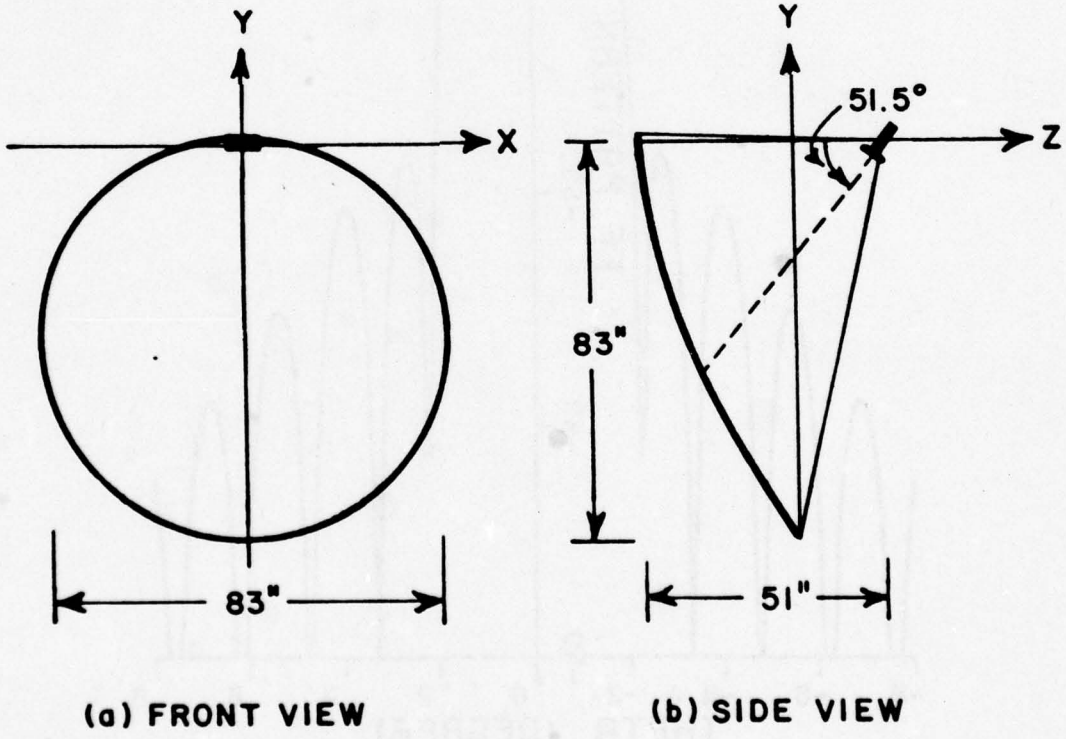

Figure 28. Offset reflector with circular porjected rim.

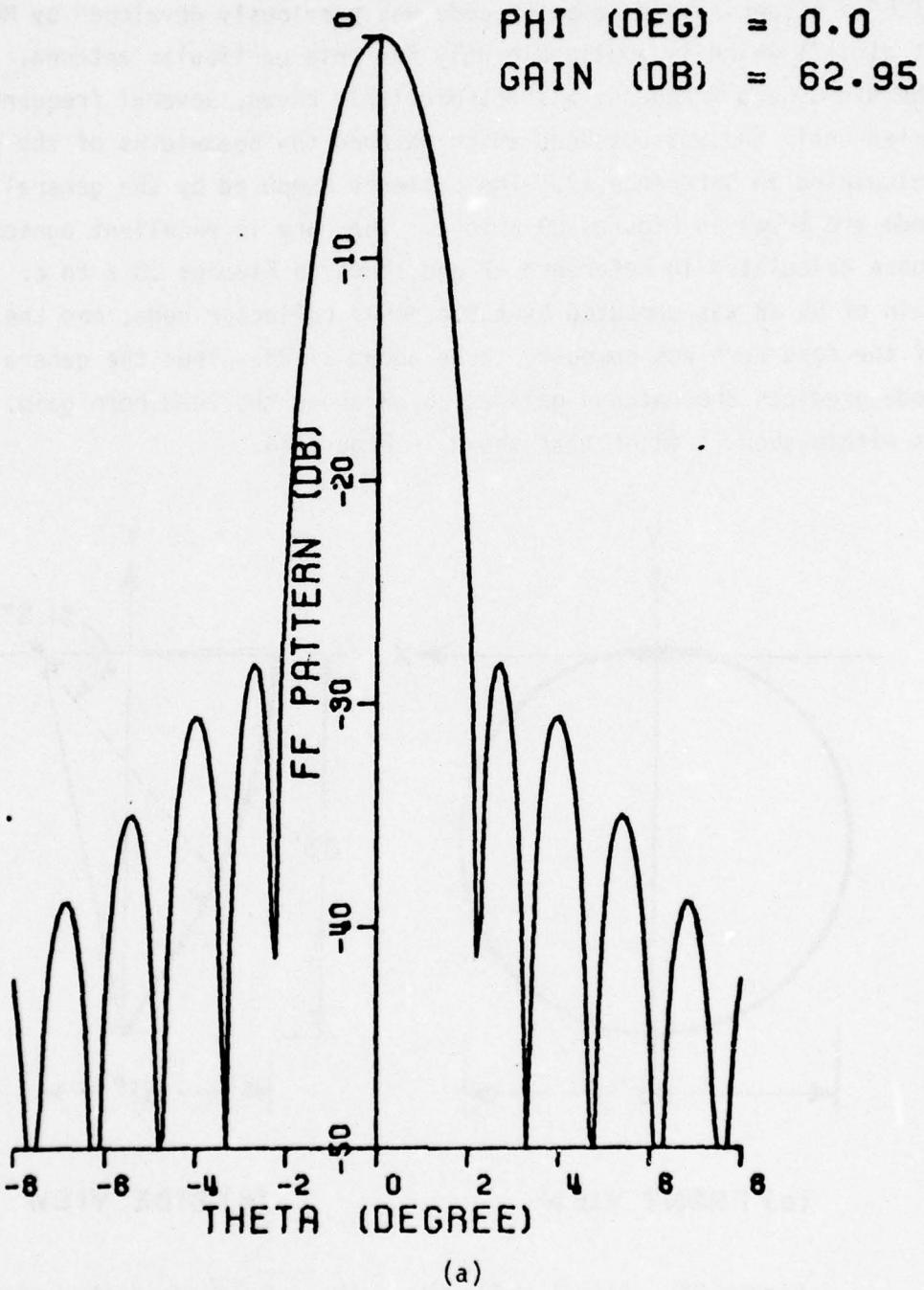

(a)

Figure 29. Far field patterns of offset reflector with circular projected rim computed by general reflector code.

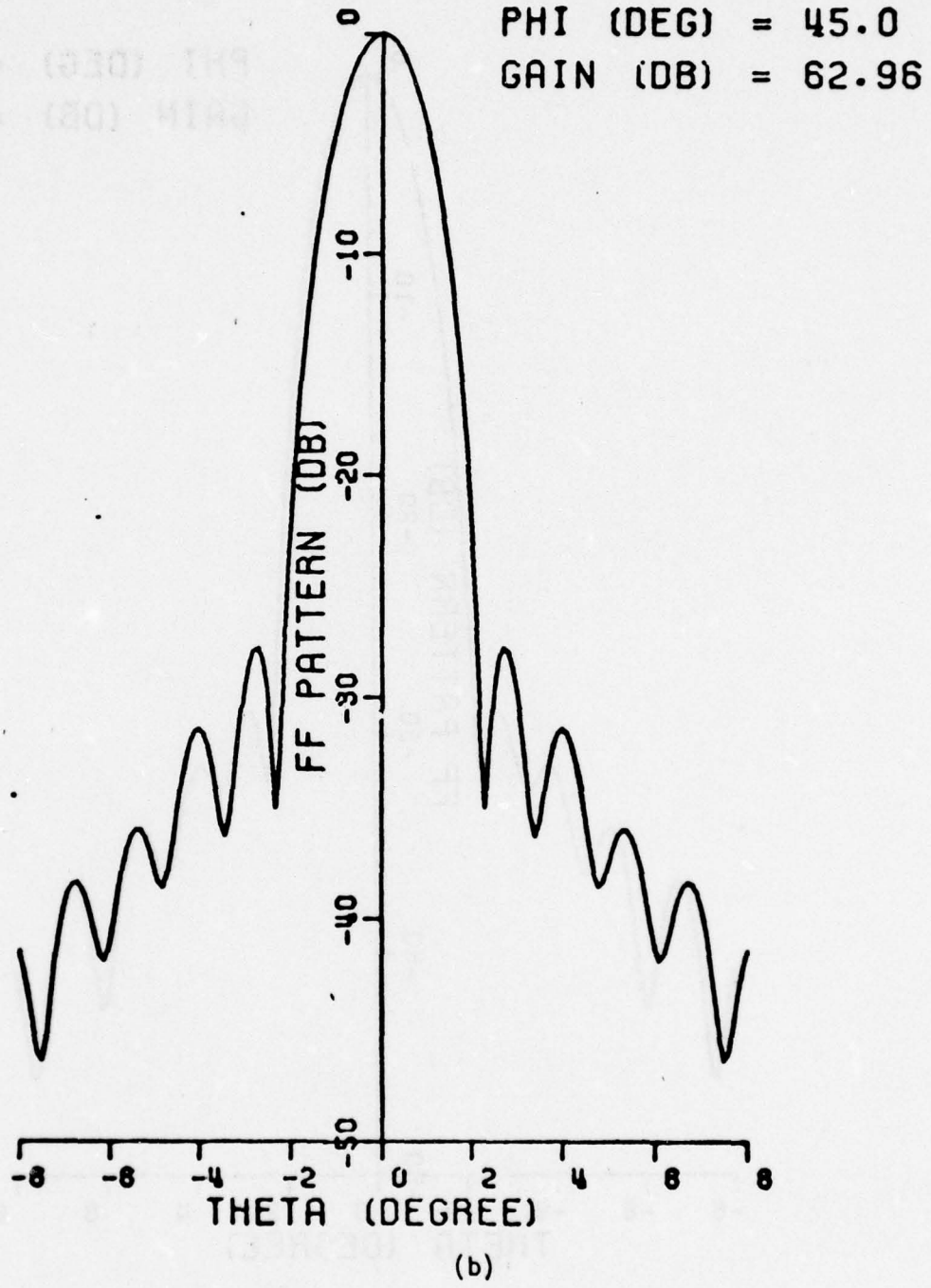

(b)

Figure 29. (Continued)

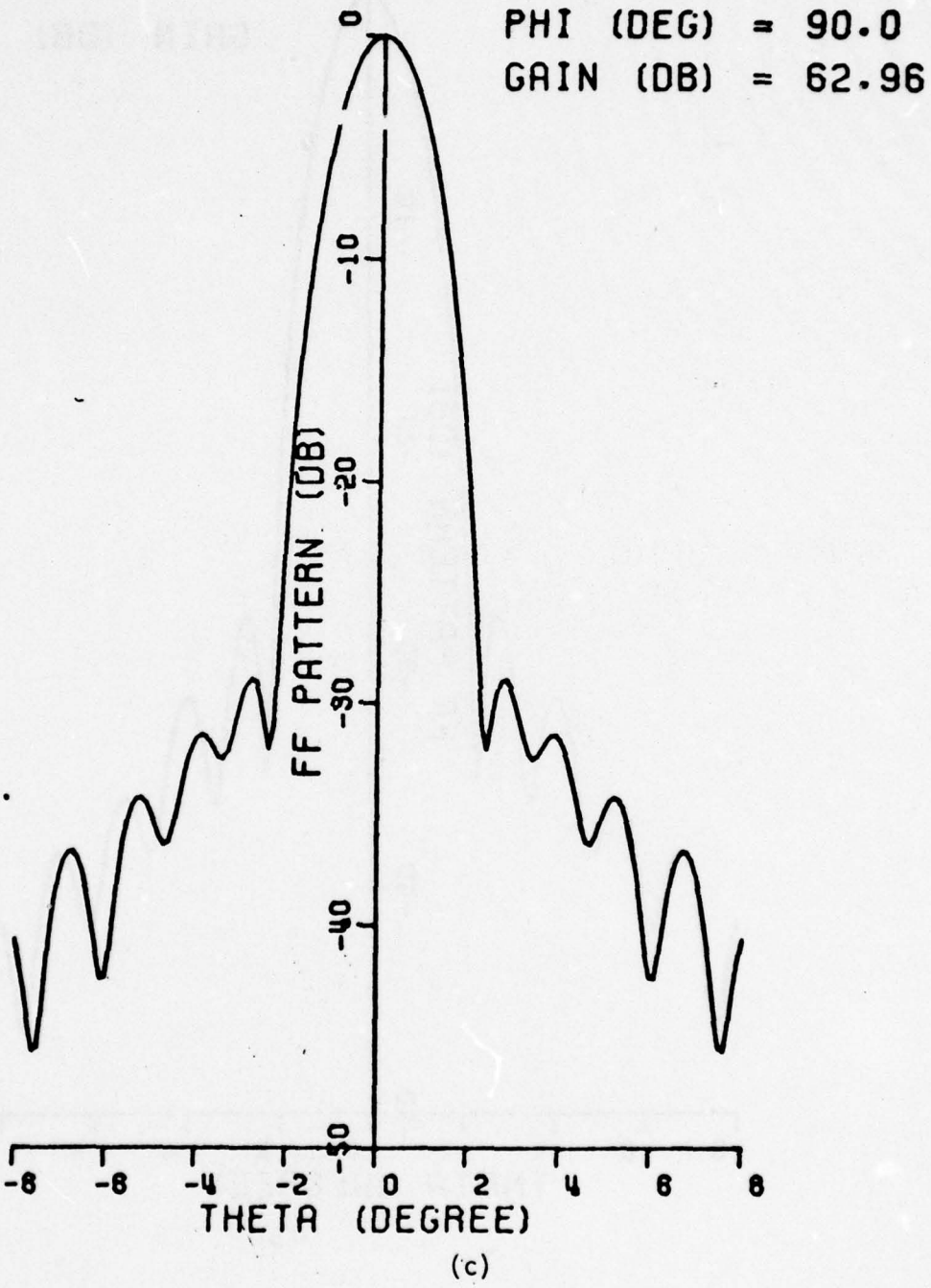

(c)

Figure 29. (Continued)

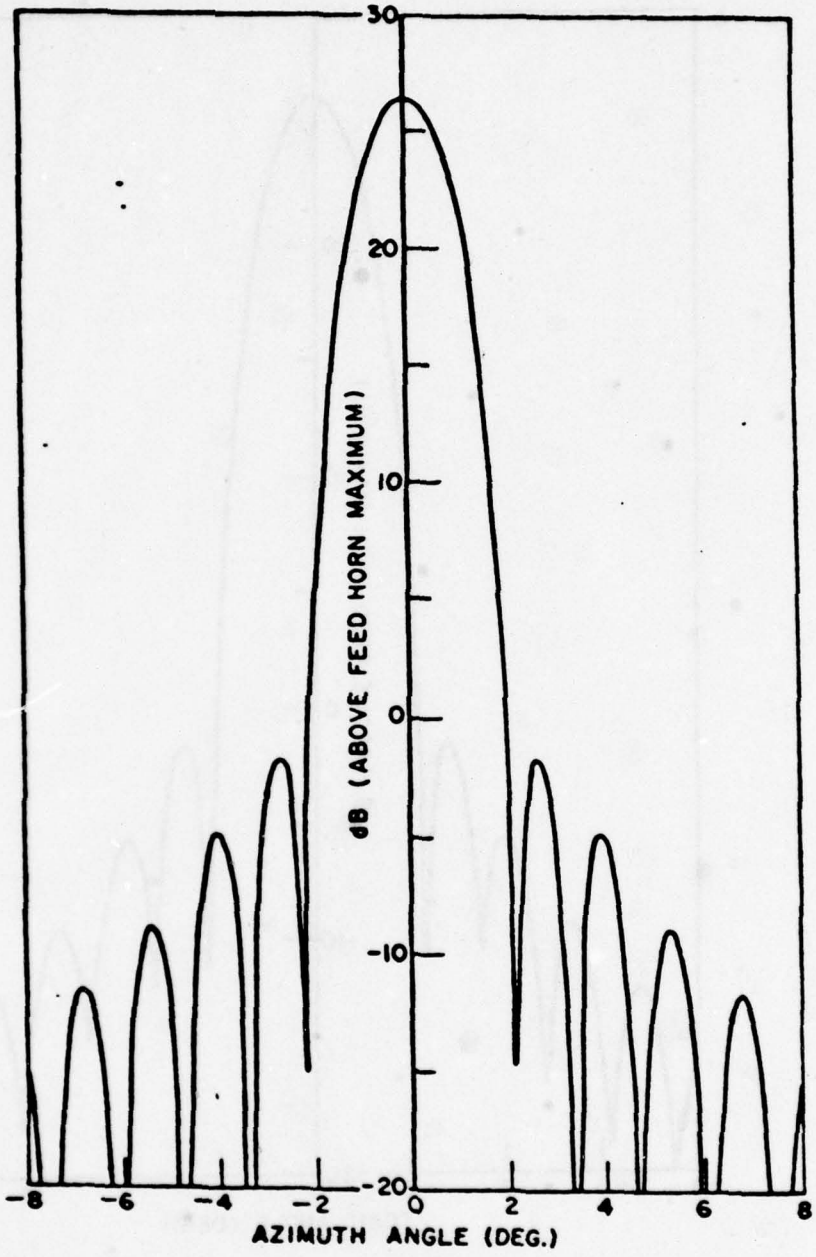

Figure 30a. $\phi=0^{o}$ pattern from Reference 17.

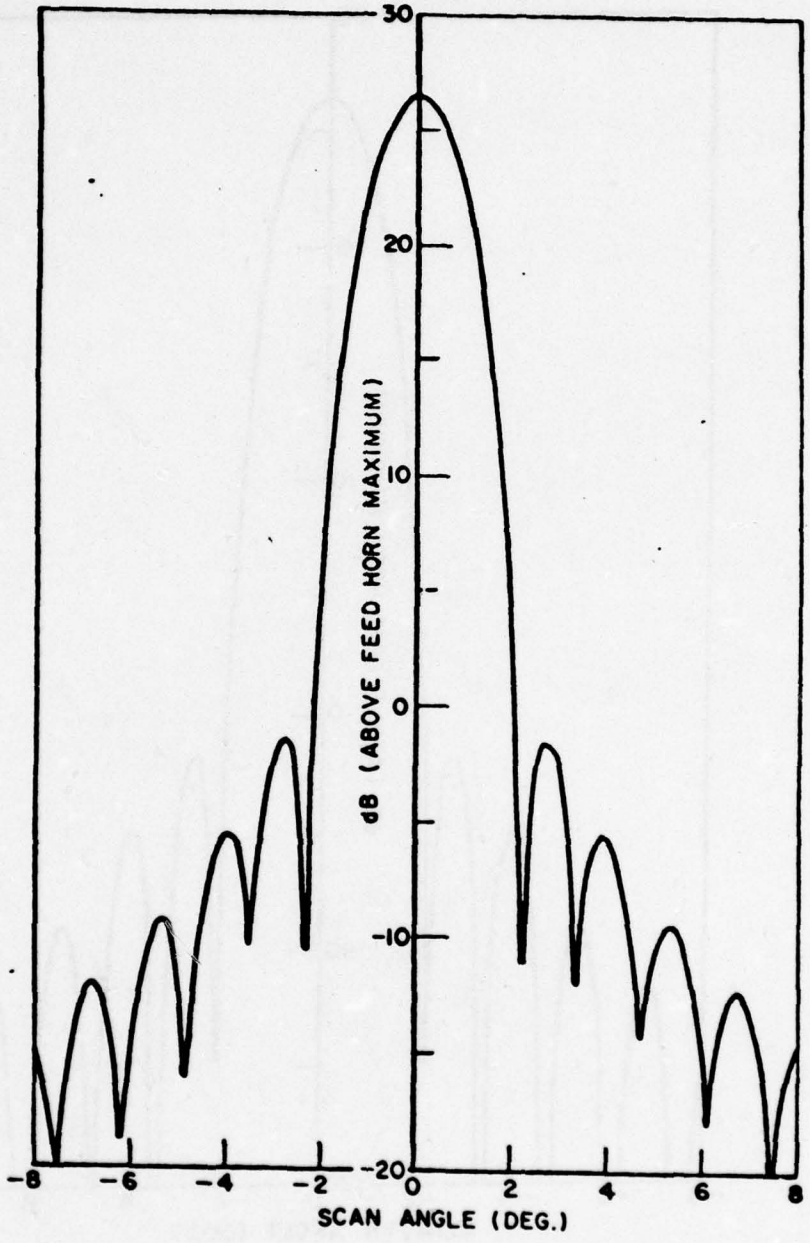

Figure 30b. $\phi = 45^{o}$ pattern from Reference 17.

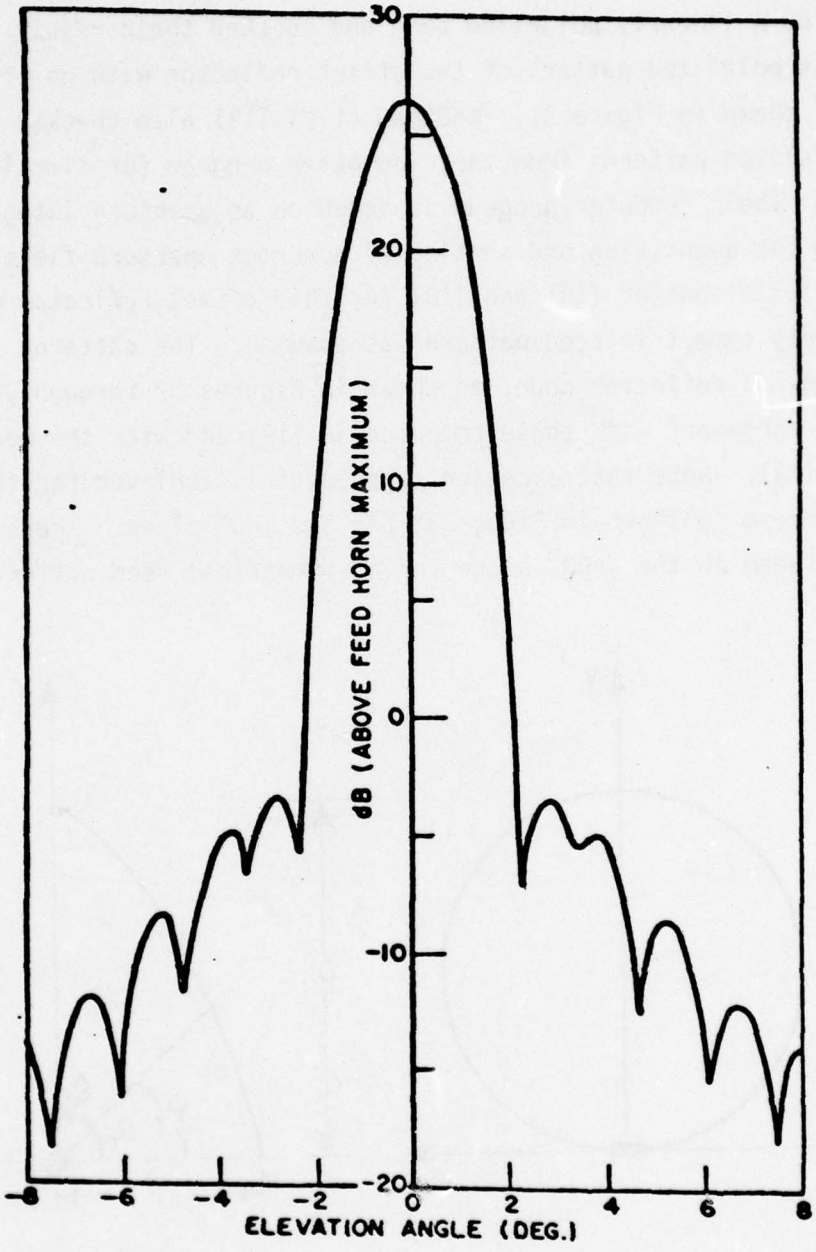

Figure 30c. $\phi=90^{o}$ pattern from Reference 17.

The depolarization properties of offset reflector antennas were studied by Chu and Turrin [18]. They calculated the maximum cross polarization produced by a linearly polarized feed and checked their result with a measured cross polarized pattern of the offset reflector with an offset angle of $\theta_c=45^o$ shown in Figure 31. Kaufman et al [19] also checked this case with calculated patterns from their computer program for circular reflector antennas. Their computer program is based on an aperture integration analysis involving the quantizing and sorting of numerous aperture field data. In the calculations of [18] and [19] for this offset reflector example, a circularly symmetric feed pattern was assumed. The patterns computed by the general reflector code, as shown in Figures 32 through 34, are in excellent agreement with those computed in [19] and with the measured patterns of [18]. Note that excellent agreement is achieved for the cross polarized beam as shown in Figure 33 for the $\phi=0^o$ plane. There is no cross polarized beam in the $\phi=90^o$ plane for a symmetrical feed pattern.

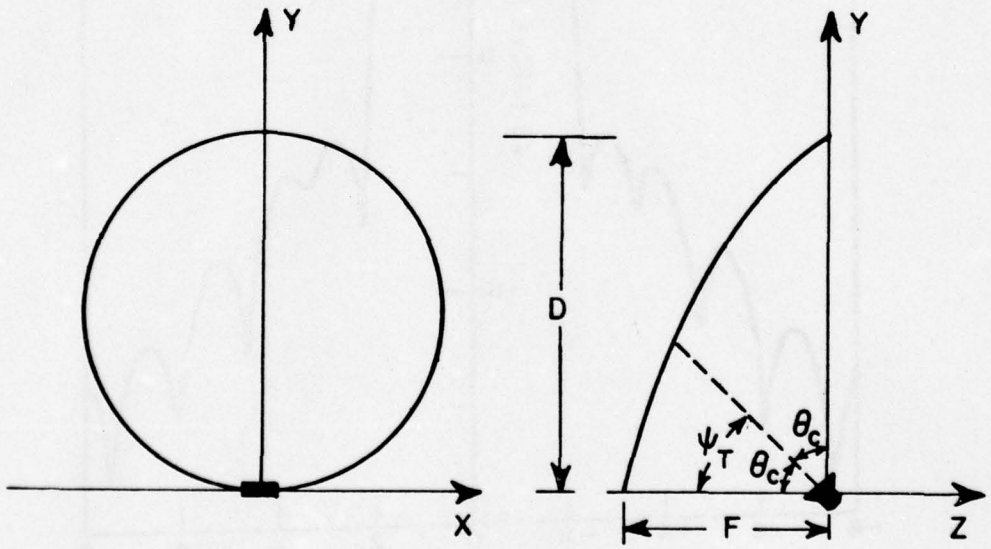

(a) FRONT VIEW (b) SIDE VIEW

Figure 31. Offset reflector geometry for example of Chu and Turrin [18]. D = 12 inches, $\psi_T=\theta_c=45^o$, f/D=0.25 and frequency = 18.5 GHz.

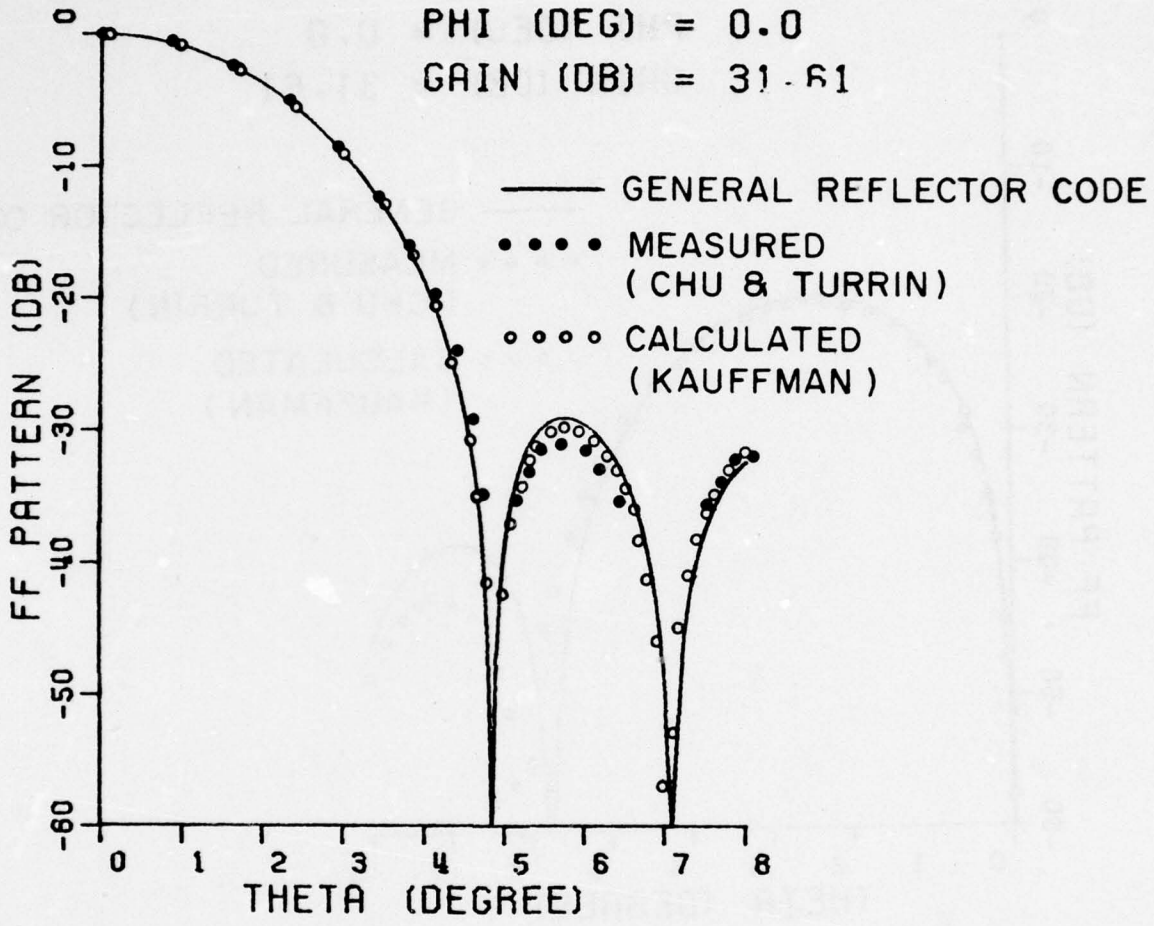

Figure 32. Far field pattern for example of Reference 18, computed by general reflector code. Principal polarization is $\phi=0^{o}$ plane.

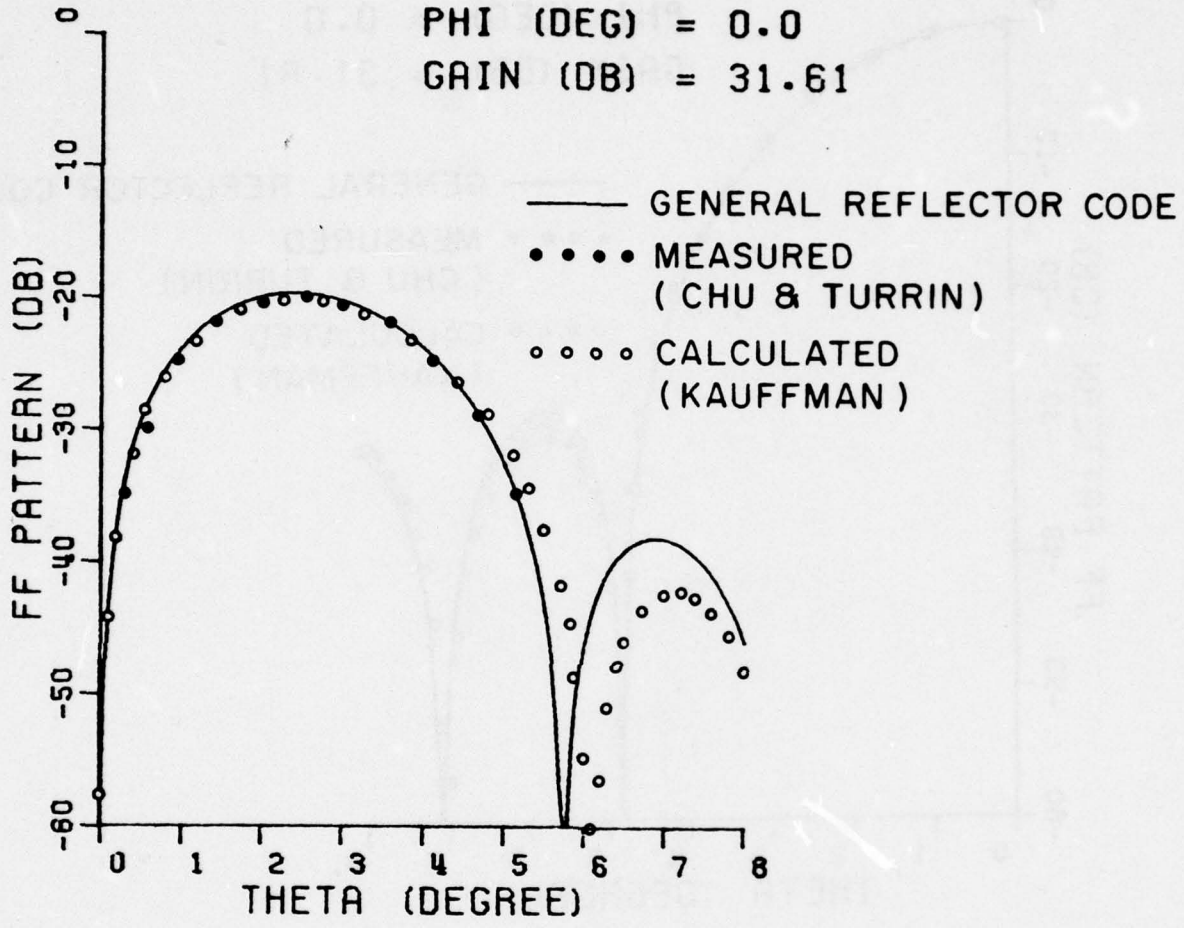

Figure 33. Far field pattern for example of Reference 18, computed by general reflector code. Cross polarization in $\phi=0^{o}$ plane.

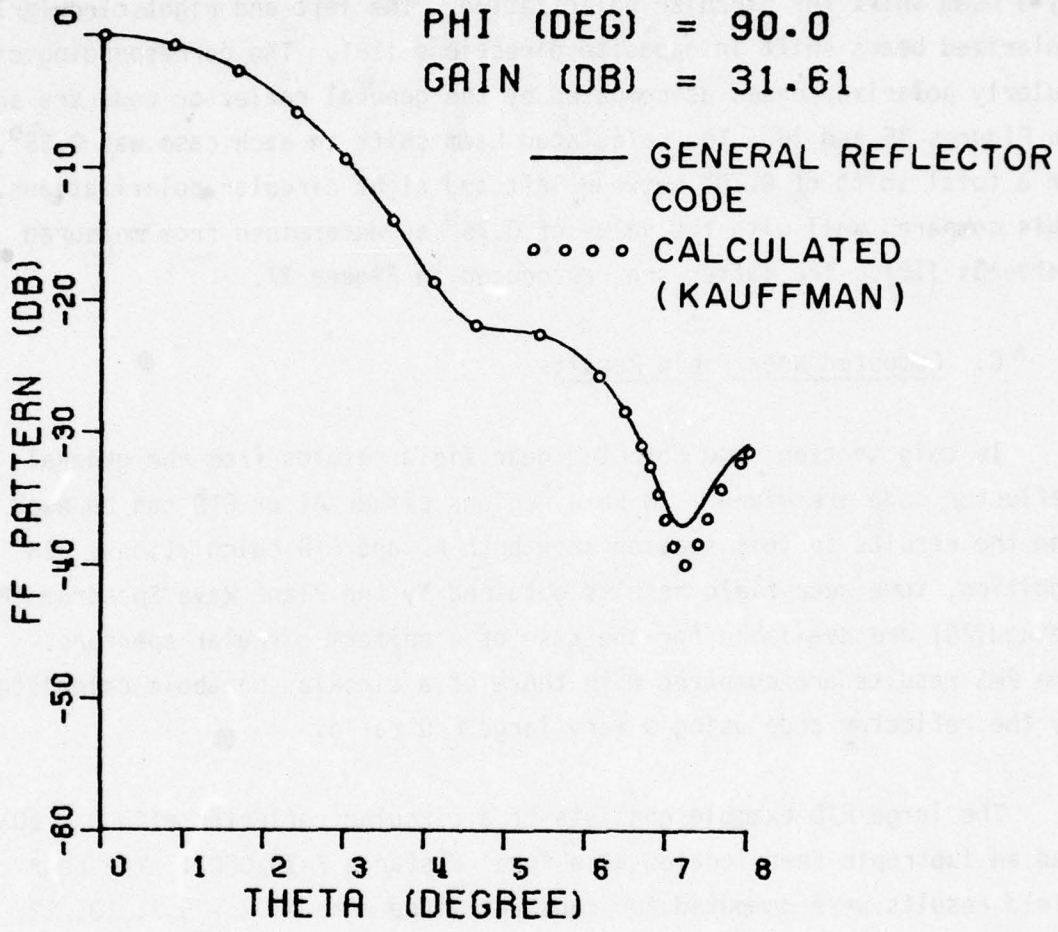

Figure 34. Far field pattern for example of Reference 18, computed by general reflector code. Principal polarization in $\phi=90^{0}$ plane.

No cross polarization occurs when the offset reflector is fed by a circularly polarized feed; but the depolarization property manifests itself by a beam shift for circular polarization. The left and right circularly polarized beams shift in opposite directions [18]. The corresponding circularly polarized cases as computed by the general reflector code are shown in Figures 35 and 36. The calculated beam shift in each case was 0.35^{o}, or a total shift of 0.70^{o} between left and right circular polarizations. This compares well with the value of 0.75^{o} as determined from measured patterns [18]. The latter are reproduced in Figure 37.

C. Computed Near Field Results

In this section some computed near field results from the general reflector code are given. In some regions either AI or GTD can be used and the results in this section show both AI and GTD calculations. In addition, some near field results obtained by the Plane Wave Spectrum (PWS) method[20] are available for the case of a uniform circular aperture. The PWS results are compared with those of a circular parabola calculated by the reflector code using a very large F/D ratio.

The large F/D example consists of a circular reflector with $D = 10\lambda$ and an isotropic feed located at a focal distance $F=10{,}000\lambda$. The near field results were computed for constant plane cuts at $Z = 5.3, 10, 12, 40\lambda$ as shown in Figures 38 through 43. Part a of each figure shows the near field as calculated by AI and part b shows that for GTD. The PWS results for the uniform circular aperture are shown in Figure 44 for the corresponding Z cuts. As seen from these figures, all AI, GTD and PWS are in excellent agreement. Note that the minor E_z components in the $Z=10\lambda$ (Figure 40) and $Z=40\lambda$ (Figure 43) cuts also check with that of PWS (Figures 44 b, c). Even though a reflector antenna with such a large focal distance is not practical to build, this example does show the validity of the code for near field calculations.

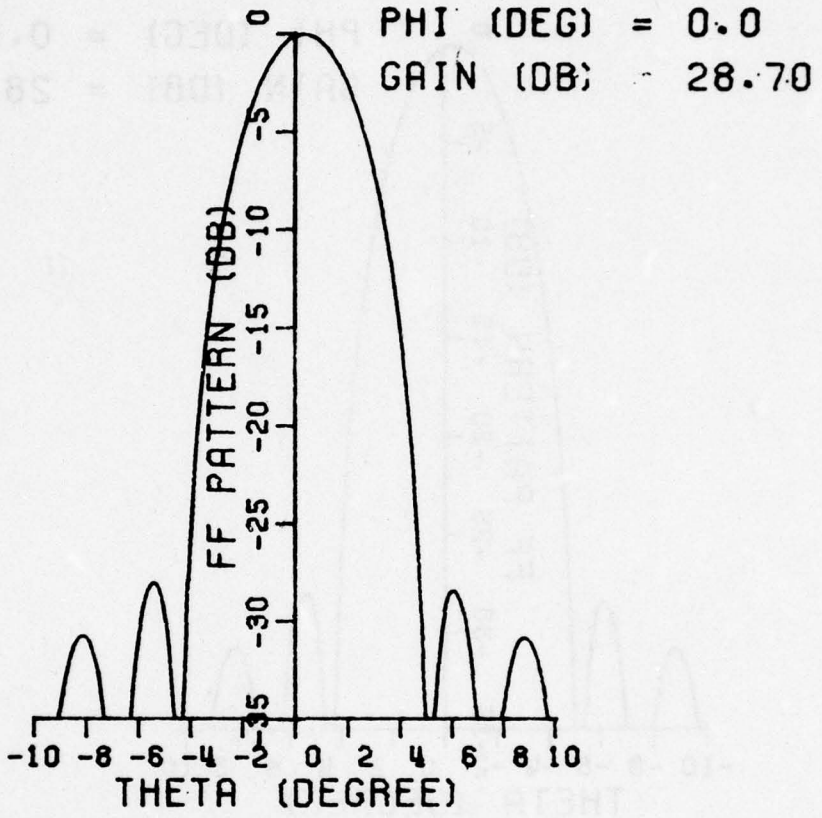

Figure 35. Far field pattern for example of Reference 18, computed by general reflector code. Left circular polarization in $\phi=0^{0}$ plane.

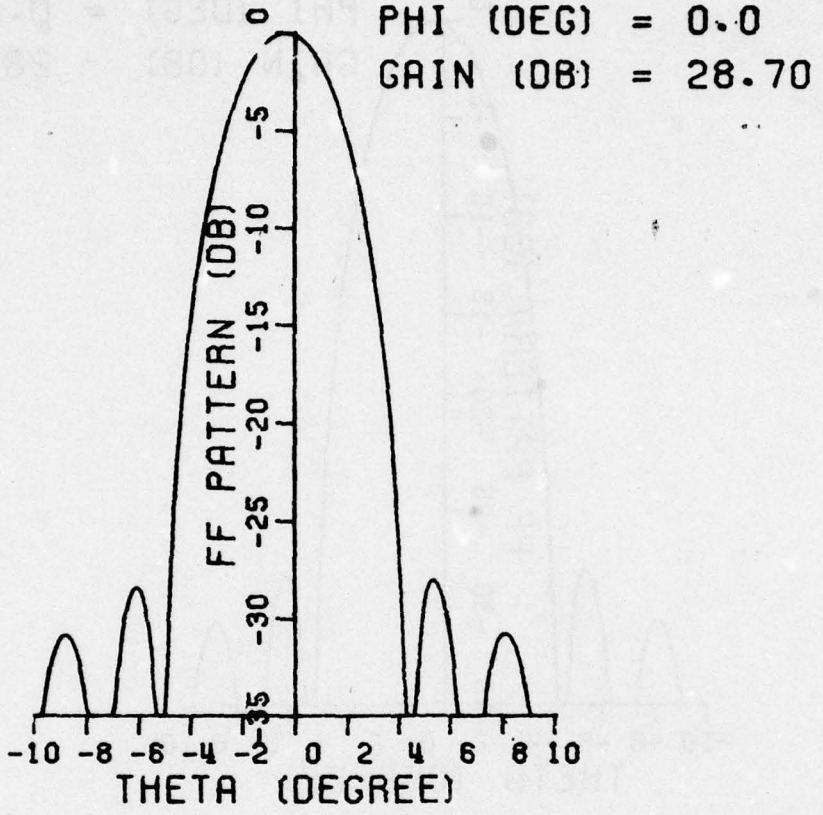

Figure 36. Far field pattern for example of Reference 18 computed by general reflector code. Right circular polarization in $\phi=0^{0}$ plane.

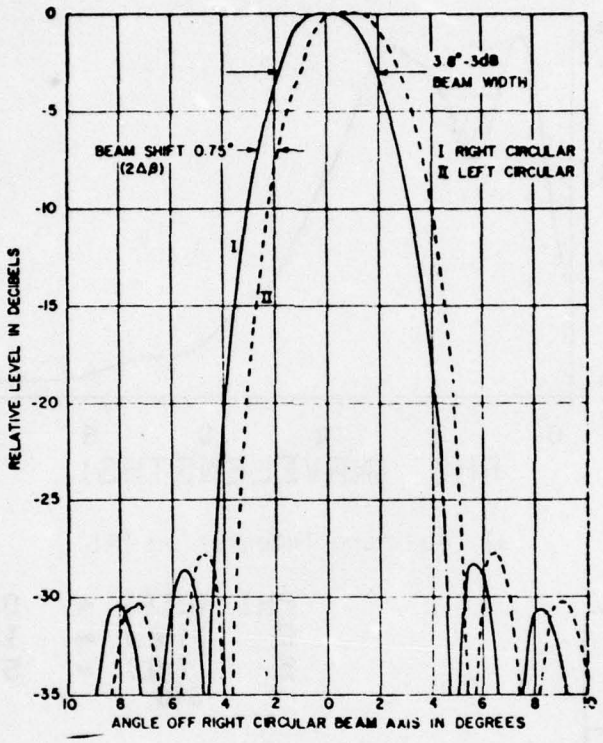

Figure 37. Measured far field patterns from Chu and Turrin [18]. Circular polarization in $\phi=0^{o}$ plane.

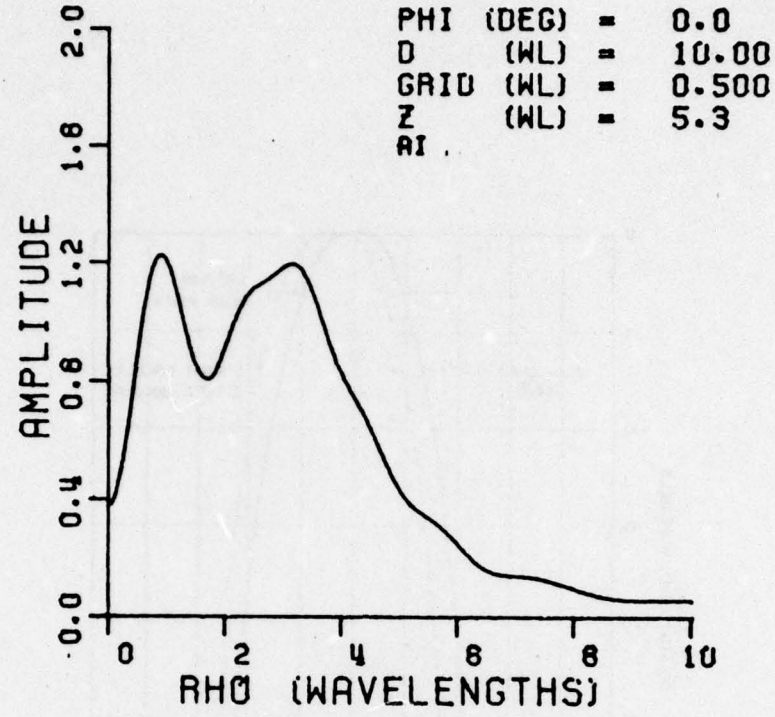

(a) Aperture Integration (AI)

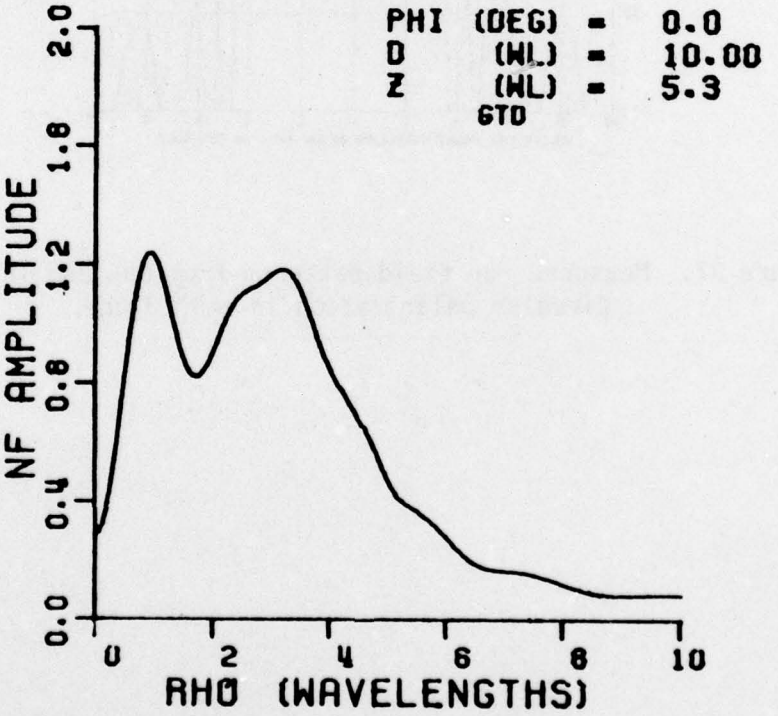

(b) GTD

Figure 38. Near field component E_v for 10λ diameter circular reflector. $Z \cong 5.3\lambda$.

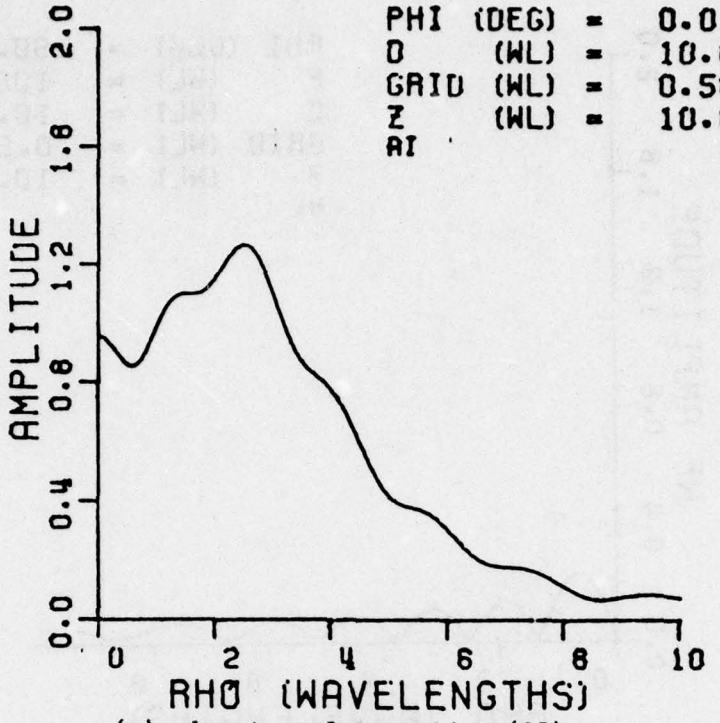

(a) Aperture Integration (AI)

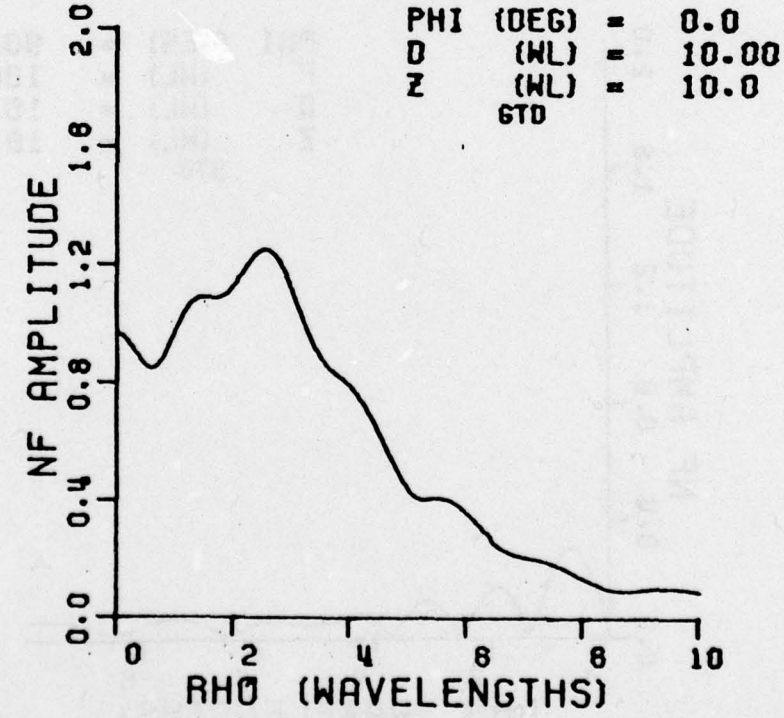

(b) GTD

Figure 39. Near field component E_y for 10λ diameter circular reflector. $Z=10\lambda$.

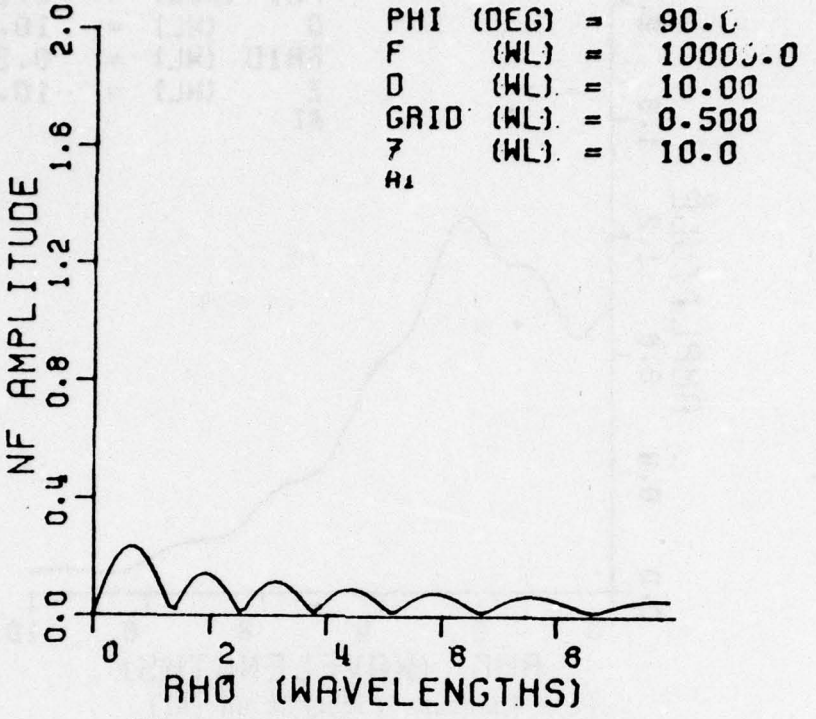

(a) Aperture Integration (AI)

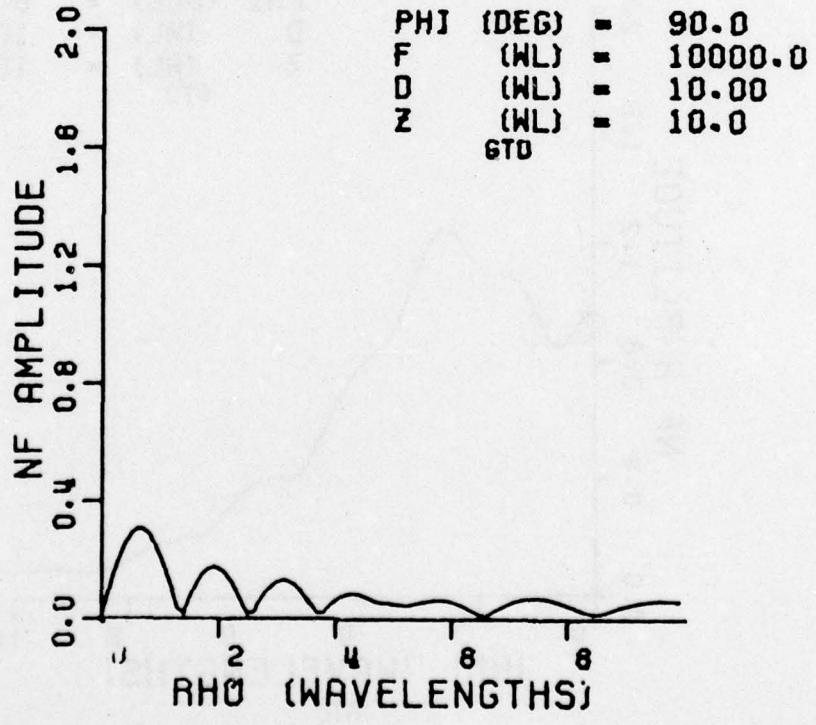

(b) GTD

Figure 40. Near field component E_z for 10λ diameter circular reflector. $Z=10\lambda$.

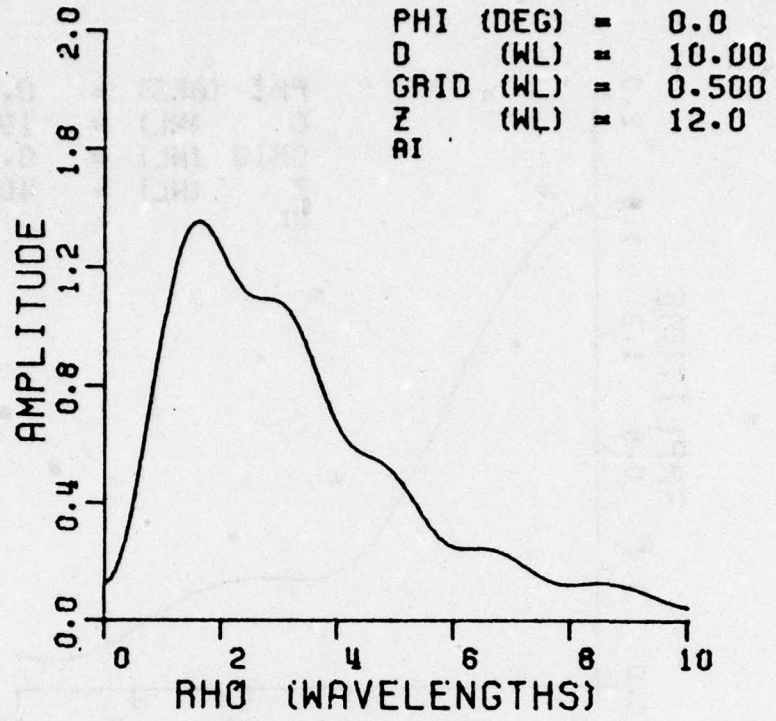

(a) Aperture Integration (AI)

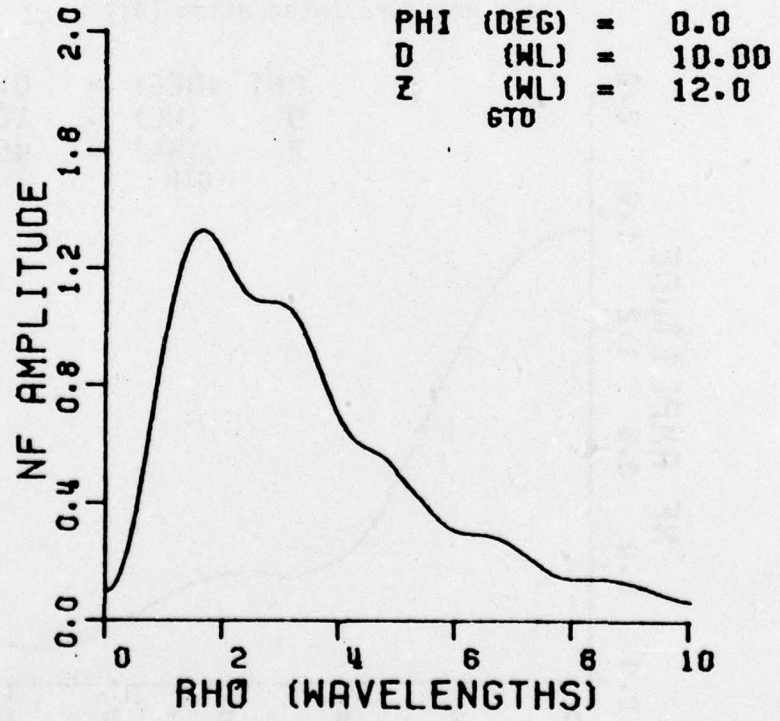

(b) GTD

Figure 41. Near field component E_y for 10λ diameter circular reflector. $Z=12\lambda$.

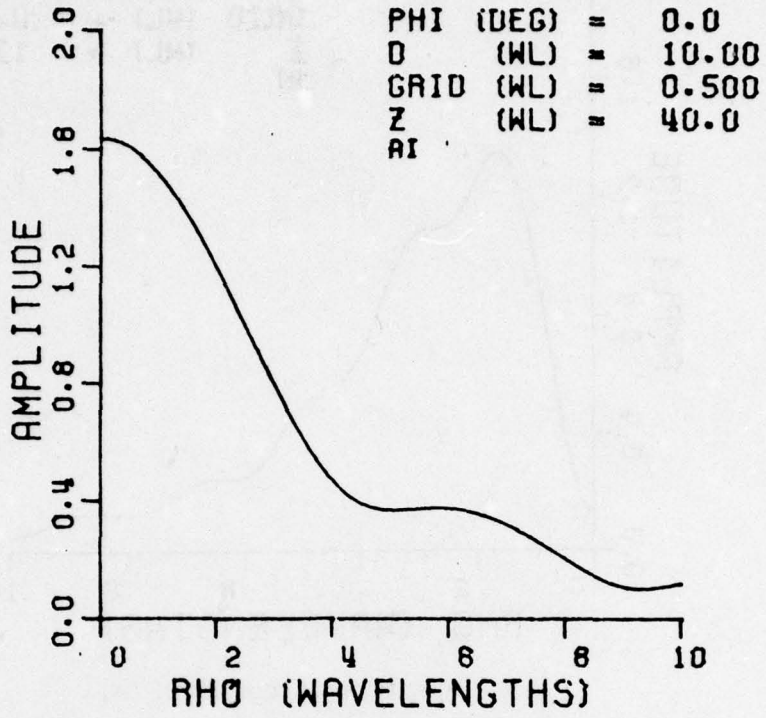

(a) Aperture Integration (AI)

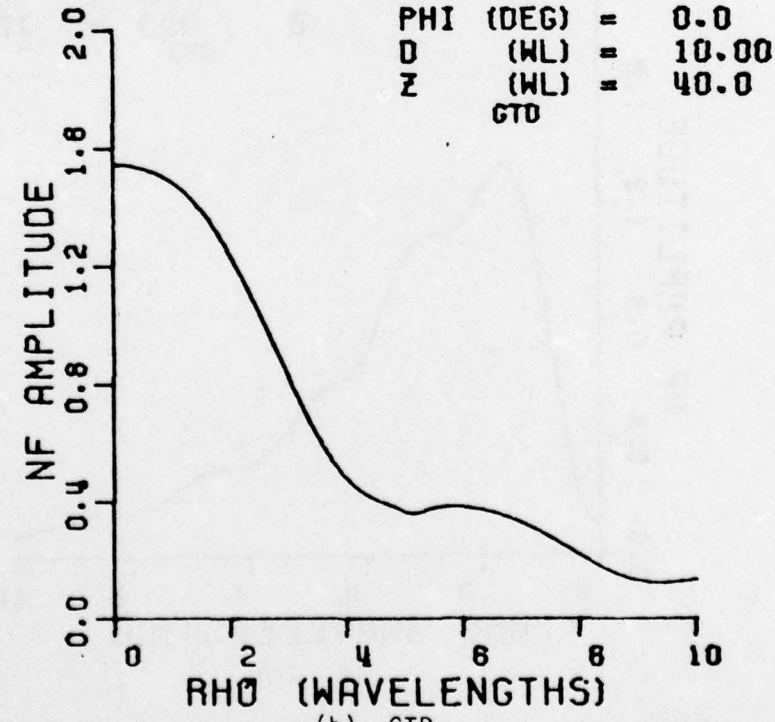

(b) GTD

Figure 42. Near field component E_y for 10λ diameter circular reflector. $Z \geq 40\lambda$.

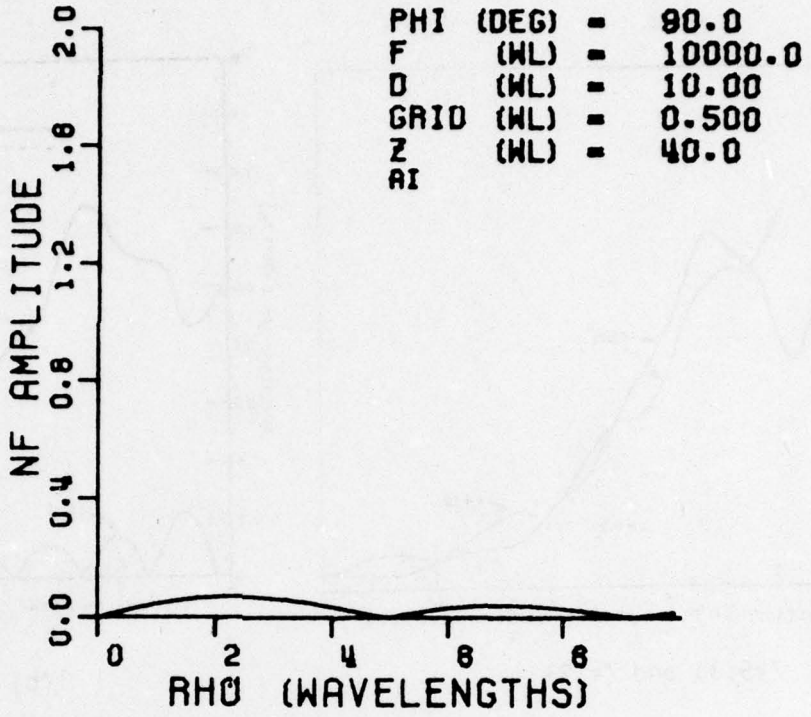

(a) Aperture Integration (AI)

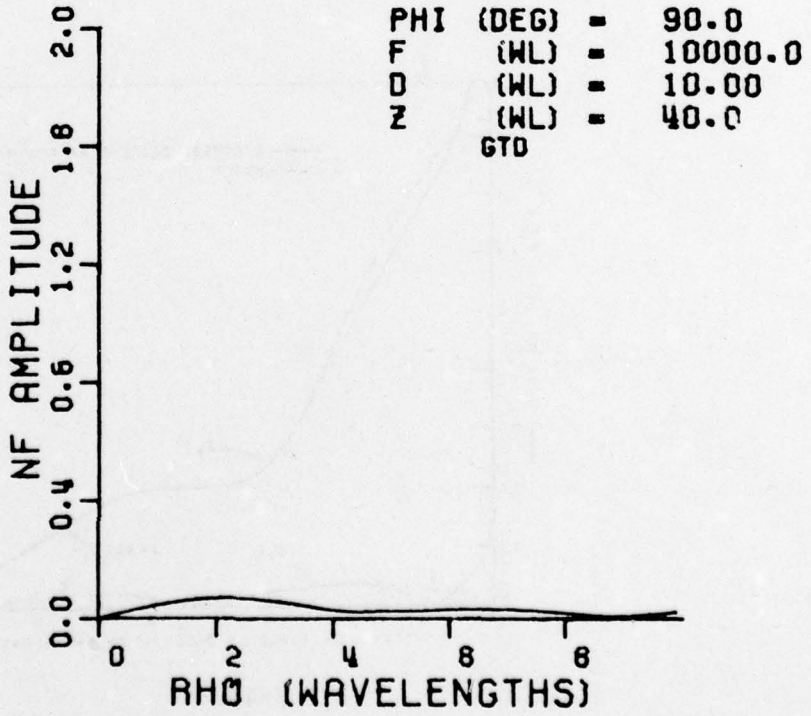

(b) GTD

Figure 43. Near field component E_z for 10λ diameter circular reflector. Z=40λ.

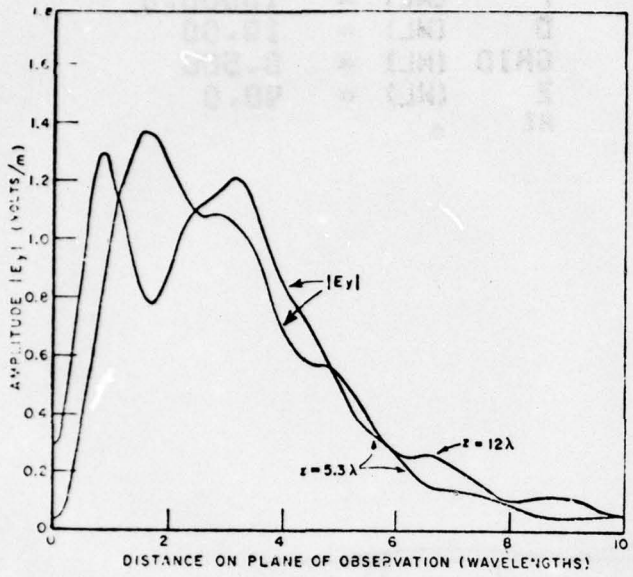

(a) Z=5.3λ and Z=12λ

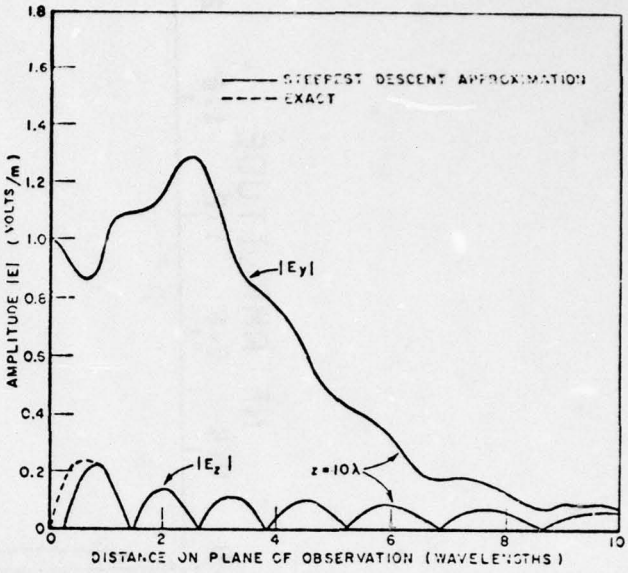

(b) Z=10λ

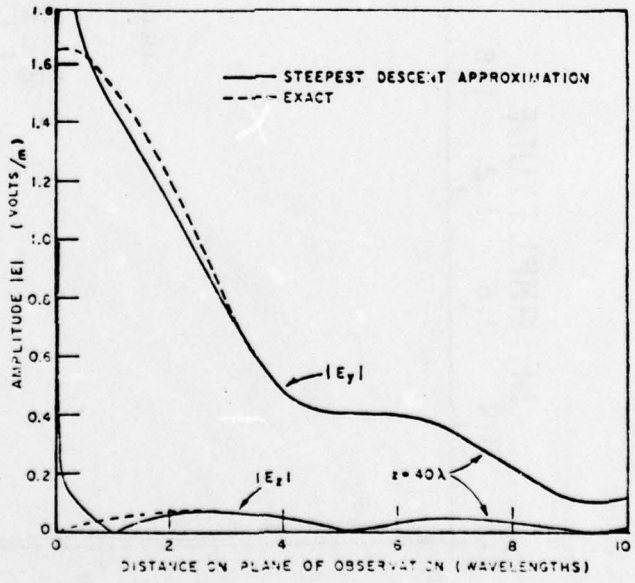

(c) Z=40λ

Figure 44. PWS calculations for near field of uniform circular aperture. 10λ diameter.

The next example presents the near fields of the 24" diameter (22.35λ) reflector antenna for which far field comparisons are given in Figures 21 to 23. This reflector has an F/D ratio of 1/3 and the patterns correspond to a frequency of 11 GHz. Figure 45 shows the near fields of this reflector at range R=40λ by AI (a) and GTD (b). As can be seen the AI and GTD calculations are in very good agreement. The reflector code would normally use GTD over the whole pattern region for this example which shows the good agreement between AI and GTD even in the near axis region. Figure 46 shows the near fields of a constant range at R = 100λ. The agreement between AI and GTD is also good in the AI region except near the axis. Both AI and GTD would normally be used for this example: AI for $\theta<12^{o}$ and GTD for $\theta>12^{o}$. As can be seen from Figure 46 AI and GTD overlap in a wide region.

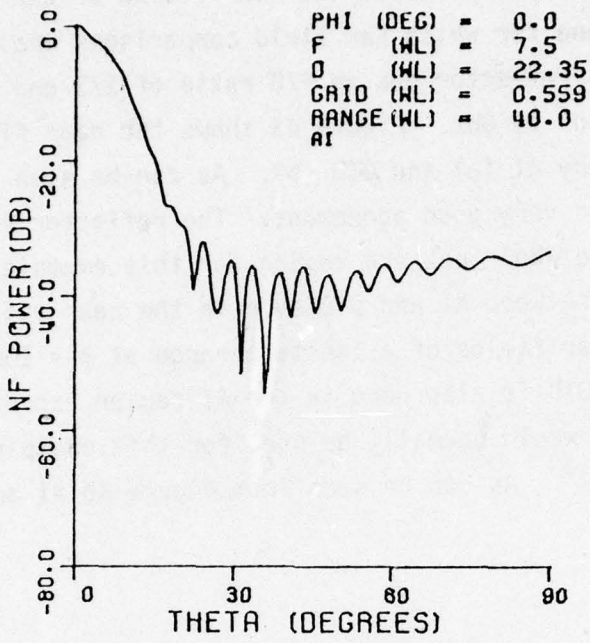

(a) Aperture Integration (AI)

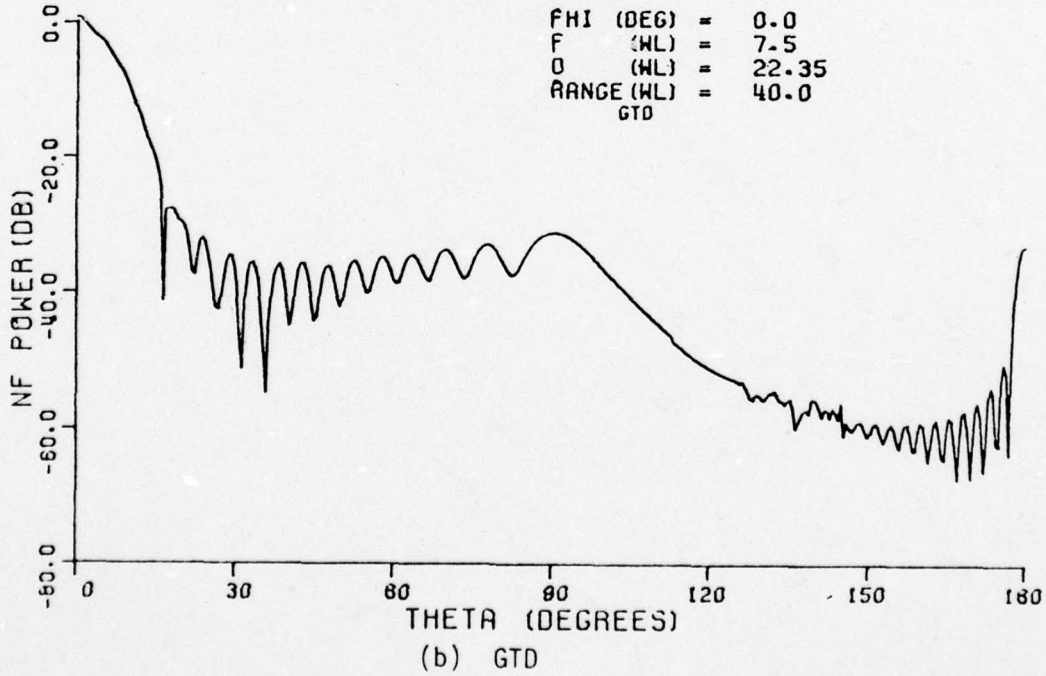

(b) GTD

Figure 45. Principal near field component for 22.35λ diameter circular reflector. R=40λ.

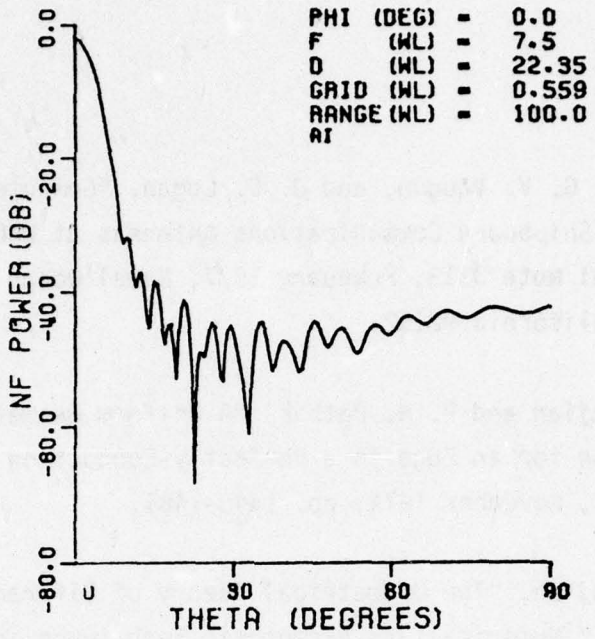

(a) Aperture Integration (AI)

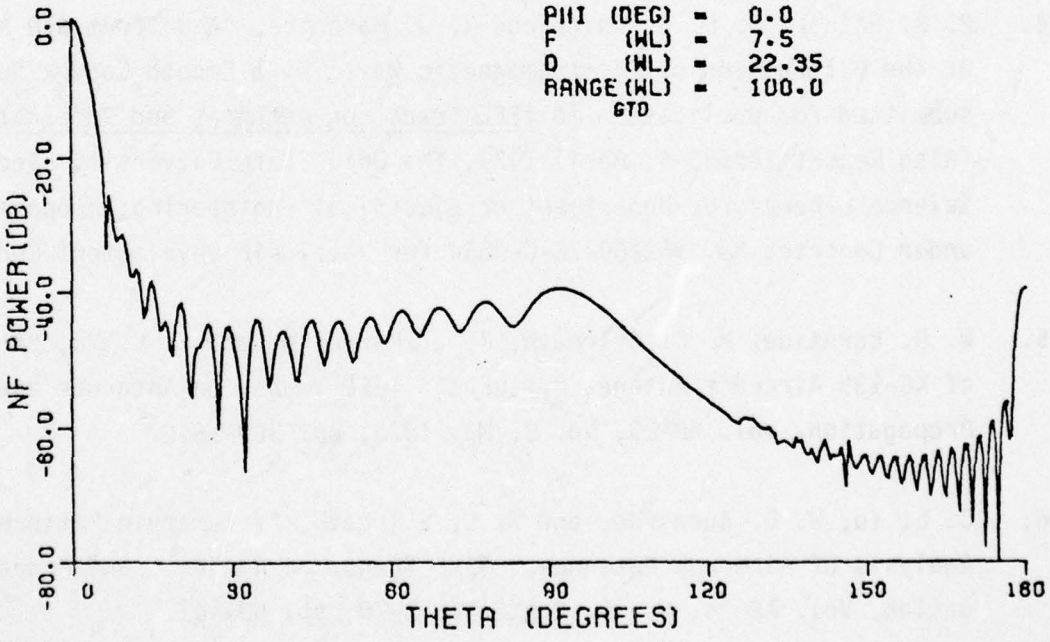

(b) GTD

Figure 46. Principal near field component for 22.35λ diameter circular reflector. R=100λ.

REFERENCES

1. R. L. Mather, G. V. Vaughn, and J. C. Logan, "Computer Techniques for Modeling Shipboard Communications Antennas at UHF and Above," NELC Technical Note 3313, February 1977, Naval Ocean Systems Center, San Diego, California 92152.

2. R. G. Kouyoumjian and P. H. Pathak, "A Uniform Geometrical Theory of Diffraction for an Edge in a Perfectly-Conducting Surface," Proc. IEEE, Vol. 62, November 1974, pp. 1448-1461.

3. R. G. Kouyoumjian, "The Geometrical Theory of Diffraction and Its Applications," Numerical and Asymptotic Techniques in Electromagnetics, edited by R. Mittra, Spring-Verlapg New York, 1975.

4. P. H. Pathak, W. D. Burnside and R. J. Marhefka, "A Uniform GTD Analysis of the Diffraction of Electromagnetic Waves by a Smooth Convex Surface," submitted for publication to IEEE Trans. on Antennas and Propagation. (Also Report 784583-4, April 1979, The Ohio State University Electro-Science Laboratory, Department of Electrical Engineering; prepared under Contract No. N62269-76-C-0554 for Naval Air Development Center.

5. W. D. Burnside, M. C. Gilreath, R. J. Marhefka, and C. L. Yu, "A Study of KC-135 Aircraft Antenna Patterns," IEEE Trans. on Antennas and Propagation, Vol. AP-23, No. 3, May 1975, pp. 309-16.

6. C. L. Yu, W. D. Burnside, and M. C. Gilreath, "Volumetric Pattern Analysis of Airborne Antennas," IEEE Trans. on Antennas and Propagation, Vol. AP-26, No. 5, September 1978, pp. 636-41.

7. R. J. Marhefka, "Analysis of Aircraft Wing-Mounted Antenna Patterns," Report 2902-25, June 1976, The Ohio State University ElectroScience Laboratory, Department of Electrical Engineering; prepared under Grant No. NGL 36-008-138 for National Aeronautics and Space Administration.

8. G. J. Burke and A. J. Poggio, "Numerical Electromagnetic Code (NEC) - Method of Moments," NOSC/TD 116, July 1977, Naval Ocean Systems Center, San Diego, California 92152.

9. R. J. Marhefka and W. D. Burnside, "Numerical Electromagnetic Code (NEC)- Basic Scattering Code. Part I: User's Manual," Report 784508-18, September 1979, The Ohio State University ElectroScience Laboratory, Department of Electrical Engineering; prepared under Contract No. N00123-76-C-1371 for Naval Regional Procurement Office.

10. F. W. Schmidt and R. J. Marhefka, "NEC-Basic Scattering Code. Part II: Code Manual," Report 784508-14, September 1979, The Ohio State University ElectroScience Laboratory, Department of Electrical Engineering; prepared under Contract No. N00123-76-C-1371 for Naval Regional Procurement Office.

11. H. Bach, "Pattern Measurements of High Frequency Satellite-Mounted Antennas," Electromagnetic Institute, Technical University of Denmark, R154, January 1976.

12. D. W. DuBrul and L. M. Peters, "Shipboard Antenna and Topside Arrangement Guidance," NELC Technical Document 356, September 1974, Naval Ocean Systems Center, San Diego, California 92152.

13. R. C. Rudduck, S. H. Lee, "Numerical Electromagnetics Code (NEC)- Reflector Antenna Code. Part I: User's Manual," Report 784508-19, September 1979, The Ohio State University ElectroScience Laboratory, Department of Electrical Engineering; prepared under Contract N00123-76-C-1371 for Naval Regional Procurement Office.

14. S. H. Lee and R. C. Rudduck, "Numerical Electromagnetic Code (NEC) - Reflector Antenna Code. Part II: Code Manual," Report 784508-16, September 1979, The Ohio State University ElectroScience Laboratory, Department of Electrical Engineering; prepared under Contract No. N00123-76-C-1371 for Naval Regional Procurement Office.

15. P. A. J. Ratnasiri, R. G. Kouyoumjian and P. H. Pathak, "The Wide Angle Side Lobes of Reflector Antennas," Report 2183-1, March 1970, The Ohio State University ElectroScience Laboratory, Department of Electrical Engineering; prepared under Contract AF 19(628)-5929 for Air Force Cambridge Research Laboratory.

16. S. Silver, Microwave Antenna Theory and Design, MIT Rad. Lab Series, Vol. 12, McGraw Hill (1949), pp. 455-457.

17. C. A. Mentzer, P. H. Pathak and L. Peters, Jr., "Pattern Analysis of an Offset Fed Parabolic Reflector Antenna," Final Report 3220-2, Department of Electrical Engineering; prepared under Contract N00178-71-C-0264 for U. S. Naval Weapons Laboratory.

18. T. S. Chu and R. H. Turpin, "Depolarization Properties of Offset Reflector Antennas," IEEE Trans. on Ant. and Prop., AP-21, pp. 339-345, May 1973.

19. J. H. Kauffman, W. F. Croswell and L. J. Powers, "Analysis of Radiation Patterns of Reflector Antennas," AP-24, pp. 53-65, January 1976.

20. R. C. Rudduck and C. J. Chen, "New Plane Wave Spectrum Formulations for the Near Fields of Circular and Strip Apertures," IEEE Trans. on Antennas and Propagation AP-24, No. 4, July 1976, pp. 438-449.